DEVELOPMENT OF POLY(LACTIDE-CO-GLYCOLIDE) MICROSPHERES FOR CONTROLLED RELEASE OF THYMOSIN BETA-4 IN THE HEART

APPROVED BY SUPERVISORY COMMITTEE

J. Michael DiMaio, MD _____

Robert Eberhart, PhD _____

Jinming Gao, PhD _____

Kevin Nelson, PhD _____

Zoltan Schelly, PhD _____

Noelle Williams, PhD _____

DEDICATION

I would like to thank the members of my Graduate Committee, my parents Larry & Kathy Thatcher, my sister Jennifer Thatcher, friends, and co-workers for providing their scientific and emotional support throughout the years.

DEVELOPMENT OF POLY(LACTIDE-CO-GLYCOLIDE) MICROSPHERES FOR CONTROLLED RELEASE OF THYMOSIN BETA-4 IN THE HEART

by

JEFFREY EDWARD THATCHER

DISSERTATION

Presented to the Faculty of the Graduate School of Biomedical Sciences

The University of Texas Southwestern Medical Center at Dallas

In Partial Fulfillment of the Requirements

For the Degree of

DOCTOR OF PHILOSOPHY

The University of Texas Southwestern Medical Center at Dallas

Dallas, Texas

May, 2012

Copyright

by

JEFFREY EDWARD THATCHER, 2012

All Rights Reserved

DEVELOPMENT OF POLY(LACTIDE-CO-GLYCOLIDE) MICROSPHERES FOR CONTROLLED RELEASE OF THYMOSIN BETA-4 IN THE HEART

JEFFREY EDWARD THATCHER, Ph.D.

The University of Texas Southwestern Medical Center at Dallas, 2012

Mentor
J. MICHAEL DIMAIO, M.D.

Thymosin β-4 is of great importance because it improves heart function after heart attack in animal models. In order to limit the number of interventions in Thymosin β-4 therapy, a localized and controlled release formulation is necessary. Our goal was to generate controlled release microsphere formulations of poly(lactic-co-glycolic acid) that overcame a common problem of burst-release and to establish a method to modulate the release rates between formulations. Burst-release is the rapid release of drug from the formulation occurring in the initial 24 hours of elution. This event causes undesirable loss and potentially toxic levels of therapeutic from the microsphere. Modulation of release is of particular importance in these studies because little is known regarding the

therapeutic dose of Thymosin β-4 in humans. A class of non-ionic surfactants, alkyl glucosides, were used as excipients in preparation of poly(lactic-co-glycolic acid) double-emulsion microspheres for controlled release of the protein albumin or the peptide Thymosin β-4. We specifically chose octyl-glucopyranoside and decyl-glucopyranoside for their ability to stabilize the primary emulsion step during microsphere synthesis. We demonstrate that the addition of alkyl glucosides of differing hydrocarbon chain length can modulate the rate of protein and peptide release from these microspheres. In albumin formulations, octyl-glucopyranoside reduced overall release compared to decyl-glucopyranoside and formulations prepared without surfactant, whereas in TB4 formulations decyl-glucopyranoside reduced overall release. In albumin containing microspheres burst release was high in formulations that did not contain any surfactant, 23%. Addition of decyl-glucopyranoside reduced burst release to 6% while addition of octyl-glucopyranoside further reduced burst release to 3%. Thin sections revealed smaller and more uniform internal porosity in microspheres containing surfactant, of which octyl-glucopyranoside porosity was less than decyl-glucopyranoside porosity. This difference in porosity corresponds with the reduction in initial burst release and overall release of albumin. With these surfactants we established a group of formulations with differing drug release rates. This research suggests that formulations containing Thymosin β-4 can be beneficially used in future *in vivo* testing to determine a controlled release profile capable of generating a therapeutic response in ischemic heart disease.

TABLE OF CONTENTS

LIST OF FIGURES

LIST OF TABLES

LIST OF APPENDICES

LIST OF DEFINITIONS

ANOVA	Analysis of variance
BCA	Bicinchoninic acid assay
BSA	Bovine serum albumin
CTAB	Cetyltrimethylammoniumbromide surfactant
pBC 264	Cholecystokinin agonist peptide
CD	Circular dichroism
DCM	Dichloromethane
AOT	Dioctyl sodium sulfosuccinate
DSC	Differential Scanning Calorimetry
EE	Encapsulation efficiency
FT-IR	Fourier Transform infrared spectroscopy
G	Gauge
ΔG	Gibbs free energy
T_g	Glass transition temperature
GA	Glycolic Acid
GH	Growth hormone
HSA	Human serum albumin
HUVECs	Human vein endothelial cells
HLB	Hydrophobic-lipophilic balance
IGF	Insulin-like growth factor-I

LA	Lactic Acid
LC-MS	Liquid Chromatography-Mass Spectrometry
NoSf	Microsphere formulation without surfactant
MI	Myocardial infarction
G10	n-Decyl-β-D-Glucopyranoside
NGF	Nerve growth factor
G7	n-Heptyl-β-D-Glucopyranoside
G9	n-Nonyl-β-D-Glucopyranoside
G8	n-Octyl-β-D-Glucopyranoside
O/W	Oil-in-water
PTH	Parathyroid hormone
PBS	Phosphate buffered saline
PEG	Poly(ethylene glycol)
PEO	Poly(ethylene oxide)
PLG	Poly(glycolic acid)
PLA	Poly(lactic acid)
PLGA	Poly(lactic-co-glycolic acid)
PPO	Poly(propylene oxide)
PVA	Poly(vinyl alcohol)
RM-ANOVA	Repeated measures analysis of variance
SEM	Scanning Electron Microscopy

SDS	Sodium dodecyl sulfate
TB4	Thymosin β-4
Sn(Oct)2	Tin (II) 2-ethylhexanoate
TEM	Transmission electron microscopy
TFA	Trifluoroacetic acid
VEGF	Vascular endothelial growth factor
W/O	Water-in-oil
W/O/W	Water-in-oil-in-water double emulsion

CHAPTER ONE
Introduction & Review of Literature

INTRODUCTION

The peptide Thymosin beta-4 (TB4), first isolated in 1981, has been discovered to have therapeutic benefits in a number of pathologies. In an animal model of ischemic heart disease, improvements in heart function have been attributed to administration of TB4 for two weeks beginning at induction of myocardial ischemia. Previous failures in delivery of peptides to the heart in humans lead us to seek a formulation that both protects TB4 from premature degradation, and reduces the concentration and frequency of dose. Poly(lactic-co-glycolic acid) microspheres synthesized with specific tolerances for intramyocardial injection are proposed here as a method to achieve controlled and local delivery of TB4. The dose of TB4 remains unknown; therefore we began testing alkyl glucoside surfactants as excipients in the microsphere formulation to determine their effect on release kinetics of a model drug, albumin (BSA). After establishing an effective surfactant hydrophobic-lipophilic balance number (HLB) and concentration we applied the same concept to the controlled release of TB4. The results of these studies demonstrate the effectiveness of surfactants in the control of peptide and protein release from PLGA devices as well as the establishment of a microsphere formulation designed for intramyocardial controlled release of TB4.

PEPTIDE & PROTEIN CONTROLLED RELEASE

The need for advancements in drug delivery is increasing rapidly. In the past, chemicals that were easiest to deliver through traditional routes of administration were sought after while difficult to deliver drugs could be ignored. For example, nucleic acid and amino acid based molecules have been known for years to elicit

many cellular effects, but were not developed as a result of short half-lives in the body as well as potential side effects in other tissues. In recent years however, advancements in biotechnology and the pace at which we are able to identify new drug targets has increased rapidly making these types of molecules more important as therapeutics. With these molecules at the cutting edge of medicine, we cannot ignore the need for improvements in routes of administration and drug formulations.

Polymer encapsulation, one such improvement in drug formulations, has gained a great deal of interest in the delivery of biomolecules, because it reduces the number of interventions and protects the drug from premature degradation in the body. The rationale behind the delivery of drugs from polymer matrices is the entrapment of therapeutic molecules from the outside environment by a network of polymer which delays the diffusion of drug into the surrounding tissue. The local release of therapeutic following implantation of the polymer device occurs by diffusion of the drug through the polymer network and into the tissue. The drug becomes available to the target tissue once it is freed from the matrix. The rate of drug release from the matrix depends on the configuration of the polymer implant as well as the physical and chemical characteristics of the drug and the polymer. The interactions caused by polymer chemistry, implant structure, and the rate of drug release are all important factors in the design of a polymeric drug delivery system (Saltzman, 2001).

Controlled release of macromolecules such as proteins and peptides has been achieved through entrapment in biodegradable polymers including poly(amides), poly(amino acids), poly(alkyl-a-cyano acrylates), poly(esters), poly(orthoesters), poly(urethanes), and poly(acrylamides) (Jain, 2000). This technology has been applied to a multitude of pharmaceutical applications

including the release of antigens for immunization (Alonso, et al., 1993; Schwendeman, et al., 1996), peptides to promote tissue regeneration (Camarata, et al., 1992; Cleland, et al., 1997), and hormone replacement therapy (Kostanski, et al., 2000; Okada, et al., 1994).

The three most important aspects of polymer controlled release formulations include the compatibility of the formulation with the body, the target tissue's access to the released drug, and finally the activity of the drug after being liberated from the matrix. In the case of PLGA controlled release devices, the tissue is generally compatible with the polymer and its acidic degradation products (Athanasiou, et al., 1996; Fournier, et al., 2003). Drug release occurs by a complex mechanism that includes diffusion and drug-polymer interactions. Lastly, the activity of the released drug is affected by the processing parameters in device synthesis as well as changes that occur to the matrix after being re-hydrated in the tissue. Drug interactions with the polymer and its degradation products, other drug molecules, and additional excipients in the formulation add to the complexity of the system. For these reasons, formulations are numerous and customized to specific therapeutic molecules to achieve desirable encapsulation and release properties.

In one of the most useful configurations for polymer delivery systems for controlled release of biomolecules is the microsphere. Microspheres are small polymer beads with typical sizes ranging from 1 to 500 microns (μm) in diameter; however they can be generated in nanometer (nm) ranges by some techniques. Their size and shape makes them amenable to delivery by injection through a small gauge (G) needle directly into the target tissue. Formulations can be tailored to release drug over durations from days to months.

For TB4 delivery, the drug delivery system should be one that can continually release therapeutically active TB4 and be deployed directly into the myocardium. Polymer microspheres fulfill this role. Peptides encapsulated within microspheres are protected from degradation by enzymatic cleavage, or cellular digestion enabling their prolonged delivery as active therapeutic molecules (Hinds, et al., 2005). The following sections discuss the synthesis of polymer microspheres and the factors that contribute to the elution of drugs, especially proteins and peptides, from PLGA microspheres.

REVIEW OF PARAMETERS IN PLGA MICROSPHERE SYNTHESIS

Lactic Acid Derived Polyesters & Their Degradation

The most commonly used polyesters for peptide delivery are poly(lactic acid) (PLA), poly(glycolic acid) (PLG), poly(lactic-co-glycolic acid) (PLGA), PLGA-poly(ethylene glycol) (PEG) block co-polymers (Carrascosa, et al., 2004; Cho, et al., 2001; Ehtezazi, et al., 1999; Rosa, et al., 2000). PLA, PLG and their co-polymers are hydrophobic. PLA is semi-crystalline when synthesized from one stereoisomer configuration of lactic acid (either the d- or the l- form). These crystalline regions make the polymer more resistant to water penetration resulting in prolonged polymer duration in the presence of water. Polymers made from both d- and l- lactic acid isoforms are amorphous, because the racemic polymer does not arrange into crystalline regions. Lack of crystallinity gives water easier access to all regions of the polymer chain leading to more rapid degradation. The polymer consisting of glycolic acid, PLG, is a highly crystalline polymer that is more hydrophilic than PLA. Owing to its hydrophilicity it does not maintain mechanical strength as well as PLA. Polymer degradation rates vary for different forms of these polyesters being influenced by molecular weight and monomer ratios (Huh, et al., 2003).

Synthesis of lactic acid and glycolic acid containing polyesters is achieved for higher molecular weights using ring-opening melt polymerization (Figure 1.1). This process begins with cyclic diesters of lactic acid and/or glycolic acid with the desired stereochemistry. Many initiators have been used in ring opening polymerization including zinc (II) and titanium(IV), however the most often utilized catalyst is tin (II) 2-Ethylhexanoate (Sn(Oct)2) for a number of reasons including high reaction rates, ability to produce high molecular weights, and its low toxicity which is useful in biomedical applications (Platel, et al., 2008). The mechanism of this reaction for metal complexes, such as Sn(II) is by coordination-insertion. A more detailed mechanism for this reaction has been proposed (Kowalski, et al., 2000).

Co-polymerization of lactic acid with glycolic acid results in a polymer with many beneficial characteristics for drug delivery. This polymer is amorphous making it a good substrate for drug entrapment. Consistent with its constituent polymer properties, PLGA microspheres degrade much more quickly than PLA microspheres (Kim and Park, 2004). One of the advantages of this system is that the microsphere degradation rate can be modified by altering the LA:GA ratio. Microspheres fabricated from PLGA 50:50 degrade slightly faster than those form PLGA 75:25, both of which degrade much faster than PLA (Cui, et al., 2005). Like microsphere degradation, peptide release can be altered by manipulating the LA:GA ratio. For instance, PLGA 75:25 can release nerve growth factor (NGF) more quickly than PLGA 50:50 (Pean, et al., 1998), Bovine serum albumin (BSA) was released faster in PLGA 50:50 than in PLGA 75:25 or 85:15 (Wei, et al., 2004), and finally melittin was released more quickly in PLGA 50:50 than PLGA 75:25 (Cui, et al., 2005). These results demonstrate that PLGA

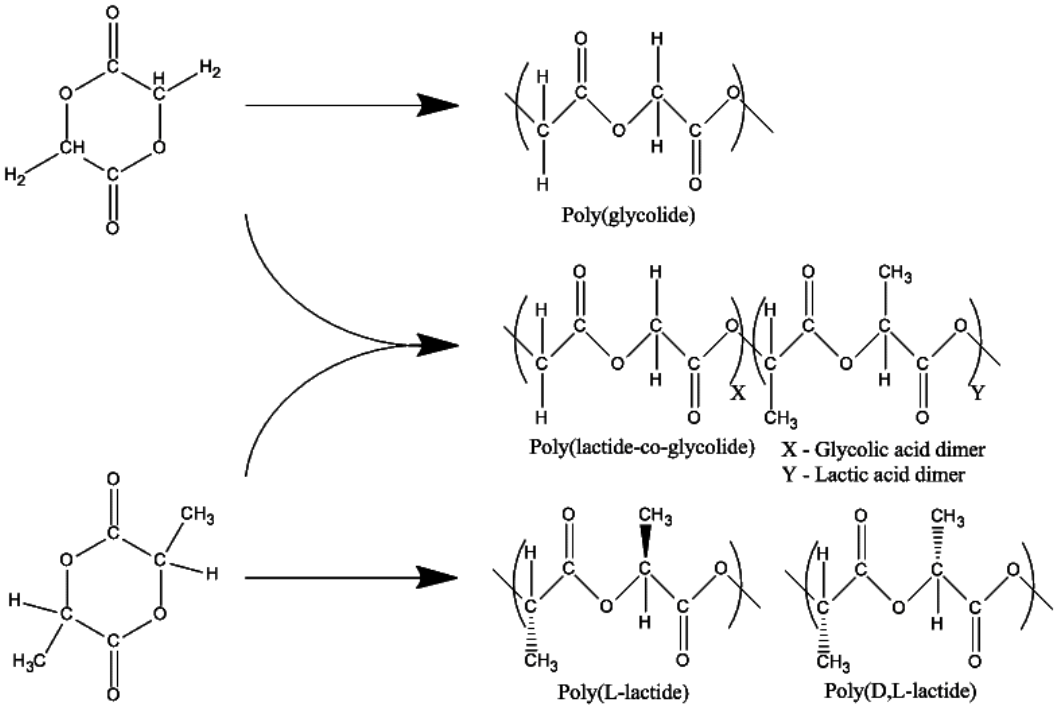

Figure 1.1 – Polymerization of PLGA by ring-opening melt polymerization of cyclic diesters. Structures of PLA, PLGA, and PGA achieved through ring opening polymerization.

50:50 is not always the fastest peptide releasing polymer, likely a result of the difference in the drug-polymer interaction. Also, these results support the effect of modulating the co-polymer ratio to alter drug release rate.

Polymer molecular weight (M_w) has an effect on the mass loss of polyester microspheres. Microsphere mass-loss results from polymer chain scission and the subsequent diffusion of oligomers and monomers from the bulk of the sphere. This tends to occur in a heterogeneous pattern in PLGA materials of dimensions greater than 300 μm and homogeneously in PLGA materials with at least one dimension less than 300 μm (Grizzi, et al., 1995). In general, drug release rates from polyesters are reduced for polymers of increasing M_w (Cui, et al., 2005). However, microspheres synthesized from higher M_w PLGA (40,000 Da to 80,000 Da) can release protein in short durations based on the method of preparation (Cleek, et al., 1997; Ruan, et al., 2002; Ungaro, et al., 2006; Wei, et al., 2007). Therefore, it is more important to choose polymer M_w for polymer residence time and rate of monomer formation than its effect on drug release. Microspheres fabricated by double-emulsion (W/O/W) from PLGA of M_w 12,000 Daltons (Da) will completely disintegrate in one month (from spheres to polymer mass), while microspheres of M_w 30,000 Da retain their integrity over the same duration (Diaz, et al., 1999).

Different polyester microsphere formulations and their drug release duration have been reported (Table 1.1). Release rates vary widely and depend on both drug and polymer chemistry. Based on the release data accumulated in this table, a polymer M_w in the range of approx. 15 to 75 kDa is sufficient to release amino-acid based molecules, such as TB4, in the four week timeframe we later suggest for clinically effective TB4 release.

Table 1.1 – Effect of polyester Mw on duration of drug release

Polymer	Monomer Ratio	M_w [KDa]	Encapsulated Peptide	Cumulative Drug Release [%]	Duration of Release [days]	Additional Excipients	Ref. Number
PLGA	(45:55)	12.0	EGF	100	30		Diaz '99
PLGA	(50:50)	14.1	insulin	80	18		Ibrahim '05
PLGA	(50:50)	14.3	calcitonin	100	25		Ruan '02
PLGA	(50:50)	15.0	GH	60	35		Kim '04
PLGA	(50:50)	41.9	BSA	85	28		Ungaro '06
PLGA	(50:50)	42.2	IgG	10	22		Cleek '97
PLGA	(50:50)	42.2	IgG	100	22	5% PEG	Cleek '97
PLGA	(75:25)	17.5	BSA	60	35	NaCl	Péan '98
PLGA	(75:25)	75.0	GH	50	30		Wei '07
PLGA	(75:25)	75.0	GH	70	30	pluronic & sucrose	Wei '07
PELA*	(10% PEG)	80.0	HSA	100	28		Ruan '02

* PELA: poly(lactide-co-ethylene glycol), contains a hydrophilic PEG segment between the hydrophobic PLA segments

Degradation of PLGA & PLGA Microspheres

Polyesters of lactic acid and/or glycolic acid are considered biodegradable by the scission of the ester linkages in the presence of water. The reaction can be catalyzed in the presence of acids, bases, salts, or enzymes (Ratner and Hoffman, 2004). The degradation of PLGA devices occurs by bulk degradation or surface erosion; however the dimensions of the device must be large to achieve surface erosion (Rothstein, et al., 2009). When configured into microspheres bulk degradation occurs, because the rate of water penetration far exceeds the rate of PLGA degradation. Therefore, the entire microsphere is wetted prior to any significant loss of PLGA. Hydrolysis occurring within the microsphere leads to formation of acidic PLGA oligomers. The retention of acidic oligomers influences the degradation mechanism of the microspheres.

Owing to these insoluble PLGA oligomers the degradation of a PLGA microsphere is a heterogeneous process occurring faster inside than outside of the microsphere. The reason for faster polymer degradation of the inside of the microsphere is initially attributable to the inability of polymer strands in the interior of the microsphere to diffuse into solution. This causes an elevated concentration of degradation products inside the microsphere. These degradation products contain carboxylic acid end-groups which, as mentioned earlier, are known to increase the rate of PLGA hydrolysis. This increased rate in the presence of degradation products is called autocatalysis and is the reason why the interior of microspheres degrades faster than the exterior (Vert, et al., 1994). The morphological result of autocatalysis is the appearance of a hollow microsphere interior (Figure 1.2).

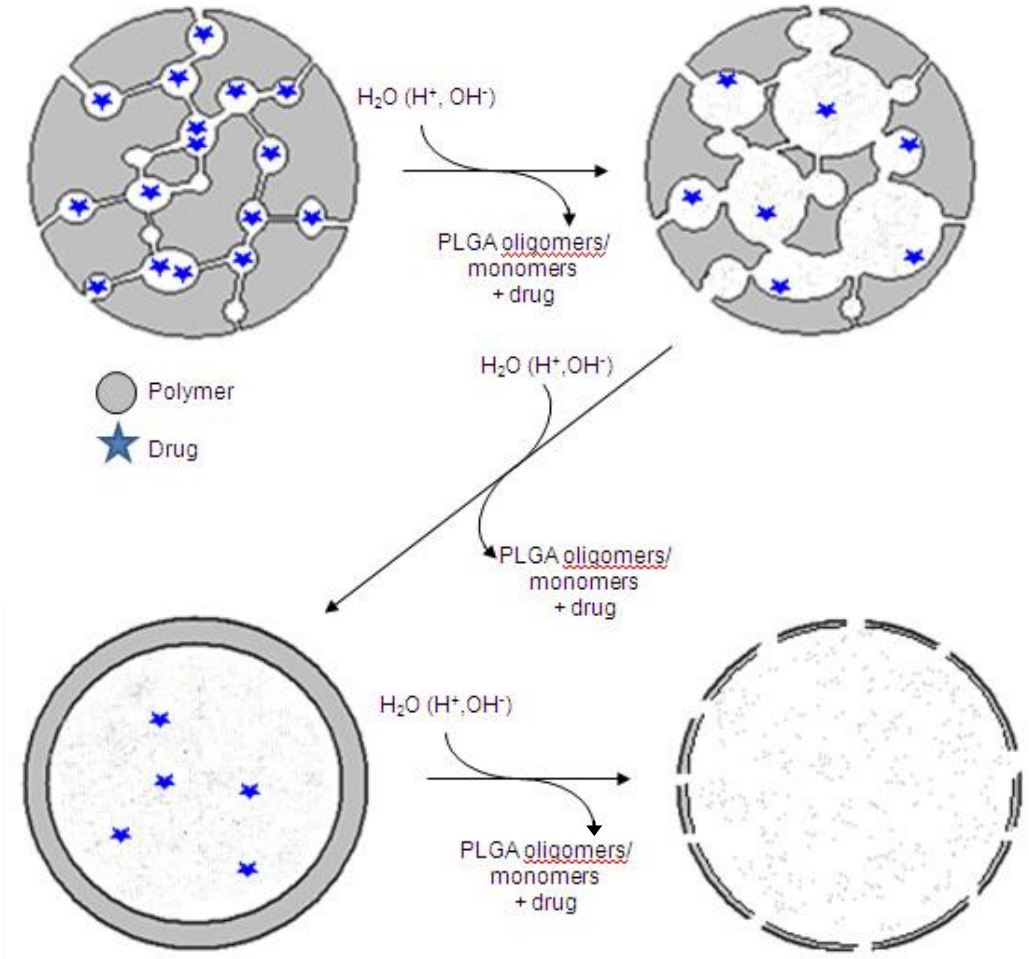

Figure 1.2 – *In vitro* bulk degradation of a PLGA microsphere in cross-section.

Occurring simultaneously with hollowing of the interior is the formation of a thick shell of crystalline polymer on the microsphere surface. The thick shell further exacerbates autocatalysis by trapping small and acidic water soluble PLGA degradation products in the interior causing a deeper drop in internal pH. The pH can be 3.0 and lower according to pH measurements made on PLGA films 30 – 100 μm thick (Shenderova, et al., 2004). Furthermore, this thick shell inhibits drug release. An additional event that inhibits drug release is hydrogen-bonding of encapsulated drug with carboxylic end-groups of the degraded PLGA fragments molecules further slowing their diffusion.

The heterogeneous degradation process is typically what leads to a commonly reported "tri-phasic" release profile of drug from microspheres. Initially, drug at or near the surface of the newly wetted microspheres can quickly escape. This initial release occurs within the first 24 hours and is called burst-release. Between 24 hours and approximately two weeks the thickening of the outer shell takes place which inhibits drug encapsulated in the interior of the microsphere from escaping. This phase of very little drug release is called the lag phase. Eventually the outer shell thins and becomes porous, allowing drug trapped within to escape. This is the late release phase.

Polymer End-Group

The polymer end-group is determined by the choice of initiator used in the polymerization reaction. Uncapped PLG has a free carboxyl group at the terminal where polymerization was initiated (Figure 1.3). Capped PLG has a more hydrophobic alkyl end attached at the initiator site by an ester linkage (Tracy, et al., 1999). Uncapped PLGA with free carboxyl termini is more hydrophilic and has

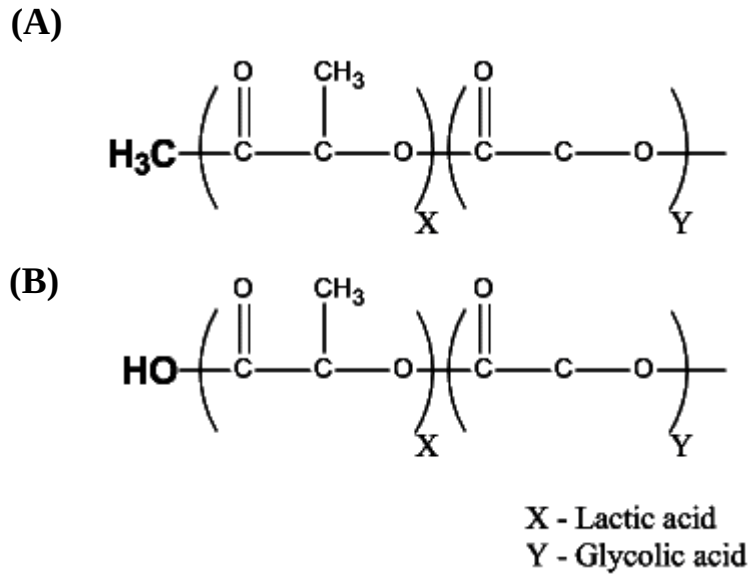

Figure 1.3 – The chemical structure of end-group capped (A) and uncapped (B) PLGA.

higher hydrolysis rate than the end-capped species with an alkyl group residing at the carboxyl terminus (Luan and Bodmeier, 2006).

PLGA with a carboxylic acid terminus, or the uncapped PLGA degrades more rapidly than its more hydrophobic counterpart. Degradation studies of disks made of 12.7 kDa uncapped and capped PLGA shows that the disks made from capped end-groups lost 85 % of their weight in 35 days, while uncapped PLGA disks lost the same weight percentage in only 20 days (Tracy, et al., 1999). The end-group chemistry plays an important role in that uncapped polymers degrade 2-3 fold faster *in vitro* and 3-4 fold faster *in vivo* than capped polymer (Tracy, et al., 1999). Increased water-uptake and acidic end-groups is regarded as the reason for this difference.

In addition to degradation rates, there also appears to be significant difference in the release of peptides from capped vs. uncapped end-groups. Microspheres made from uncapped end-groups and loaded with recombinant insulin-like growth factor-I (IGF) released 100 % of their encapsulated drug in 30 days, while their capped counterpart released 80 % in the same duration. Release of vascular endothelial growth factor (VEGF) was 90 % in 32 days with uncapped PLGA while capped PLGA released 90 % in 41 days (Lam, et al., 2000). The burst release from capped PLGA is also much higher showing a 25 % increase for IGF and 15% increase for VEGF (Cleland, et al., 2001). Initial burst-release was higher in capped PLGA likely caused by less hydrogen-bonding between encapsulated drug and polymer during the initial release stage. In later stages, release was more rapid in uncapped PLGA, which is probably a result of its increased degradation rate (Lam, et al., 2000).

Microsphere Synthesis Technique

The standard manufacturing techniques to generate peptide loaded microspheres are water-in-oil-in-water double emulsion (W/O/W), oil-in-water (O/W) single emulsion, coacervation (oil-in-oil single emulsion), and spray drying. Each method can work with different polymer-peptide combinations. Spray drying, coacervation, and O/W emulsion generally begin by mixing the polymer and drug in the polymer solvent together. The drug can be in solid or aqueous form.

In O/W emulsion the drug is hydrophobic and soluble in the organic solvent, or the drug is processed in its crystallized form in such a way it can be easily dispersed in the organic solvent. The polymer (e.g., PLGA) is dispersed into a volatile organic solvent (e.g., dichloromethane (DCM)), and upon addition of this mixture to a water phase, under constant mixing, the organic phase partitions into small spheres surrounded by water. Over time the polymer dissolved in the organic solvent precipitates as the organic solvent evaporates. The resulting precipitate is polymer microspheres containing the drug that was dispersed in the organic solvent. During solvent evaporation the microspheres are usually stabilized with the amphiphlic surfactant polyvinyl alcohol that has been dispersed in the water phase. This method has poor drug encapsulation efficiency (EE) with water soluble drugs because they generally escape from the oil phase into the water phase during processing. Microspheres are collected after the organic solvent is evaporated.

In coacervation, a fourth component is added to the drug-polymer-organic solvent mixture. This fourth component is another organic solvent that is slowly added to precipitate the polymer from the initial organic solvent. This yields two phases, a supernatant without polymer or drug, and a second dispersed phase

containing polymer and drug. Upon homogenization these two phases generate microspheres that are stabilized by the addition of the microsphere solution to a final organic phase. This method has the advantage of being able to encapsulate hydrophilic drugs with high EE, because the primary oil phase is never subjected to a water phase. The drawback to this method is that the formed particles tend to aggregate and it is difficult to remove residual solvents from the microspheres (Takada, et al., 1995).

The W/O/W emulsion is similar to the O/W emulsion with the addition of a pre-emulsion step to add the drug to the organic phase (Figure 1.4). In this step, small volume of a water-drug mixture is added slowly to a polymer-organic solvent mixture followed by vigorous mixing. This forms the primary W/O emulsion that consists of hydrophilic drug in water droplets surrounded by an organic phase containing dissolved polymer. This W/O solution is added slowly to a second water phase with more mixing. In the second water phase polymer microspheres are formed that contain small droplets of water containing drug. This method is effective for encapsulation of hydrophilic drugs. However, it requires many steps with rigid temperate and viscosity controls (Takada, et al., 1995). A more detailed review of the three methods mentioned has been provided (Jain, 2000).

Spray drying involves the atomization of a polymer mixture into a stream of heated air. The polymer mixture contains polymer, drug (usually in solid form), and an organic solvent. Prior to spray atomization, the three components of this solution are mixed well. During atomization the organic solvent instantly evaporates and the microspheres are collected from the air in a cyclone separator. The advantages to this method are: the microsphere properties are not highly

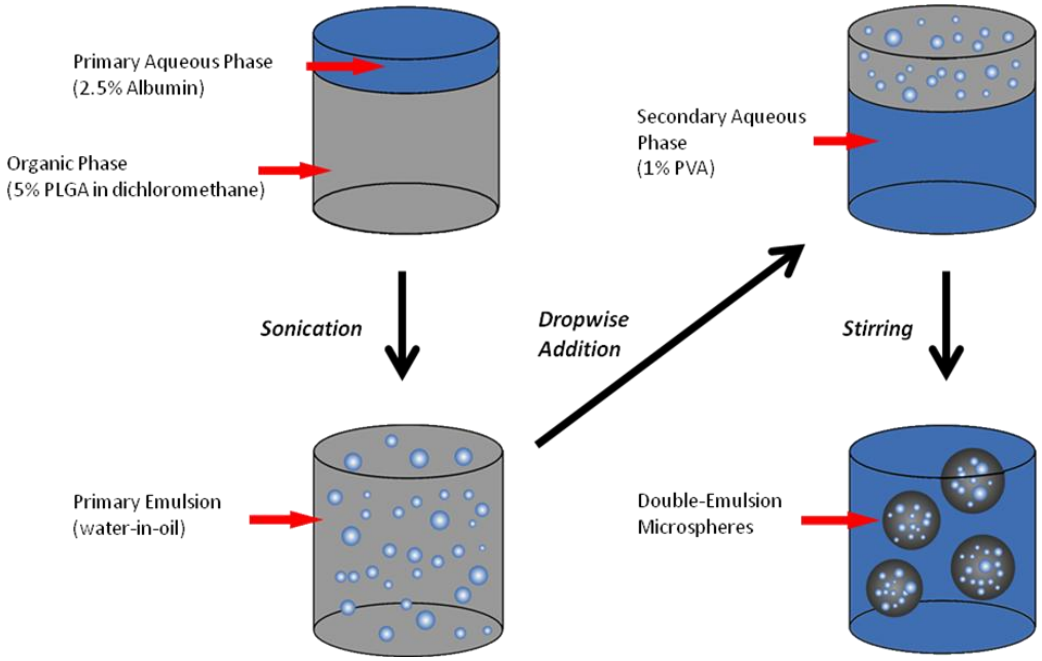

Figure 1.4 – The double emulsion (W/O/W) method of microsphere synthesis (See text for details).

dependent on strict polymer conformity, and drugs are not subjected to an oil-water interface. Disadvantages include high initial cost for both the atomizer and collection devices as well as the lyophilization equipment needed to pre-process the peptide. Furthermore, these particles are somewhat sensitive to aggregation (Sinha and Trehan, 2003). Our method of microencapsulation is the W/O/W method because of its relative ease in encapsulating proteins and peptides with high efficiency. When processing parameters are discussed in the remainder of this review, they are the parameters relevant to this method.

Internal Aqueous Phase Volume

The internal aqueous phase contains the peptide, water, and may contain other excipients such as sugars or ions. This phase will be dispersed into an emulsion contained by the organic phase. Therefore, it must be of considerably smaller volume (e.g., 1 – 10 % of the volume of the organic phase). In a W/O/W preparation for encapsulation of melittin in PLGA (9.5 kDa) where the internal aqueous phase volume was increased stepwise from 5 to 20 %, a decrease in microsphere size was observed by about 60 %. Conversely, melittin EE increased from 60 % to 80 %. This suggests that higher aqueous phase volume allowed these microspheres to be broken into smaller sizes during the second emulsion step. Furthermore, higher drug concentration in the aqueous phase leads to better retention of melittin during microsphere synthesis. The cumulative melittin release was affected very little, but rates increased slightly as the internal aqueous phase increased in volume (Cui, et al., 2005). In calcitonin loaded PLGA (M_w 12 kDa) microspheres prepared by W/O/W, an increase in internal aqueous phase from 10 % to 20 % slightly increased overall microsphere diameter. Using PLGA (M_w 30 kDa) size increased by almost 100 %. Burst-release was always higher in formulations with the highest internal aqueous phase (Diaz, et al., 1999). This

demonstrates increasing the internal aqueous phase volume leads to a change in both drug release and overall microsphere size.

In a review by Li et al. (2008) (Li, et al., 2008), the authors rationalize that during processing the main mechanism for loss of drug is the migration of internal water droplets to the second aqueous phase. Furthermore, microspheres with high drug loading must be more porous. This porosity is responsible for more loss of drug during processing as well as higher bust release during drug elution studies. Lastly, the maximum internal aqueous phase volume can be only about 50 % of the microsphere volume (Eq. 1). It is important to note that during the solvent evaporation process the microsphere volume decreases down to the volume of the polymer that was dissolved in the organic solvent while the internal aqueous phase volume remains nearly constant. Since the volume of internal aqueous phase remains the same, it is more important to consider the volume fraction of the polymer in the microsphere formulation than the volume of the organic solvent when estimating internal aqueous phase volume. Eq. 2 indicates the drug loading is highest when the water droplets of the primary emulsion are spaced as close together as possible, but do not combine into larger droplets. As we will come to find out it is difficult to control these last two parameters during microsphere synthesis. However, they do have an important impact on the drug release characteristics of proteins and peptides from microspheres.

$$N_d = \frac{\left(\frac{\pi}{6}\right) D_d^3}{L^3} \qquad \textbf{(Eq. 1)}$$

Equation 1 – Total drug loading in porous double-emulsion (W/O/W) polymer microparticles (Li, 2008). Assuming that the drops are homogeneously distributed and they are of equal size and distance from one another, the total drug loading Nd (%, v:v) is a function of the drop diameter (Dd) and the cubic space that circumscribes the drop of length L.

Amount of Drug Added to Microsphere Preparation

The amount of drug added to the internal aqueous phase will depend on the solubility of the drug in the water or buffer used. Increasing drug concentration will result in an increase in the quantity of drug loaded per volume of microspheres. While more drug is loaded in the microsphere this way, the efficiency of encapsulation tends to decrease. Furthermore, release during the initial burst release phase will increase owing to the increase in drug concentration within the microsphere. In melittin releasing microspheres generated from PLGA 50:50, increasing peptide concentration in the internal aqueous phase decreased the EE from 94 % with 3.2 % theoretical loading to EE of 80 % with 14.3 % theoretical drug loading. Higher drug loading also increased particle size (Cui, et al., 2005). Furthermore the burst-release increased with drug loading followed by only a minor decrease on the rate of release following the initial burst. It has also been reported that increasing cyclosporine-A loading from 2.5 % to 10 % increased burst release by 20 %, but had little effect on drug release after the initial burst release (Luan and Bodmeier, 2006).

Emulsification Method

There are two mixing steps in the W/O/W method of microencapsulation. The first emulsion is generated at a higher intensity of mixing compared to the second. This will ensure the water droplets contained within the organic phase are smaller than the organic phase droplets of the second emulsion. The emulsions can be created by mechanical stirring, sonication devices, and in some rare cases they spontaneously occur owing to the correct combination of surfactants and emulsion enhancers. The speed of stirring or intensity of sonication influences the size of the phase dispersed in the emulsion. It has been demonstrated that increasing the intensity of emulsification of the first emulsion step results in microspheres with an internal morphology composed of a higher

number of smaller and more densely packed pores (Ehtezazi, et al., 1999). This research was performed in the absence of drug loading and the authors conclude that the internal pore structure is predictable based on the Saltykov unfolding method.

In vortex mixing, high shear stress and turbulent flow characterized by high Reynold's number separates the bi-phasic mixture into smaller dimensions. In the laboratory environment a bench-top vortex mixer is often employed. The intensity of vortex mixing is low and often does not generate emulsion droplets in the desired size range. For this reason sonication devices are commonly applied during the primary emulsion step. The energy from an ultrasonic probe causes intense mixing that creates small emulsion droplets. This emulsion is more stable than emulsions created by vortex mixing. The disadvantage of sonication is in the mechanism of sonic irradiation. During irradiation with ultrasound, acoustic cavitations occur. Cavitation is the formation, growth, and implosive collapse of bubbles irradiated with sound (Leighton, 1994). The compression of the bubbles during cavitation is more rapid than thermal transport, which generates a short-lived localized hot-spot. Experimental results have shown that these bubbles have temperatures around 5000 Kelvin (K), pressures of roughly 1000 atm, and heating and cooling rates above 1010 K/s (Flint and Suslick, 1991; Suslick, et al., 1986). These cavitations can create extreme physical and chemical conditions in otherwise cold liquids.

The repercussion of this type of mixing is the potential for disruption of the chemical structure of the molecules being sonicated. Intra- and inter-molecular interactions are being broken which could lead to destruction of the secondary structure molecules in the emulsion. This can be particularly damaging to the encapsulation of biological molecules such as proteins or peptides. With

the unfolding of large and structured molecules such a protein, the hydrophobic residues are exposed which can lead to aggregation of molecules (e.g., protein-protein or protein-polymer) causing a deactivation of the protein's function or precipitation of protein from solution. This unfolding can also cause proteins to become trapped at the O/W interface. It is possible that these proteins can be salvaged because the organic solvent is eventually extracted from the system, however it will depend on the thermodynamics of protein re-folding. This could be complicated by the presence of other molecules in the formulation. In general, long chain polypeptides, such as proteins, are unlikely to spontaneously refold into their native conformation while peptides in some cases can successfully re-fold spontaneously in solution.

While the energy of the first emulsion affects internal morphology, the second emulsion energy affects microsphere diameter. In a comparison study where all other variables remained constant, PLGA microspheres loaded with BSA could be generated at sizes of 20 to 50 μm with mechanical stirring of the second emulsion at 700 rpm, or sizes less than 1.0 μm using sonication. The release rates for the sonicated microspheres were greater compared to the stirred particles (Ruan, et al., 2002). Similarly, it has been reported that increasing the stirring speed of the second emulsion from 800 to 1,200 rpm decreased particle size from 55 to 25 μm. In the same study homogenization at 20,000 rpm decreased the size further to less than 10 μm. Protein loading efficiency of human serum albumin (HSA) decreased 5 % and 10 % as mixing speeds increased from 800 to 1,200 rpm (Wei, et al., 2004).

It is desirable to generate microspheres within a stringent size range for both ease of delivery and retention at the site of injection. To be formulated as an injectable, the microspheres should be less than the diameter of a 24 G needle.

The smallest commercially available needle is 33 G and has an inner diameter of 89 μm while a 24 G needle has an inner diameter of 292 μm. Testimony from our supervising cardiothoracic surgeon suggests that a 24 G needle is at the upper size limit of acceptable direct myocardial injection (J. Michael DiMaio, personal communication, January, 2010). This number indicates a pragmatic upper limit of diameter to be less than the internal diameter of.

Localization of the injectate for cardiac applications requires that the microspheres be larger than the capillaries of the myocardium so they will not be swept away by local circulation. One of the standard methods for determination of regional blood flow in organs is perfusion of that organ with radiolabeled microspheres of uniform size. In this method microspheres are trapped by the small capillaries of the tissue giving information on the smallest diameters of these micro-vessels. Intravascular perfusion of radiolabeled microspheres in the excised dog or cat heart showed complete retention of microspheres at the size range of 14.6 μm and diminishing retention as this size decreased, indicating that the smallest capillaries in the heart are between 8.6 and 14.6 μm (Hof, et al., 1981). We can assume retention of microspheres injected directly into the myocardium will occur with better certainty when their diameters are greater than 15 μm. One simple method we employed to ensure our PLGA microsphere formulation does not contain particles below this specific size range was to wash the final microsphere preparation over a sieve of specific pore dimensions.

An equation for prediction of the size of microspheres created from an emulsion process has been proposed (Eq. 2) (Li, et al., 2008). This equation is based on the maximum diameter of a drop (d_{32}) the diameter of the agitator (D, meters), the density of the continuous phase (ρc, kg/m^3), the agitation rate (N, turns/s), the interfacial tension between the dispersed phase and the continuous

phase (σ, N/m), the constant (c_5), the volume fraction of the dispersed phase to the continuous phase (Φ), and their viscosity ratio (η_c/η_d). These types of equations are useful for estimating the mixing intensity necessary to generate microspheres in the correct size range given the solution parameters of the microsphere formulation.

$$\frac{d_{32}}{D} = c_5 \Phi \left(\frac{\rho_c N^2 D^3}{\sigma}\right)^{-3/5} \left(\frac{\eta_d}{\eta_c}\right)^{0.25} \quad \textbf{(eq. 2)}$$

Equation 2 – prediction of microsphere size (Li, et al., 2008).

Concentration of Polymer in Organic Phase

The concentration of polymer in the organic phase is another aspect of the W/O/W emulsion technique that can be altered that affects drug encapsulation and release. The increase in polymer concentration usually results in a decrease in the burst release of microspheres. The burst release decreased in melittin loaded microspheres from 50 to 20 % as polymer concentration increased from 3.75 to 15 % in the organic phase, but did not affect the length of time to total peptide release. EE decreased with increasing PLGA concentration, and microsphere size increased with increasing PLGA concentration slightly (Cui, et al., 2005). Similar results were found for BSA loaded PLGA microspheres with increasing PLGA in the organic phase. The only difference was that release durations were longer in higher PLGA concentrations and increasing polymer concentration increased EE (Yang, et al., 2001).

Stabilizer Concentration

Poly(vinyl alcohol) (PVA) is used to stabilize particles generated during the second emulsion step in concentrations typically between 0.5% and 5%. Higher PVA concentrations tend to decreased particle size by 50% or more. Researchers have found that the protein BSA and peptides parathyroid hormone (PTH) and melittin have higher encapsulation efficiencies as PVA increases with little effect on drug release rates (Cui, et al., 2005; Wei, et al., 2004).

Additives

Lastly, there have been numerous studies on additives to the microsphere formulation that include surfactants, ions, and polymer blends, to name a few. The addition of surfactants to the internal aqueous phase is thought to stabilize the loaded peptide from adverse chemical reactions and denaturation. Here the addition of surfactants on release rate will be discussed. Some of the surfactants used in conjunction with PLGA W/O/W microspheres were poloxamer 188, polysorbate 20 (Tween 20), or sorbitan monooleate 80 (Span 80). In a study involving the encapsulation, storage, and release of insulin from PLGA microspheres it was found that surfactants decreased the microsphere mean diameter and altered their spherical morphology (Rosa, et al., 2000). They also increased insulin release and reduced EE in a concentration dependent manner. This group favored polysorbate 20 at 3% (w:v) for insulin controlled release based on encapsulation efficiency and data involving insulin storage and chemical reactions in the microspheres.

Similar to surfactants, co-encapsulation with sugars, PEG, vitamins, or other peptides is performed to improve drug stability. Their effect on drug release is discussed in this section. IGF was co-encapsulated with albumin, succinylated gelatin, or PEG and addition of these substances blunted burst release except

when albumin and gelatin were used together (Meinel, et al., 2001). The addition of NaCl to the dispersing phase of the W/O/W emulsion was studied in NGF loaded microspheres. It was shown to markedly reduce burst release, along with microsphere size. However, the NaCl also induced a pronounced NGF denaturation (Pean, et al., 1998). The difficulties in detecting NGF were circumvented by using ^{125}I iodinated NGF. Denatured NGF was accounted for as the difference in released ^{125}I-NGF and ELISA detectable NGF. In HSA loaded PLGA microspheres, addition of a small amount of vitamin E dramatically increased burst release, while large amounts of vitamin E dramatically decreased burst release. Adding PEG slightly lowered burst release. Finally, the addition of organic solvents such as acetone or ethyl acetate to the DCM increased particle size (Ruan, et al., 2002).

The diblock copolymer p(PEG:Histidine) plays an interesting role in stabilizing encapsulated proteins. The R-group of histidine becomes protonated at pH lower than approx. 6, which occurs in degrading PLGA microspheres. The positively charged hisitdine blocks of this co-polymer interact with encapsulated proteins, protecting them from denaturation. As the p(PEG:Histidine)-protein complexes diffuse from the microsphere and enter physiologic pH 7.4, histidine R-groups return to neutral charge and release their complexed protein. As additives, this copolymer also affects protein release kinetics. BSA was encapsulated in PLGA microspheres blended with p(PEG:Histidine) in order to maintain protein secondary structure (Kim, et al., 2005). This blend increased release rate and burst release of the microspheres. While increasing the PEG:Histidine ratio of p(PEG:Histidine) decreased release rate and burst release. The addition of p(PEG:Histidine) increased EE and particle size, and microsphere degradation occurred faster with the blend of p(PEG:Histidine).

In another article recombinant human growth hormone (GH) was stabilized with the addition of pluronic F127 or sucrose. The addition of pluronic alone or pluronic and sucrose increased release rate and burst release. Furthermore, pluronic decreased EE while addition of pluronic plus sucrose did not affect EE (Wei, et al., 2007).

PRIMARY EMULSION STABILITY

Primary Emulsions in the W/O/W Technique

The primary emulsion is the first step in generation of double-emulsion microspheres. The emulsion is generated by the mixing of water (the dispersed phase) into a larger organic phase (the continuous phase). In the case of the double-emulsion microspheres generated in this study, the water phase contains our water soluble protein or peptide while the organic phase contains the degradable polymer PLGA. Once the emulsion is generated by adding energy in the form of mixing or sonication tiny water droplets are dispersed in the organic phase. These droplets are thermodynamically unstable and over time tend to rise to the surface of the organic phase (creaming) where they aggregate and combine into larger droplets. If the system is left unperturbed for a long period of time the water and organic phase separate completely, called phase separation (Figure 1.5).

In the emulsions prepared for our double-emulsion microspheres, the route of breakdown occurs by creaming. This can be detected by observing the turbid layer of emulsion rise to the surface of a sealed cuvette (Figure 1.6). It is also important to note that our ability to see the emulsion layer is evidence that the water droplets in the emulsion are on the larger scale of the colloid range (> 500 nm).

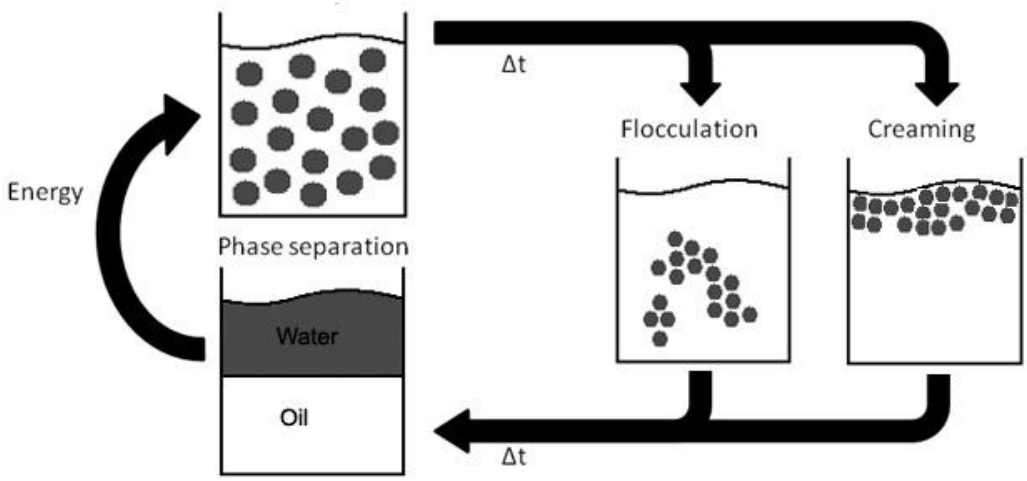

Figure 1.5 – Breakdown of an emulsion over time by the flocculation and creaming pathways.

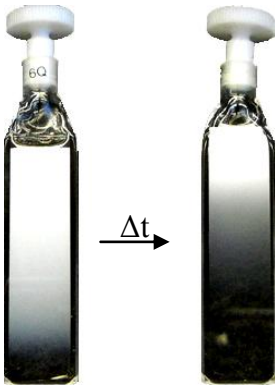

Figure 1.6 – Turbidity of the primary emulsion as it changes over time. The "white" layer depicts water droplets rise under the influence of gravity due to the density difference with the organic phase.

The importance of primary emulsion characterization is its connection to the internal and external morphology of the resulting microspheres. The size of the primary emulsion droplets dictate the size of the internal porosity of the final microspheres. Once the primary emulsion is generated it is then transferred to a second water phase where the microspheres are formed. During formation of microspheres, the volatile organic phase slowly evaporates over a period of approximately six hours. While the organic solvent is extracted, the water droplets of the internal aqueous phase are free to travel throughout the organic solvent. During this process the polymer-DCM solution becomes increasingly viscous. This rise in viscosity is what suspends movement of the water droplets dispersed in the organic phase.

Any length of time between emulsion generation and suspension of internal water droplet movement (solvent extraction) is time for the primary emulsion droplets to interact with each other or the second aqueous phase. Interaction between primary emulsion droplets can lead to aggregation and coalescence resulting in large internal porosity inside the final microspheres. In extreme cases, large porosity may include pores with radius half the diameter of the microsphere or even larger. Interaction of the primary emulsion droplets and the secondary aqueous phase results in loss of drug from the microspheres during their formation.

When microsphere internal porosity is large, drug diffusion from the microsphere is uninhibited. Our study with albumin demonstrates increasing internal porosity results in greater burst-release of protein from the microspheres. This is consistent with the non-uniform degradation of microspheres where the initial drug release is dependent on initial microsphere morphology, while late

stage release is blunted by the formation of a shell of PLGA around the exterior that inhibits drug release until its breakdown.

Application of Emulsion Theory to W/O/W Primary Emulsions

The hypothesis that generating more stable primary emulsions containing smaller water droplets would reduce drug release kinetics from PLGA microspheres was tested. In order to alter the rate of primary emulsion breakdown we added surfactants to the continuous phase of the primary emulsion. We chose alkyl glucosides as the surfactants in this work (Ch. 2, Table 2.1). These non-ionic surfactants were chosen for their non-toxic nature, ability to dissolve in DCM, and their wide range of hydrophilic-lipophilic balance (HLB) numbers.

HLB number is used to characterize the solubility of a surfactant in aqueous or organic solvents. It was first characterized by Griffin in 1954 and later revised by Davies in 1957 (Davies, 1957; Griffin, 1954). The advantage of the second method is that it could be applied to specific chemical groups. Lower HLB numbers represent surfactants that are soluble in organic phases while higher numbers represent surfactants soluble in aqueous phases. These numbers have been applied to their effectiveness as emulsification enhancers. Non-ionic surfactants with values from 7 to 11 are typically good W/O emulsifiers while values from 12 to 16 correspond to good O/W emulsifying agents. This is consistent with the rule of thumb that a surfactant should be selected by its ability to be dispersed in the continuous phase of the emulsion.

Surfactants aid in both the generation of an emulsion as well as in the prevention of its breakdown. Surfactants orient themselves at the interface

between two immiscible layers, in this case between the water and organic solvents. They are organized at this surface in a single layer with a specific configuration such that their polar groups are facing the aqueous phase and their alkyl chains are facing the organic phase. This specific molecular orientation was described in a paper by Irving Langmuir in 1917 and his work in this field resulted in him being awarded the Nobel Prize in 1932 (Langmuir, 1917). The organization of surfactant at the interface occurs spontaneously, lowers surface tension, and increases the surface viscosity. These properties play an important role in emulsion generation and stability. Emulsification is a complex process that involves large droplets being broken down into smaller droplets by shearing, necking which causes elongation, and eventually separation into discrete droplets. The reduction of the surface tension of the water phase caused by addition of surfactants allows for the stabilization of smaller water droplets and a much larger W/O interfacial surface area.

Surfactants also aid in increasing the emulsions resistance to break-down. In order to understand this role it is important to define emulsion stability and describe the forces involved in this process for our W/O system. For a more in-depth reading of the following discussion the reader is referred to Hiemenez & Rajagopalan (Hiemenez and Rajagopalan, 1997).

We define emulsion stability as the resistance of the dispersed particles in the emulsion to coagulation. Coagulation is the process in which individual droplets of the dispersed phase come together with one or more droplets to a point where a group of droplets act as a single unit. The stability of a colloid (i.e., its resistance to coagulation) is determined by thermodynamic and kinetic effects. At a macroscopic scale, thermodynamic considerations determine the equilibrium state of the emulsion while kinetics determine how quickly that state is achieved.

Taking into account that our W/O emulsion is unstable, these two properties of the system play an important role in emulsion breakdown. Kinetics is a result of flow and buoyancy of the water droplets in our system. Thermodynamic forces include attractive van der Waals forces, repulsive electrostatic forces, and steric interaction of molecules adsorbed at the water droplet surface. As a result of the size of the water droplets in the system (approx. 1.5 μm), we can ignore the effects of diffusion. Therefore, droplet-droplet interaction is mainly the result of kinetic forces. For instance, in an undisturbed emulsion, creaming of the dispersed phase as a result of buoyant forces causes droplets to aggregate at the emulsion's surface. Also, during preparation of double-emulsion microspheres there is a considerable movement of the water droplets in the organic phase because of the constant mixing of the microsphere solution during solvent extraction process.

Therefore, there must be a repulsive force that provides resistance to coagulation and nucleation of droplets. We know this, because despite considerable bumping together of water droplets, the emulsion does not break-down before the solvent extraction step in microsphere synthesis is complete. Furthermore, emulsions that consist simply of water as the dispersed phase and DCM + 9 % PLGA as the continuous phase break-down almost instantaneously (Nihant, et al., 1994). When molecules are added, the rate of phase separation occurs much more slowly. Small amounts of BSA added to the inner aqueous phase decrease the time to complete phase separation to approximately 3 days, showing that a small amount of amphipathic polymer added to the system causes a dramatic resistance to coagulation. Since the continuous phase of the emulsion is an organic solvent, it is unlikely that an ion atmosphere surrounding the water droplets is present and capable of generating electrostatic resistance. Instead the

presence of protein and surfactant molecules adsorbed to the W/O interface causes the resistance to water droplet coalesence.

As an example, we will consider a water-in-oil emulsion with a non-ionic polymer in the dispersed phase as a stabilizing agent. The non-ionic polymer is found adsorbed at the surface of the water droplets. As the distance between two water surfaces separated by the organic phase decreases, the molecules adsorbed at the surface begin to overlap. The crowding of molecules in the overlapping region provides a stabilizing effect, called steric stabilization. These overlapping polymer chains cause an increase in the Gibbs free energy (ΔG) during coagulation. The degree to which the polymer coats the W/O interface is important and depends on the concentration of polymer in the system. At low polymer concentration, aggregation of emulsion droplets can be induced. As polymer concentration increases a stabilizing effect against aggregation is generated.

This stabilizing effect can be described in a thermodynamic sense. When polymer chains are freely dangling from the surface of the water droplet, the loose ends are free to move in the solvent. When the chains from one droplet come in contact with the chains adsorbed to the surface of another droplet, there is a restriction of movement of the free ends of the polymer chains. This restriction of movement is thermodynamically unfavorable and causes repulsion between the droplet surfaces. Characterization of this interaction is made troublesome by the chemical make-up of specific polymers with differing polymer-polymer interactions. Therefore, it is difficult to quantify these interactions; however it is evident that a ‘good’ solvent of the polymer is necessary to maintain a positive ΔG during particle-particle interaction. The net repulsive force is maintained in a

'good' solvent by reason of favorable polymer-solvent interactions and unfavorable polymer-polymer interactions.

Surfactant hydrocarbon tails protruding into the organic phase from the water droplets will act in a similar manner as adsorbed polymer on the surface (Figure 1.7). The surface should be completely covered with surfactant to prevent them from being pushed out of the way during droplet interaction.

As we have described, there are many forces involved in emulsion stability. The direct measurements of which are very difficult to perform. Therefore, we are charged with determining a method to characterize our emulsions on a macroscopic scale that will provide evidence to compare emulsion stability between formulations. By reason of the size of our emulsion droplets we can consider to things, the diffusion of water droplets is negligible, and the buoyant force is large enough to determine the rate of creaming, which is the initial route of destabilization for this particular W/O emulsion. In addition, the rate of creaming is related to the size of the dispersed water droplets which is also important in generating microsphere internal porosity.

According to Stokes' law (Eq. 3) as a particle, or water droplet in our case, moves through a fluid, the fluid exerts a resistant force on the particle in the opposite direction.

$$\mathbf{F} = 6\pi\eta R_s\mathbf{v} \qquad \textbf{(Eq. 3)}$$

Equation 3 – Stokes' law written as the force acting in resistance to the movement of a spherical particle through a fluid. Force (**F**) and velocity (**v**) are vectors. $6\pi\eta R_s$ is the friction factor for a spherical particle (R_s is the radius of the sphere). η is the dynamic viscosity.

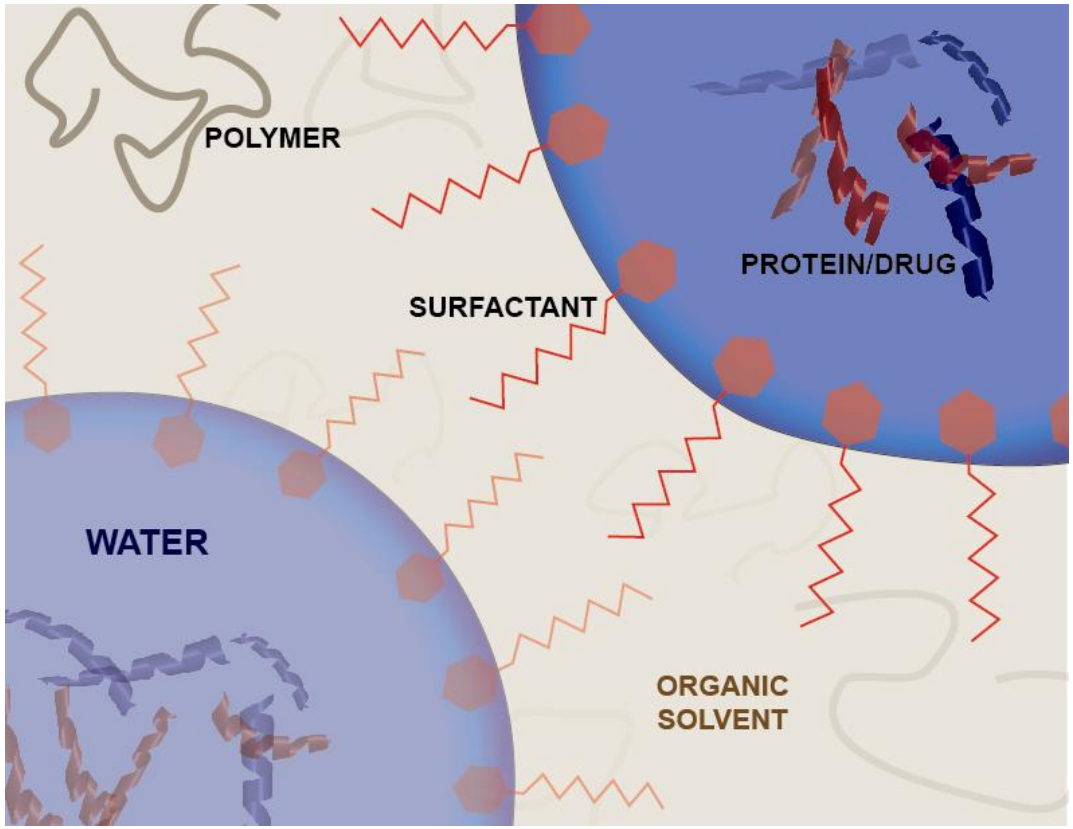

Figure 1.7 – Depiction of molecular orientation in the primary emulsion during microsphere synthesis. Alignment of surfactant and polymer molecules on the surface of the water droplets plays an important role in stabilizing the droplets from coagulation (image by Kristin Yang).

An object that moves through a fluid is subject to gravitational force buyout force, and a viscous force. Stokes Law, Eq. 3, shows that as an object moves through a fluid there is a frictional force exerted on the object by the fluid that resists the motion of the object. As the velocity of the object increases, the resistant force increases until these forces balance and the particle reaches a steady state velocity. This force is directly proportional to the radius and velocity of the sphere, and the viscosity of the fluid. We can solve this equation for a spherical particle to relate the velocity of the particle to the particles radius (Eq. 4; see Hiemenez & Rajogopalan, 1997)

$$R_s = \left(\frac{9\eta v}{2(\rho_2 - \rho_1)g}\right)^{1/2} \qquad \textbf{(Eq. 4)}$$

Eq. 4 gives the radius of a spherical particle (R_s) traveling in a fluid with viscosity (η) in normal gravity (g) at steady state velocity (v) where the difference in density between the particle and the fluid are given as $\Delta\rho$. It is evident from this equation that particles that travel faster have larger radii.

For the sake of estimation if we assume that the water droplets in our primary emulsion are spherical and act independently we can estimate the radius of droplets from the emulsion analysis presented in Ch. 2. In this experiment a spectrophotometer is used to measure rate of water droplet creaming in a W/O emulsion. Initially, the water droplets are evenly dispersed throughout the cuvette. Light passes through a point centered 15 mm above the base of the cuvette. Initially, the turbid emulsion scatters much of the light that passes though the cuvette. This is indicated by the spectrophotometer detecting a high amount of absorbance by the emulsion. Over time the water droplets cream and

rise to the surface. As more droplets rise, less light is scattered and absorbance readings decrease. The change in absorbance results from larger droplets creaming out of the emulsion while smaller water droplets remain at the measurement point 15 mm from the bottom of the cuvette. At any given time in this experiment, we know that the largest droplets contained between the base of the cuvette and the point of measurement (15 mm) have velocities less than or equal to a droplet that traveled at a rate equal to 15 mm x time.

If we take the emulsions after being subject to 28 x gravity for 720 seconds and apply Eq. 4, we can calculate the droplets in the path of the light beam are ≤ 1.23 μm in diameter (calculation in Appendix B). This assumes that the density and viscosity of the organic phase (DCM) and the water phase are not affected by any other additives. The gravitational force provided by the centrifuge is considered to be constant throughout the experiment. Lastly, any molecule adsorbed to the surface of the water droplets does not affect the movement of the water droplets. This estimation of droplet radius is near the size of the smaller internal pores of the microspheres as seen by transmission electron microscopy (TEM) (Figure 2.6).

We are limited by this analysis in that we can only compare the change in emulsion turbidity over time between similar emulsions. We can also estimate the size of the droplets that have not yet creamed out of the emulsion at a specific timepoint. The decrease in absorbance between two time points results from water droplets of a specific velocity (and therefore radius) completely creaming out of the emulsion. However, we cannot accurately estimate the distribution of water droplets contained within the emulsion. This would require that the absorbance values we collect using the spectrophotometer be the result of water droplets absorbing light. This is not the case, because the water droplets scatter

the 720 nm light passing through the emulsion. Light scattering does not directly correlate to droplet density owing to the properties of our system that influence light scattering. These include water droplet concentration and water droplet size. In an emulsion with a high concentration of water droplets, such as ours, light that passes through is scattered many times by the sample before leaving the cuvette. The probability of light scattering multiple times decreases as the concentration of water droplets decreases. A second event that complicates the correlation of absorbance values to the droplet distribution is that different droplet sizes do not scatter light in the same way. Droplets smaller than the wavelength of light, 720 nm, cause very little scattering compared to droplets larger than this wavelength. For this reason very small droplets are underrepresented by this analysis even if they make-up a large portion of the emulsion. Similarly, large droplets with less curvature at their surface may allow light to pass through with minimal scattering.

In summary, the size of the water droplets in the primary emulsion determines the size of the pores within the final microspheres. The size of these droplets is affected by the energy of emulsion, addition of surfactants, and the rate of emulsion breakdown. Addition of surface active molecules, such as amphiphilic polymers or surfactants to W/O emulsions improves emulsion stability by preventing rapid coagulation of water droplets. This increase in stability is attributed to a thermodynamic resistance that occurs when two surfaces with adsorbed polymers or surfactants come in contact. These parameters are difficult to measure directly; therefore we implemented an analysis of the rate of emulsion creaming to determine emulsion stability. Stokes' law gives a physical basis for the estimation of emulsion stability by the creaming method. Through this law we can interpret the size of the droplets passing through the light beam in the spectrophotometer depend on the duration the emulsion has spent in a

gravitational field. More rapid decrease from the initial absorbance reading is associated with a higher concentration of large droplets in the emulsion.

DELIVERY OF THYMOSIN BETA-4 TO THE HEART

TB4's Role in Ischemic Heart Disease

Heart disease is remains the most common cause of death for both men and women in the U.S (Roger, et al., 2011). A new paradigm for treatment is the regeneration of the ischemic myocardium by molecules that promote myocyte survival or induce the formation of new blood vessels in the heart. One such molecule that has become a principal candidate to treat myocardial infarction is TB4. TB4 is a 43 amino acid peptide originally isolated from the thymus in 1981 (Low, et al., 1981). It is one of a group of 16 peptides that share a high degree of conservation in their sequences and are expressed in many tissues throughout the body (Huff, et al., 2001). TB4 is a strong regulator of actin polymerization and is also a g-actin sequestering peptide in the cytoplasm (Cassimeris, et al., 1992; Sanders, et al., 1992).

TB4 is known to be involved in many processes including angiogenesis, dermal and corneal wound healing, and transition of cancers to a malignant stage. The process of new blood vessel formation is important to the growth of new tissues, wound healing, as well as cancer malignancy. Evidence for the involvement of TB4 in angiogenesis was determined by the significant increase in TB4 mRNA expression levels in endothelial cells during the process of tube formation *in vitro* (Grant, et al., 1995). Addition of TB4 to endothelial cells *in vitro* and *in vivo* demonstrates an increase in cell migration as well as nascent blood vessel formation, respectively. This effect is demonstrated at ng concentrations of exogenously administered TB4. TB4 promotes corneal wound

healing by endothelial cell migration and modulation of anti-inflammatory pathways (Sosne, et al., 2001). In dermal injuries, the administration of very small concentration of TB4 has been shown to accelerate wound healing (Malinda, et al., 1999). This involvement is useful in the repair of diabetic ulcers (Philp, et al., 2003).

Cancer metastasis presents a challenging problem with the administration of TB4 to promote tissue regeneration. Over expression of the TB4 gene is associated with metastasis in colon cancer (Wang, et al., 2004). There is also evidence that supports the involvement of TB4 in metastasis of fibrosarcoma, a cancer originating in the bone (Kobayashi, et al., 2002). The mechanism for this activity was shown to be induction of cell migration and activation of angiogenesis (Cha, et al., 2003). These adverse effects of TB4 are expected to be avoided by local delivery to the myocardium through direct injection of TB4 bearing polymer microspheres. The localization of the dose to the heart is important to avoid multiple systemic dosing at high concentration necessary for intracoronary administration (Freedman and Isner, 2001).

At present, the cellular mechanism through which TB4 acts to increase cell migration, angiogenesis, and wound healing is not well described. For many years TB4 was speculated to induce angiogenesis through a discrete pathway involving a unique cell surface receptor. A recent paper using human vein endothelial cells (HUVECs) suggests that extracellular binding of TB4 to the β subunit of ATP synthase is responsible for induction of cell migration (Freeman, et al., 2011).

TB4 was recently shown to have beneficial effects on cardiac cell survival and function in mice after heart attack (Bock-Marquette, et al., 2004; Srivastava,

et al., 2007). TB4 also participates in coronary artery development, stimulates migration of embryonic epicardial cells, and causes thickening of the adult mouse epicardium. This evidence, along with continuing experiments in our lab generously support the hypothesis that TB4 also stimulates neovascularization in the ischemic adult myocardium (Bock-Marquette, et al., 2009). This list of TB4's beneficial effects provides a strong argument for its clinical use which has been explored by the company RegenRx. Like many peptides, the structure and function of TB4 make it especially difficult to administer, therefore attention to effective drug delivery is necessary for TB4 to have success in clinical trials.

Chemical Characterization of TB4

TB4 is a water soluble 43 amino acid peptide. It has M_w of 4963.5 Da, and an isoelectric point of 5.1. The sequence of TB4 (*Homo sapiens*) is as follows:

[Ac-**S**-**D**-**K**-**P**- -**D**-**M**-**A**-**E**- -**I**-**E**-**K**-**F**- -**D**-**K**-**S**-**K**- -**L**-**K**-**K**-**T**- -**E**-**T**-**Q**-**E**-
-**K**-**N**-**P**-**L**- -**P**-**S**-**K**-**E**- -**T**-**I**-**E**-**Q**- -**E**-**K**-**Q**-**A**- -**G**-**E**-**S**-COOH]

The N-terminus contains an acetylserine (ac-S). TB4 is a short peptide of typical hormone length. It has no disulfide bonds or tertiary structure (Figure 1.8). An important physical characteristic is that it is extremely hydrophilic. There are two regions of TB4, residues 4-12 and 32-40, which were identified to contain high alpha-helical potential (Low and Goldstein, 1982).

To determine the water solubility of TB4 we evaluated the hydrophobic and hydrophilic nature of the molecule based on its amino acid sequence. A hydropathy plot is used for this assessment. In a hydropathy plot, each amino-acid is ranked based on the hydrophobicity or hydrophilicity of the R-group. A number of different scales are used for ranking, but the most common is the scale developed by Kyte and Doolittle (Kyte and Doolittle, 1982). A plot of the ranked

amino acid sequence is used to predict the solubility of different regions of the amino acid sequence. Using the Kyte and Doolittle index, we generated a TB4 hydropathy plot (Figure 1.9) showing the maximum score to be 0.014, and the minimum score as -2.886 with almost all residues scoring in the negative region. The negative regions of TB4 are consistent with hydrophilic peptide segments and the positive regions indicate hydrophobicity.

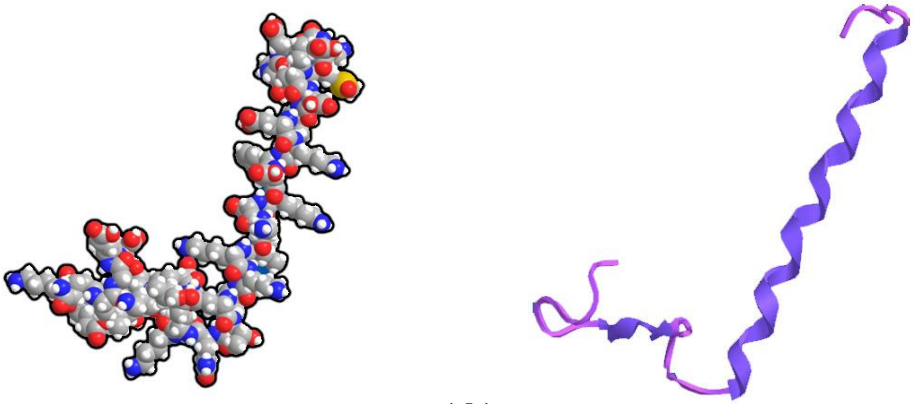

(A) **(B)**

Figure 1.8 – (A) Space filling and (B) ribbon model of TB4 generated from primary sequence using ChemBioOffice Ultra software.

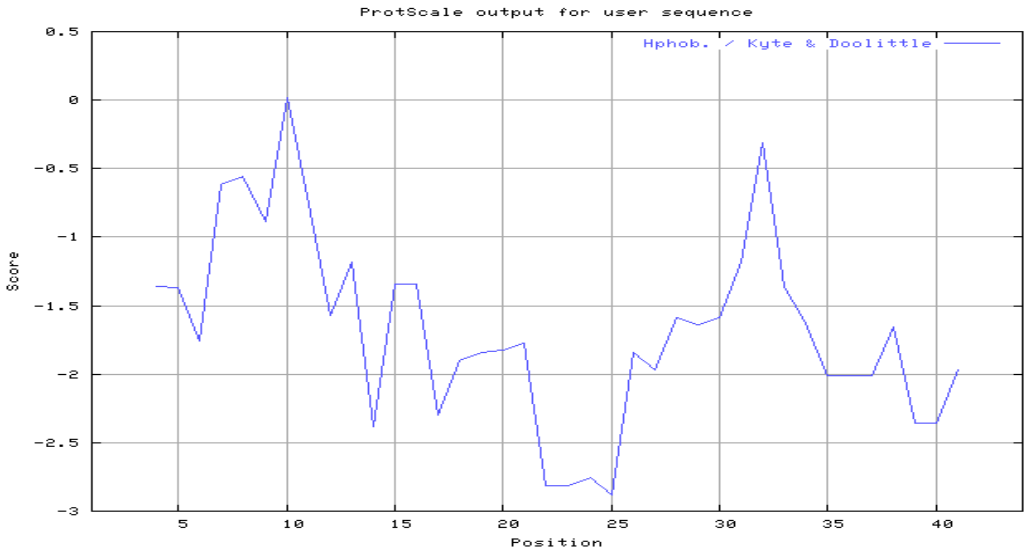

Figure 1.9 – TB4 hydropathy plot using linear weight variation model window size 7, and Kyte and Doolittle amino acid residue index. The maximum score is 0.014, and the minimum score is -2.886. TB4 residues are mostly in the negative score demonstrating the very hydrophilic nature of this peptide [from: http://expasy.org/tools/protscale.html].

***Peptide Delivery to the Ischemic Myocardi*um**

Previous failures with therapeutic peptides underline the importance of developing a drug delivery system for TB4. Many attempts to deliver peptides and proteins to the heart in humans and large animals revealed that peptides do not have significant effects when delivered intravascular owing to short serum half-life, poor tissue uptake, and systemic side effects (Aiello, et al., 1994; Cooper, et al., 2001; Jain, et al., 2007; Laham, et al., 2005; Lazarous, et al., 1997; Lucerna, et al., 2007; Virmani, et al., 2005). Furthermore, TB4 has been associated with cancer metastasis, such that a high systemic dose may lead to undesirable development of occult neoplasms (Kobayashi, et al., 2002; Wang, et al., 2004; Yamamoto, et al., 1993). More successful attempts to deliver peptides to treat heart disease have been performed by direct myocardial injection; however this procedure is difficult and invasive in nature and therefore unlikely to be acceptable for multiple dosing regimens (Fuchs, et al., 2003; Grossman, et al., 2002; Hamano, et al., 2001; Hofmann, et al., 2005; Penicka, et al., 2005; Perin, et al., 2003; Stamm, et al., 2003; Tse, et al., 2003).

Controlled release drug delivery systems including polymer implants, microspheres, nanoparticles, and liposomes offer characteristics beneficial to peptide delivery. They provide: fewer interventions, improved patient compliance, are simple to implant, protect their payload from systemic exposure and degradation. These types of improvements to peptide delivery will likely be the key to realizing future therapy involving TB4. This underlines the benefit of developing a controlled drug delivery system customized to TB4's molecular composition and biological effects.

Location of TB4 Delivery to the Heart

The preferential location of delivery of TB4 to the heart is dependent on the cells in which TB4 promotes its therapeutic effects as well as the pathological process of myocardial infarction (MI). Previously, we mentioned that TB4 has effects on the cardiomyotyes in the ischemic region of the heart as well as the epicardial cells surrounding the heart. In order to gain full efficacy of TB4 we must localized the molecule in the ischemic region of the heart. In order to determine this region, the anatomical changes in the heart resulting from myocardial infarction will be discussed.

MI typically results from the blockage of a coronary artery where the severity of tissue damage depends on the length of time the heart goes without blood supply. Studies in the canine heart were performed by temporarily or permanently occluding the left circumflex coronary artery to define the pattern and location of MI (Reimer and Jennings, 1979; Reimer, et al., 1977). The progression of MI occurs in what is described as a "wavefront" pattern (Figure 1.10). The shortest ischemic durations, 20 – 40 min of total arterial occlusion followed by reperfusion, cause only subendocardial tissue damage (infarction) that may involve one of the two papillary muscles. As ischemic times increase to 3.0 hrs, the MI extends to the middle myocardium and eventually to the subepicardium. Permanent occlusion results in a transmural infarct (i.e., full thickness necrosis) with only minor subepicardial tissue sparing.

There are two reasons for this pattern of tissue sparing. During systole, intramyocardial tension is highest in the subendocardial myocardium and limits perfusion to this zone relative to subepicardial myocardium. Also, collateral circulation is present in the subepicardial tissue, because neighboring coronary

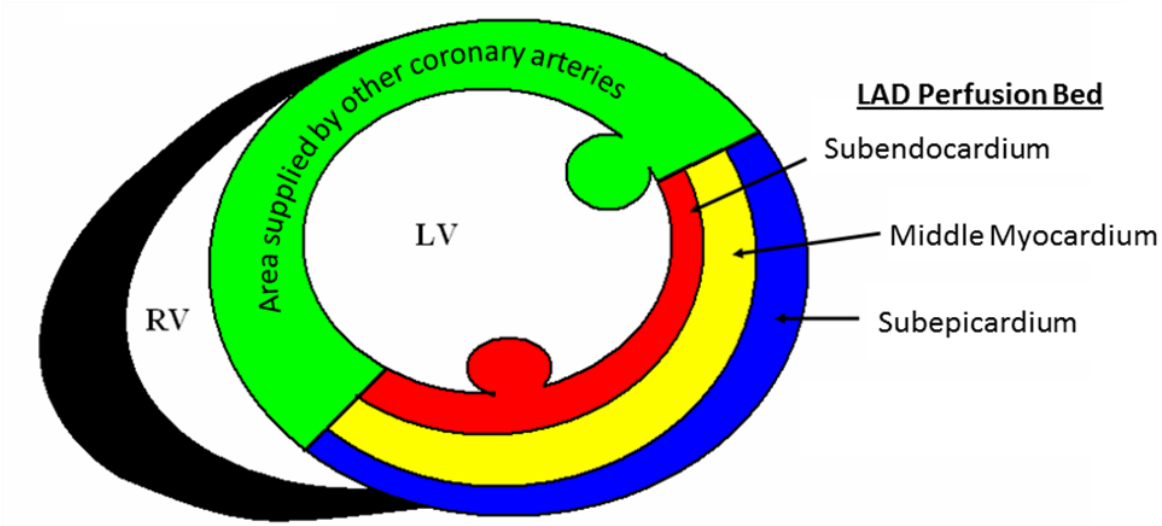

Figure 1.10 – Diagram of a transverse section of the heart representing a typical left anterior descending coronary artery (LAD) perfusion bed and the areas at risk by layer: subendocardial (red), middle (yellow), and sub epicardial (blue). The "wavefront" of permanent tissue damage at the advent of total arterial occlusion occurs in the order of 1) subendocardial, 2) middle, 3) subepicardium.

arteries intersect in this region. This collateral circulation protects the subepicardium (Reimer and Jennings, 1979). Although these studies were performed in dogs, there is evidence that the wavefront occurs similarly in humans (Christian, et al., 1992).

Controlled Release Technology to Improve Treatment of Myocardial Infarction

The therapeutic effectiveness of controlled release formulations has been successfully demonstrated in animal models. Myocardial injections of growth factors and small molecules have been performed in animal models utilizing various controlled release matrices. In general, these show improved outcomes compared to bolus injection. The materials used in these studies include gelatin hydrogel microspheres (Iwakura, et al., 2003; Liu, et al., 2006; Wei, et al., 2007; Yamamoto, et al., 2001), self-assembling peptide nanofibers (Hsieh, et al., 2006), and alginate hydrogels (Hao, et al., 2007). Hsieh et al. (2006) and Hao et al. (2007) demonstrated that their controlled release matrices lead to physiologically active drug levels for at least 14 and 15 days after injection, respectively. These are much improved therapeutic retentions compared to bolus injection. Clinical trials have assessed the administration of a heparin-alginate, slow-release matrix implanted perivascularily in the epicardial fat in humans (Laham, et al., 1999). Results from this small study demonstrate that injectable, controlled release delivery systems are safe in patients and may be effective therapy to treat ischemic myocardium that cannot be reperfused by a graft.

Engineering a TB4 Controlled Release Formulation

Within the heart TB4 elicits beneficial effects on ischemic cardiomyocytes located in the bulk of the heart, as well as epicardial cells distributed as a single cell layer on the exterior of the heart (the visceral epicardium). Our current

estimation of TB4 dose was determined from mouse models, and is very low: 400 ng given as an intraperitoneal injection 0, 3, 7 and 14 days post-infarction (Bock-Marquette, et al., 2004).

The duration exposure of the myocardium to TB4 is related to the healing process that occurs after myocardial infarction. Beginning after the initial ischemic event the heart undergoes remodeling. Apoptosis of cardiomyocytes and replacement by fibroblasts is the basic mechanism that occurs in the ischemic region followed by global changes to heart morphology. Apoptosis in the ischemic region directly follows an ischemic event, and continues to occur in the region of myocardium surrounding this initial infarct, the "border zone", for weeks to months. (Mani and Kitsis, 2003). Collagen synthesis is known to initiate at two days after the ischemic event and continues for 28 days (Sun, et al., 2000). This suggests that the largest portion of healing of the ischemic area at risk occurs in a timeframe of about one month. Our research shows that exposure of the heart in the initial two weeks after infarction is effective in reducing the severity of heart attack (Bock-Marquette, et al., 2004). This evidence suggests that local delivery of TB4 for two to four weeks will be necessary to test the efficacy of a controlled release formulation.

Delivery methods that supply this dose to reach both cell types and still avoid the systemic circulation are: direct myocardial injection or injection into the pericardial space. Direct myocardial injection would be the most effective for cardiomyocyte survival, because the dose can be localized to the ischemic region. Our previous mouse studies show that direct myocardial injection was effective in enhancing cardiac function after MI, attributable to its effect on both the myocardium and the epicardium (Bock-Marquette, et al., 2004; Bock-Marquette, et al., 2009). This straightforward method of administration shows efficacy.

However, this procedure is invasive, and a multiple dosing regimen of TB4 administered by this route would unsafe in the clinical setting.

Other routes to administer the microsphere formulation include injection into the pericardial space. Intra-pericardial injection would be employed with direct myocardial injection, because protein diffusion from the pericardial space to the subendocardium is minimal (Gleason, et al., 2002; Laham, et al., 2003). This method would have a more potent effect on the epicardium and could have excellent long-term results in combination with direct myocardial injection if the dose can be retained in this region for the four week therapeutic window.

Development of microspheres has been chosen to overcome these issues. In direct myocardial injection the size of the microspheres is expected to prevent the common problem of efflux of injectate from the needle path (Grossman, et al., 2002), as well as improve diffusion distance owing to prolonged release from the microsphere formulation. Another advantage of microsphere formulations is that they can be injected simultaneously with another form of controlled release such as an *in situ* forming hydrogel. Release of drug from the hydrogel occurs more rapidly and would be effective shortly after injection while the microspheres trapped in the hydrogel would provide release extending days after intervention.

In summary, a plausible, strong argument can be developed for the deployment of a controlled release drug delivery system directly into the subendocardial region of the myocardium to 1) reduce the number of invasive interventions, 2) protect the drug from degradation, and 3) target the cardiomyocytes most susceptible to loss of function in the ischemic myocardium. This microsphere formulation is dynamic and can, for instance, be applied to

different anatomical regions around the heart, used for treatment of dermal wound healing, or in combination with other drug delivery technologies.

CHAPTER TWO
Encapsulation & Release of Albumin from PLGA Microspheres

ABSTRACT

The purpose of this work was to assess the impact of nonionic surfactant hydrocarbon chain length on BSA containing PLGA microspheres synthesized by the double-emulsion technique (W/O/W). We used alkyl glucosides as the surfactant in the continuous phase of the primary emulsion with seven to ten hydrocarbons comprising the hydrophobic segment (G7 – G10, respectively). BSA in the dispersed phase acted as both a model protein therapeutic and a co-surfactant. To compare emulsions generated from each surfactant we determined the change in emulsion turbidity due to gravity. Emulsions containing octyl glucopyranoside surfactant (G8) had the slowest change in turbidity compared to emulsions generated with G7, G9, or G10. Furthermore, the concentration of G8 at 8.55 mM in the continuous phase was associated with less turbidity change compared to emulsions with 4.28 mM and 34.2 mM. The choice of surfactant influenced microsphere size and internal morphology. G8 microspheres were significantly larger than G10 microspheres. The internal porosity of G8 microspheres was uniform compared to G10 and surfactant free microspheres. G8 microspheres had significantly lower burst release and subsequent elution of BSA over a 37 day period compared to the G10 formulation. Differential scanning calorimetry suggests that the additives in all three microsphere formulations had a slight antiplasticizing effect on the PLGA matrix. BSA adsorption studies show that molecular interactions between G8 and BSA at the W/O interface were the likely cause of enhanced emulsion stability and control of microsphere morphology. Our results indicate a single carbon difference in surfactant hydrocarbon chain length can significantly influence emulsion stability

under gravity. G8 microspheres had more stable primary emulsions which lead to less internal porosity and lower initial burst-release of encapsulated protein.

INTRODUCTION

In PLGA microspheres a number of excipients have been studied including polymers, sugars, and surfactants. Surfactants are classified by their hydrophilic portion and fall into the general categories of ionic and nonionic. They can be further classified by their hydrophilic-lipophilic balance (HLB) number which gives a value to the surfactant's propensity to solubilize in a hydrophobic or hydrophilic solution. HLB values were first introduced by Griffin in 1949 and further revised by Davies in 1957 (Davies, 1957; Griffin, 1954). HLB values range from 0 to 20 with lower values corresponding to surfactants that dissolve in organic solutions and higher values with those that dissolve in aqueous solutions. This number is useful for predicting surfactants that will enhance stabilization of water-in-oil (W/O) or oil-in-water emulsions.

Despite the importance of the W/O emulsion in formation of double-emulsion microspheres, few studies have analyzed the impact of surfactants on characteristics of this colloid solution. Nihant, 1994 I, made the first attempt to quantify the contribution of surfactants in PLGA drug delivery using the amphiphilic co-polymer Puronic F68 (Nihant, et al., 1994). To assess primary emulsion stability 'de-mixing' rate was measured by determining the time it took for the emulsion to cream while in a sealed tube. This de-mixing study demonstrated that the absence of surfactant in the primary emulsion resulted in immediate phase separation of water from the organic phase containing polymer. This suggests that poly(lactic acid) has negligible interfacial activity at the water-dichloromethane (DCM) interface. When BSA, Pluronic F68 (an ABA block-

copolymer of polypropylene oxide (PPO) and polyethylene oxide (PEO)), or a combination of the two was added to the emulsion, stabilization improved. BSA was far more potent in this regard than Pluronic F68. The stabilizing effect of BSA was again demonstrated in their follow-up article, Nihant, 1995 II (Nihant, et al., 1995). These studies established that surfactant additives could be used to influence the internal morphology of PLGA microspheres.

Further research on the influence of surfactants in PLGA microspheres demonstrated that surfactant type and concentration were associated with emulsion stability (Mohamed and van der Walle, 2006). A variety of Pluronics (F68, F127, L31, L62, L81, and L92) poorly stabilize primary w/o emulsions with PLGA in the organic phase regardless of their concentration. However, Span/Tween surfactants with a high HLB value (Tween 20 and Tween 80) effectively stabilize the emulsion. The different outcome in emulsion stabilization involves the chemical and structural difference between these two classes of surfactant. While both surfactants have PEO as the hydrophilic segment, Pluronics contain PPO as the hydrophobic segment and Tween contains a hydrocarbon chain. Structurally, Pluronics are linear and have molecular weights between approx 1,000 and 13,000 g/M depending on the specific surfactant. Tweens have four branches originating from a central sorbitan ring with molecular weights between approx 1,230 – 1,300 g/M. DSC experiments performed in their study demonstrate that Tween 20 interacts more within the PLGA matrix compared to Pluronic L92 despite the HLB prediction that Tween 20 has a higher preference for aqueous phases. PEO is known to be soluble in DCM and is a good hydrogen bond donor and acceptor which explain why Tween 20 can interact more with PLGA despite PLGA being localized in the organic phase of the emulsion.

The interaction of proteins at the W/O interface during microsphere synthesis is important, because protein adsorption to this interface occurs by irreversible denaturation. A study by Kwon et al. (2001) shows that sorption of the peptide insulin to the water-DCM interface is dependent on time, peptide concentration, presence of PLGA in the organic phase, and the presence of surfactant (Kwon, et al., 2001). Specifically, ionic surfactants had better efficiency than non-ionic surfactants in preventing precipitation of insulin to a water-DCM interface. This study makes it apparent that the water-DCM interface induces more aggregation of peptide compared to water-air or water-solid interfaces, and that the addition of PLGA to the organic phase increases this rate of aggregation. Owing to slight solubility of DCM in water, there is a greater interfacial region where molecules of the organic solvent and molecules in the aqueous phase can interact. The efficacy of ionic surfactants in preventing insulin aggregation is clear, however, ionic surfactants such as sodium dodecyl sulfate and cetyltrimethylammoniumbromide are known to be irritants that up-regulate inflammatory pathways in cells making them undesirable excipients in implantable drug formulations (van Ruissen, et al., 1998).

There is a significant body of research on the effect of a number of surface active agents on the stability and release of drugs from PLGA microspheres fabricated by methods including double-emulsion, water-in-oil-in-oil, and solid-oil-in-oil techniques. The additives include non-ionic surfactants: poloxamers (Pluronic), sorbitans (Span and Tween), Poly(ethylene glycol), poly(vinyl alcohol), Triton X-100, phosphatidylcholine, tricaprin, and Igepal CA-630, as well as the ionic surfactant dioctyl sodium sulfosuccinate (AOT), and finally the proteins BSA and ovalbumin (Bertram, et al., 2010; Blanco and Alonso, 1998; BlancoPrieto, et al., 1996; Bouissou, et al., 2004; Bouissou, et al., 2006; Kang and Singh, 2003; Lam, et al., 2001; Mohamed and van der Walle, 2006; Paillard-

Giteau, et al., 2010; Sandor, et al., 2002; Shelke, 2010; Tobio, et al., 1999; van de Weert, et al., 2000; Wei, et al., 2007; Yeh, et al., 1996). The addition of these surfactants in the double-emulsion technique shows inconsistency in their effect on drug release. For instance, addition of Pluronic surfactant, L101 (HLB 1) or F68 (HLB >24), to microspheres caused a decrease in BSA encapsulation efficiency (van de Weert, et al., 2000) and an increase in release rates (Blanco and Alonso, 1998). In the case of hormone release from PLGA microspheres F127 (HLB ~20.5) increased GH release kinetics while F68 (HLB >24) decreased pBC 264 (a short cholecystokinin agonist peptide) release rate (Wei, et al., 2007) (BlancoPrieto, et al., 1996). The unique interactions associated with different surfactant molecules demonstrate the advantages of emulsion characterization for controlled release PLGA matrices that begin with a W/O emulsion.

In this study alkyl glycosides were used in combination with BSA for preparation of PLGA microspheres. Alkyl glucosides are amphiphilic molecules composed of a glucose head group and an aliphatic hydrocarbon chain attached in the beta linkage position to the alcohol group of the primary carbon on the glucose ring. They are considered biocompatible and are used frequently in membrane protein solubilization, because they tend to leave protein secondary structure intact (le Maire, et al., 2000). They are commercially available and can be synthesized chemically or enzymatically.

Alkyl glucosides of 7, 8, 9, and 10 carbons on their hydrocarbon chain were added to the organic phase of the primary emulsion to stabilize the W/O emulsion step of our double-emulsion microspheres. Using Davies' method we calculated the HLB of these surfactants to be 9.68, 9.20, 8.73, and 8.25 respectively (Table 2.1). These values, being below 10, suggest that these surfactants will favor solubility in an organic phase and stabilize a W/O emulsion,

such as the emulsion used in preparation of microspheres synthesized by this method.

We demonstrate a synergistic role between alkyl glucoside surfactants and BSA that drive more uniform microsphere morphology. We propose that this dual surfactant system will be useful in generating uniform microsphere morphology suitable for modulating drug release kinetics.

Our goal was to determine whether emulsion stability could have a significant impact on BSA release. We were especially interested whether our measure of emulsion stability was related to a decrease in the burst-release of protein from the formulation. Microsphere morphology would be of considerable interest, because attributes of the primary emulsion such as viscosity, water droplet size, and droplet stability would directly influence the resulting microspheres. In addition to microsphere morphology we analyzed intermolecular interactions in the polymer matrix of microsphere formulations using DSC. We sought this information because it is speculated that more intermolecular interactions, identified by higher glass transition temperature (T_g) values, are related to characteristics of drug release such as initial burst release and the subsequent lag phase (Bouissou, et al., 2006). Lastly, we characterized BSA adsorption to the W/O interface, because surfactants are expected to occupy this space and prevent protein adsorption to this interface. Interesting, surfactants induced a slightly higher BSA adsorption at the interface. We suspect G8 interaction with BSA at the W/O interface causes more BSA precipitation and improved emulsion stability which leads to smaller and more uniform internal porosity of PLGA microspheres.

Table 2.1 – Alkyl glucoside surfactant HLB and structure

Surfactant	HLB*	Structure†
n-Heptyl-β-D-Glucopyranoside (G7)	9.68	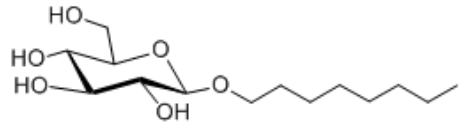
n-Octyl-β-D-Glucopyranosid (G8)	9.20	
n-Nonyl-β-D-Glucopyranoside (G9)	8.73	
n-Decyl-β-D-Glucopyranoside (G10)	8.25	

* Calculated using method described by Davies, 1957

† G8 structure

MATERIALS & METHODS

Dichloromethane (DCM), lyophilized bovine serum albumin (BSA) purified by the Cohn cold ethanol fractionation method, poly(vinyl alcohol) (PVA), and phosphate buffered saline (PBS) were purchased from Sigma-Aldrich. PLGA with a 50:50 ratio of lactic to glycolic acid and inherent viscosity of 0.35 - 0.45 dL/g (M_w 41 – 59 kDa) was purchased from Lakeshore Biomaterials. Alkyl glucoside surfactants were purchased from Anatrace. Trifluoroacetic acid, and acetonitrile were purchased from Fisher Scientific. All other chemicals were purchased from Sigma-Aldrich.

Microsphere Synthesis and Yield

Microspheres were synthesized by the water-in-oil-in-water double-emulsion method. Briefly, 250 mg PLGA 50:50 was dissolved in 5.0 ml DCM. 2.5% (w:v) BSA solution was generated and incubated for 1 hr at 37 °C. The indicated amount of surfactant was carefully weighed with an analytical balance and added to the DCM-PLGA mixture. To generate the primary emulsion, 200 µl of 2.5% (w:v) BSA in water was pipetted into the DCM-PLGA-surfactant mixture. The coarse emulsion was vortexed for 10 sec followed by indirect sonication. Sonication was achieved using a cup-horn sonication probe (Soncis & Materials Inc. model CV17) with a circulating bath of water and glycol maintained at 1.1 ± 1 °C. The emulsion was sonicated in a 50 ml Erlenmeyer flask with a flat bottom to increase surface area for transmission of acoustic energy to the emulsion. To generate the second emulsion, the sonicated mixture was added dropwise to a beaker containing 20 ml of 1.0 % (w:v) PVA being stirred at 300 rpm with an overhead stirrer (Caframo model BDC 250). DCM was extracted at RT for 6.0 hrs. The resulting microspheres were washed to remove

small particles and excess PVA using a 15 μm sieve (BioDesign Inc. of New York). Microspheres were frozen in liquid nitrogen and freeze dried in a small vacuum chamber with a liquid nitrogen moisture trap. After drying, microspheres were weighed on an analytical balance. Percent yield was calculated as the weight of dried microspheres divided by the initial weight of drug, surfactant, and PLGA used in the formulation.

Emulsion Analysis

Primary emulsion stability was compared between formulations containing different alkyl glucoside HLB numbers as well as alkyl glucoside concentration. The primary emulsion was prepared following the microsphere synthesis procedure. Directly after sonication the primary emulsion was transferred to a 2.0 mm path-length quartz cuvette and sealed with a Teflon stopcock. Baseline turbidity of each emulsion was measured on a UV/VIS/NIR spectrophotometer (Shimadzu UV-3600) at 720 nm wavelength. We chose 720 nm after performing a wavelength scan of a similar emulsion over time. At this wavelength the turbidity change over time reflected visual observations of emulsion creaming. We concluded that at this wavelength absorbance was a result of scattered light, not absorbance by components of the emulsion. Rapid creaming was achieved by placing the cuvettes in a bench-top centrifuge at 28 x gravity and measuring the change in turbidity at specific timepoints up to 12 minutes, temperature was maintained at 25°C.

***Scanning Electron Microscopy (SEM*)**

Microspheres were gold sputtered under vacuum prior to imaging. Images were generated in a high vacuum chamber using a SEM (model FEI XL30 ESEM). Images taken at 75x were used to measure the distribution of microsphere diameters. Pore number, and pore area were measured from images

taken at 3000x. Measurements taken from SEM images were performed with imageJ software.

Transmission Electron Microscopy (TEM) and Internal Porosity

Dry microspheres were embedded in acrylic resin blocks and cut into 80 nm thick sections with a microtome. Sections were stained in osmium tetroxide and viewed with a TEM (model FEI Tecnai G2 Spirit Biotwin). Quantification of internal porosity was performed on 2-D sections from three unique microspheres from each formulation (n=9). As a result of artifacts created during the sectioning process, or the obstruction of the microsphere by the mesh disk used for mounting the TEM sample, microsphere images were divided into slices from their center every 45 degrees. A random section that did not contain artifact from each divided microsphere image was selected (Figure 2.1). Internal porosity was calculated from the slice using threshold analysis on imageJ software. Internal porosity was defined as the percent of void space area compared to the total microsphere area.

Encapsulation Efficiency (EE)

Approx. 15 mg of dried microspheres were carefully weighed. 1.0 ml chloroform was added to the microspheres to dissolve the polymer and 1.0 ml of PBS buffer was added to extract the BSA. BSA concentration was determined by reverse phase HPLC (section 7.6). EE was calculated as the percent of drug recovered from the formulation divided by the amount of drug used to generate the formulation. Each surfactant group was analyzed in triplicate and compared using ANOVA.

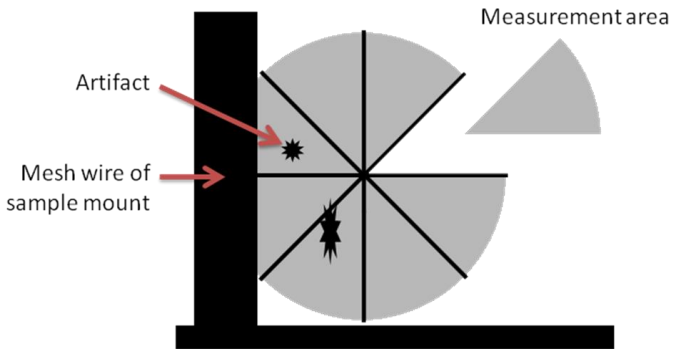

Figure 2.1 – Selection of a random area from a TEM microsphere image for analysis of internal porosity. A random section was chosen from a slice that was unobstructed and did not contain an artifact.

BSA Release & High-Performance Liquid Chromatography

2.0 ml phosphate buffered saline (PBS) was added to 75 mg of microspheres, the exact weight of microspheres was carefully recorded. BSA release was carried out in borosilicate vials in an oven at 37 ± 1.0 °C rotating horizontally at approx. 10 rpm. 1.0 ml of drug release media was collected and replaced with fresh PBS at pre-determined timepoints. BSA in the collected drug release medium was quantified by reverse phase HPLC (Dionix, UltiMate 3000) equipped with porous channel monolith type column (Proswift® RP-2H; phenyl surface chemistry; dimensions 4.6 × 50 mm). The mobile phases consisted of A: 95 % H_2O, 5.0 % acetonitrile and 0.1 % trifluoroacetic acid and B: 95 % acetonitrile, 5.0 % H_2O H and 0.1 % trifluoroacetic acid. The mobile phase decreased from 99 % A to 50 % A in two minutes using a gradient method with flow rate of 2.5 ml/min (see Appendix C for program information). BSA was detected at 214 nm with retention time at approx. 2.38 minutes.

Differential Scanning Calorimetry

Dry microspheres were transferred to an aluminum calorimetry tray such that the bottom of the tray was evenly coated one layer thick. The tray was capped and placed in the DSC (Perkin Elmer Diamond DSC) along with an empty tray as a reference. The sample and reference were cooled to 0.0 °C and stabilized for 5.0 min. Once stabilized the temperature was raised to 90 °C simultaneously in the sample and reference tray at a rate of 50 °C min^{-1}. Resulting thermograms were analyzed for T_g at the onset point using the bisector method (Figure 2.2; Software Pyris 8.0). A second heating analysis was not performed owing to alterations in intermolecular interactions within the microspheres that would have occurred upon the first analysis. The onset temperature is extrapolated at the intersection of two lines tangent to the curve at the initiation of the glass transition peak. The first tangent line is drawn at the

baseline of the T_g peak, and the second tangent line is drawn where the slope transitions from positive to negative (relative maxima of the first derivative of the curve). The onset T_g is determined where these lines intersect.

In situ BSA Aggregation at W/O interface

To clean borosilicate test tubes 0.5 ml of 5.0 % PLGA in DCM was added with or without 8.55 mM of G8 or G10 surfactant. 200 µl of 1.5% BSA was carefully added to the surface of the DCM solution in such a way that mixing did not occur. The two-phase samples were gently agitated at 30 rpm for 30 min, RT. After 30 min had elapsed, the aqueous layer was collected and analyzed for BSA concentration using Reverse Phase HPLC. 1.5% BSA in water was agitated in a glass tube as a control. Each treatment had a total of five replicates. BSA from the aqueous phase was quantified with HPLC (Dionix, UltiMate 3000) using a C18 column (Acclaim PA2, 3.0 µm Analytical; 3.0 x 150 mm) with mobile phases A: 90 % H_2O, 10 % acetonitrile and 0.05 % trifluoroacetic acid and B: 100 % acetonitrile and 0.05 % trifluoroacetic acid. The mobile phase decreased from 90 % A to 10 % A in 12 minutes using a gradient method. BSA was detected at 214 nm with retention time at approx. 8.4 minutes.

Statistics

Statistics were performed in SigmaPlot (version 11.0). For analysis of variance (ANOVA) and repeated measures ANOVA (RM-ANOVA) models, alpha was 0.05. All post-test analysis was performed using Bonferroni correction where alpha equals 0.05/number of multiple comparisons. Multiple comparisons for RM-ANOVA were performed by comparing all individual curves pairwise using RM-ANOVA.

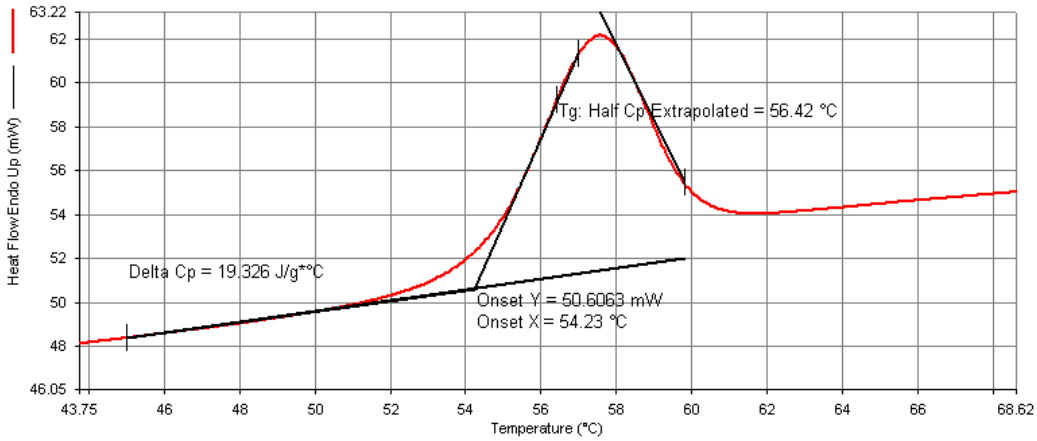

Figure 2.2 – Typical DSC thermogram for microsphere encapsulated with G8 surfactant showing the glass transition temperature peak (T_g). Onset method is demonstrated where tangent lines intersect at temperature coordinates (54.2, 50.6).

RESULTS

Emulsion Analysis

The creaming analysis was initially carried out at normal gravity; however, we found it was very time consuming and could not be repeated consistently. Therefore, we decided to perform the analysis by increasing the gravitation field using a centrifuge at 28 x g (500 rpm). Despite having to carefully transfer samples between the centrifuge and the spectrophotometer at the predetermined timepoints, the data was more consistent and reproducible. The turbidity of the solution decreases as the water droplets rise in the DCM solvent (density=1.33 g/cm3, STP) under gravity. According to stokes law, water droplets with larger radii rise faster (Hiemenez and Rajagopalan, 1997). The gradual decrease in turbidity of these emulsions, as opposed to a sharp drop-off, demonstrates the heterogeneous size distribution of the water droplets.

The results of this experiment show that addition of surfactant to the primary emulsion had an impact on the rate of creaming of the water droplets in the DCM solution. Hydrocarbon chain length was compared at a surfactant concentration of 8.55 mM in the DCM (Figure 2.3). An emulsion without surfactant was used as a reference. Between emulsions generated with different surfactants, it was clear that hydrocarbon chain length had a significant impact on the rate of creaming, even when surfactants differed by only one methyl group. G8 emulsions had significantly slower rates of creaming compared to all other surfactants (Table 2.2; $P<0.005$). G10 and G7 surfactants accounted for the most rapid creaming rates. G9 appeared to have an intermediate rate of creaming because it was significantly faster than G8 emulsions ($P<0.005$), significantly slower than G10 emulsions ($P<0.005$), and statistically trending toward slower creaming rates compared to G7 ($P=0.008$).

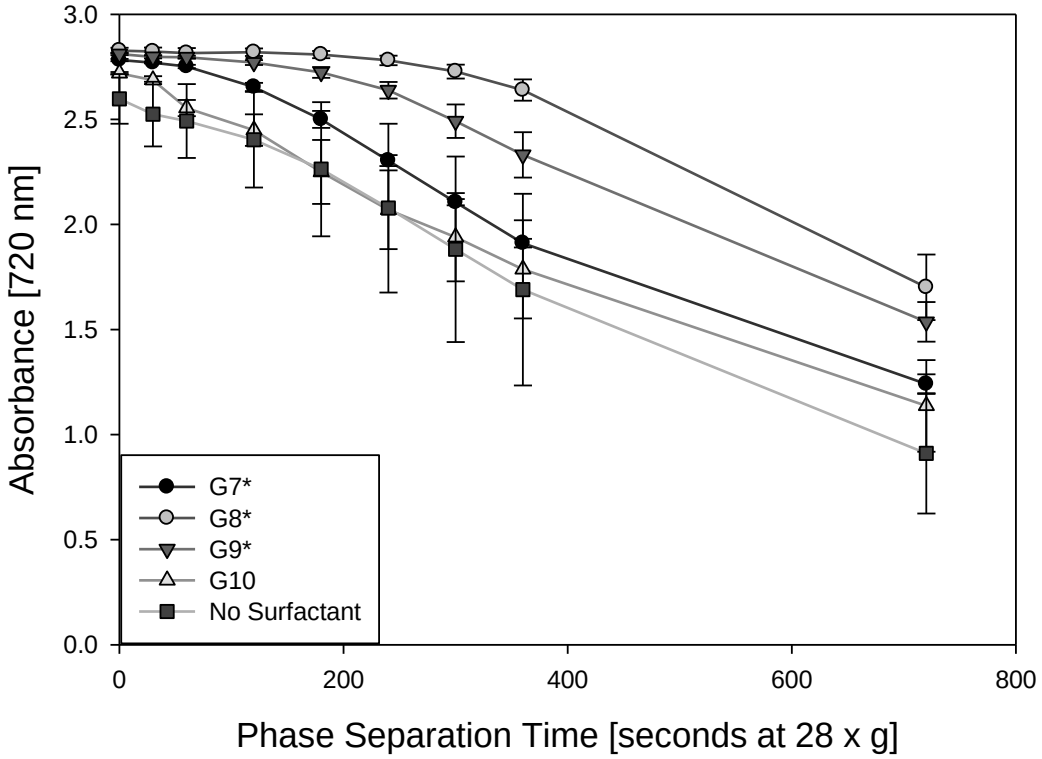

Figure 2.3 – Emulsion analysis of primary emulsions generated with alkyl glucosides of differing hydrocarbon chain length. RM-ANOVA for all treatment groups was significant (P=0.003). (*) Indicates individual comparisons between treatments were significant by RM-ANOVA (P-values in Table 2.2).

Table 2.2 – Individual comparisons of treatments in emulsion analysis for emulsions generated with alkyl glucosides of differing hydrocarbon chains. P-Values from RM-ANOVA (α=0.005; Bonferroni correction)

	G7	G8	G9	G10	NSF
G8	***<0.001***				
G9	***<0.001***	***0.02***			
G10	0.091	***0.003***	0.008		
NSF	0.215	0.027	0.053	0.666	

Surfactants stabilize the interface between hydrophobic and hydrophilic surfaces which requires enough surfactant present in the emulsion to occupy the interfacial surface area. Consequently, emulsion stability is expected to increase as surfactant concentration increases until the interfacial surface area is saturated. When the surfactant is soluble in organic solvent, interfacial saturation occurs when the exchange of surfactant molecules between the W/O interface and the organic phase does not result in interfacial area being unoccupied by surfactant. As we increased the concentration of G8 surfactant in the organic phase from 4.25 to 8.55 mM the rate of creaming trends toward improved emulsion stability (Figure 2.4; P=0.014; Table 2.3). This decrease in distribution of droplet velocity results from the presence of more surfactant stabilizing the larger surface area associated with smaller emulsion droplets. However, creaming rate increased significantly ($P<0.0083$) as surfactant concentration increased from 8.55 to 32.4 mM. We speculate reasons for poorer emulsion stability upon increase in surfactant concentration are the presence of larger water droplets, or surfactant self-association structures that result in a depletion force between emulsion droplets.

Yield

Microspheres were weighed after drying. Percent yield was calculated as the weight of lyophilized microspheres divided by the initial weight of drug, surfactant, and PLGA used in the formulation. Yield ranged between 83 and 93 % recovery with no difference between formulations (Table 2.4) (P=0.333).

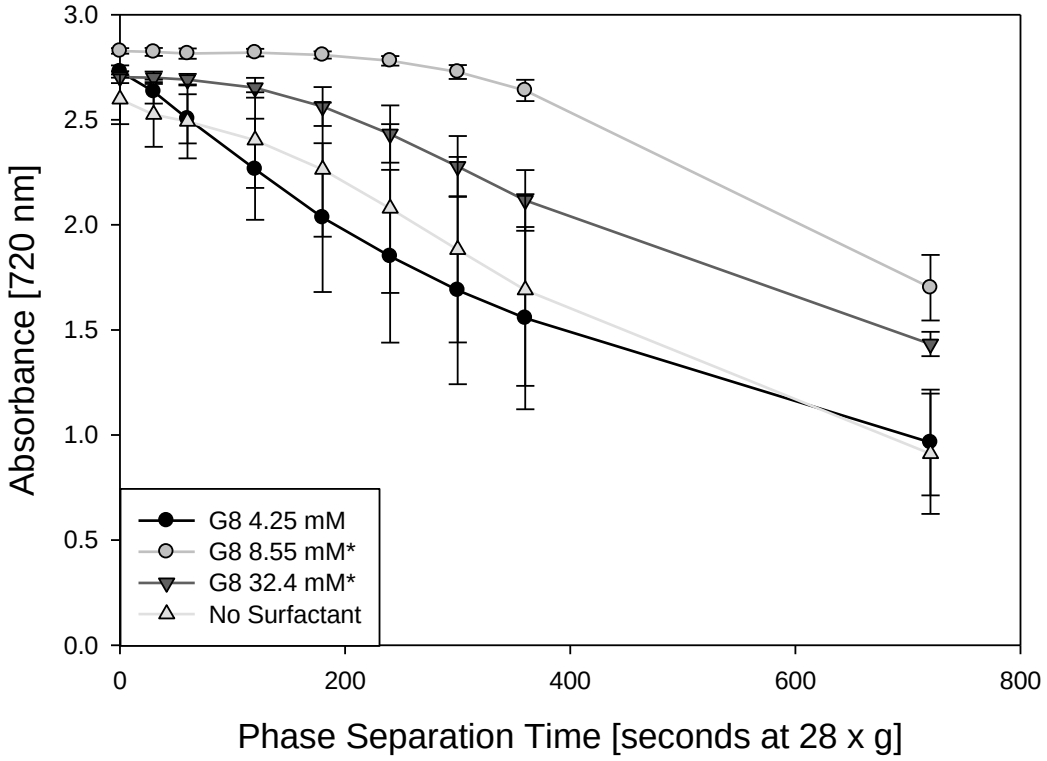

Figure 2.4 – Emulsion analysis of primary emulsions generated with G8 surfactant at different concentrations. RM-ANOVA for all treatment groups was significant (P=0.015). (*) Indicates individual comparisons between treatments were significant by RM-ANOVA (P-values in table 2.2).

Table 2.3 – Individual comparisons of treatments in emulsion analysis for emulsions generated with G8 surfactant at different concentrations. P-Values from RM-ANOVA (α=0.005; Bonferroni correction)

	G8 4.25mM	G8 8.55 mM	G8 32.4 mM	NSF
G8 8.55 mM	0.014			
G8 32.4 mM	0.076	***0.006***		
NSF	0.774	0.027	0.149	

Table 2.4 – Microsphere yield and encapsulation efficiency

Formulation	Yield [% recovered MS weight /theoretical MS weight]	Encapsulation Efficiency [% actual BSA loading /theoretical BSA loading]
G8	85 ± 3.4	46.7 ± 6.4
G10	92.6 ± 3.0	68.5 ± 7.2
NoSf	82.9 ± 9.4	65.4 ± 24.7

Values represent mean ± standard deviation

Scanning Electron Microscopy (SEM)

Surface measurements were made from SEM images to determine the distribution of microsphere diameters in each treatment (Figure 2.5). The smallest diameters observed were approx. 20 μm as a result of having washed the microsphere batches over a 15 μm sieve during preparation. Microspheres prepared without surfactant (NoSf) had the largest average diameter at 219 nm, with G8 being slightly smaller at 187 nm, and G10 represented the smallest size distribution averaging 79 nm. Individual microsphere batches had diameters that were normally distributed (Normality Test: Shapiro-Wilk; $P<0.50$). However, when the three batches that represented one treatment group were combined, normality could not be assumed. As a result, comparison of average diameters was performed using ANOVA on Ranks revealing that G10 microspheres were significantly smaller than G8 or NoSf microspheres ($P<0.01$).

Surface porosity and pore size distributions, both a potential contributor to high initial burst-release were measured. We examined the average area of individual pores on the surface of each microsphere formulation and well as the average amount of surface occupied by pores for each formulation (Figure 2.5). The average pore area for G8 was 51 nm^2, G10 was 80 nm^2, and NoSf was 66.4 nm^2 (Table 2.5). Within each group there was a large deviation in pore area measurement and there was no difference when G8, G10, and NoSf formulations were compared. The percentage of the surface of each microsphere formulation occupied by pores was calculated on a 1200 μm^2 area (n=4). The surface pore area was on average less than 1.0 % in all groups. G8 pore area measured 0.06 %, G10 was 0.78 %, and NoSf was 0.27 %. While the ANOVA model was significant ($P=0.03$) multiple comparisons only revealed a trend showing the G10 group had a nearly significantly higher surface porosity ($P<0.033$). Given the large deviations within formulations as well as insignificant statistical

comparisons it is unlikely that differences in these morphological characteristics contributed to the observed differences in drug release.

Internal Porosity (TEM)

Microsphere sections observed by TEM revealed differences in internal morphology related to the presence and type of surfactant (Figure 2.6). Without the addition of surfactant, microspheres were nearly hollow in the center with a few areas containing masses of polymer. G10 microspheres did contain a central core of interconnected pores, but were much less hollow. On the other hand, G8 microspheres demonstrate a more consistent internal porosity with discrete pores and lacking a void area in the core. These large void areas within the NoSf and G10 microspheres were likely attributed to the combination of water droplets in the primary emulsion as well as influx of water from the secondary aqueous phase. Despite the large hollow areas inside these microsphere formulations, a closer look at the polymer segments demonstrate tiny pores. These tiny pores are a result of some water droplets of the primary emulsion being sustained throughout extraction of solvent from PLGA during microsphere synthesis.

Quantification of microsphere internal porosity revealed all groups had significantly different pore composition (Table 2.5, $p<0.017$). G8 maintained the least internal porosity at 37.4 %, G10 was 53.4 %, and NoSf was 70.9 %. By calculation of the volume fraction of each chemical component in the microsphere formulation after solvent extraction but before drying (calculation not shown), we determined there influx of water from the secondary aqueous phase was greater than efflux of the primary aqueous phase during microsphere formation. If no loss of the internal aqueous phase occurred during microsphere synthesis the volume fraction would be 48 % of the entire microsphere composition. We can

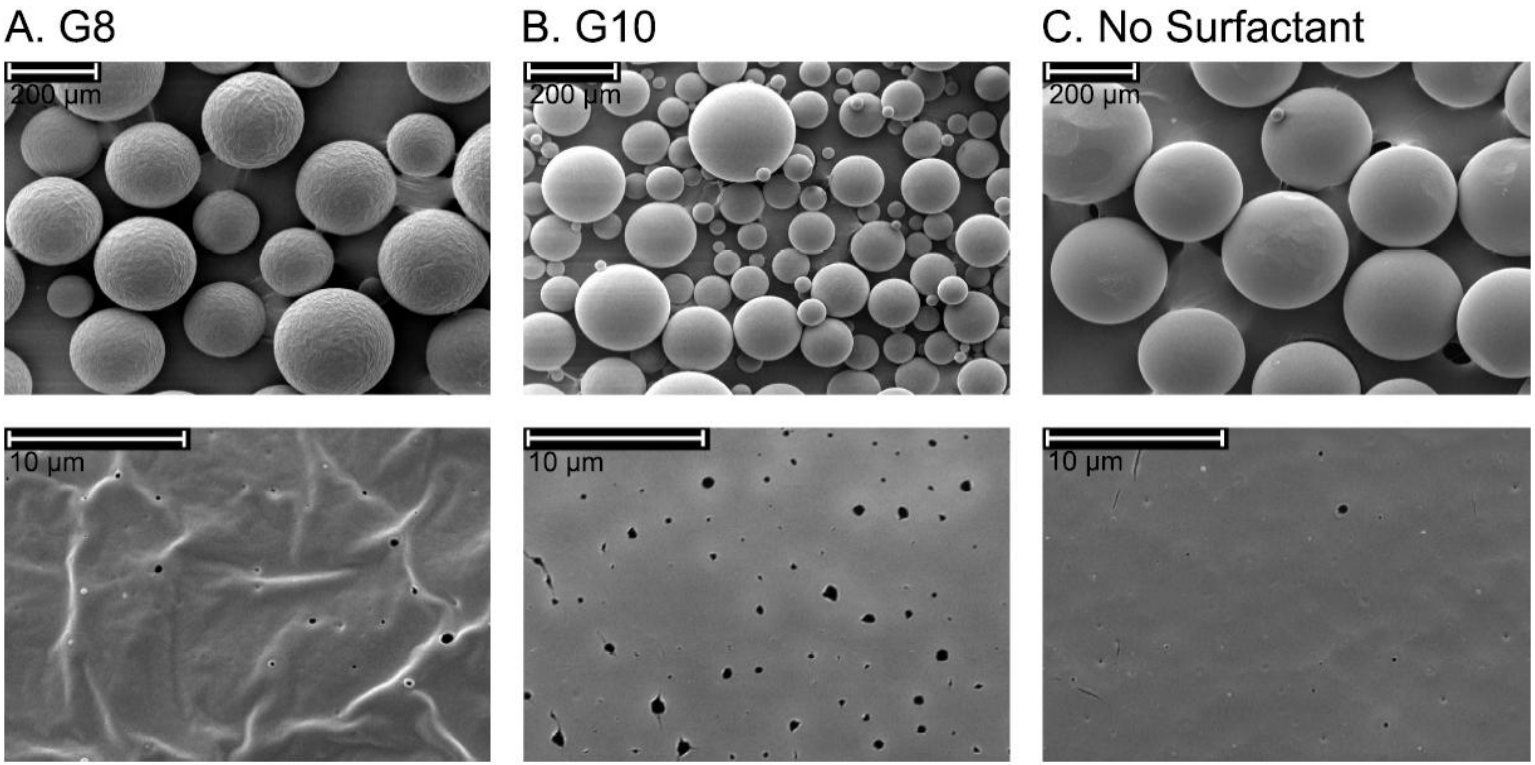

Figure 2.5 – SEM images of G8, G10, and NoSf microspheres taken for morphological analysis. The order of average microsphere diameter is: G10<G8<NoSf. Area of pores occupying the surface was greatest in G10 microspheres and similar in G8 and NoSf microspheres. Top row scale bar is 200 µm, bottom row scale bar is 10 µm.

Table 2.5 – Morphological Analysis of Microsphere Formulations

Morphological Characteristic	Formulation		
	G8	G10	NoSf
Diameter [μm]	186.5 ± 34.6	79.3 ± 51.3 †	218.7 ± 68.1
Individual Pore Area [nm^2]	50.9 ± 17.5	80.2 ± 24.5	66.4 ± 45.1
Surface Porosity [% pore area/surface area]	0.1 ± 0.04	0.8 ± 0.4 ‡	0.3 ± 0.3
Internal Porosity [% pore area/total area]	37.4 ± 5.1 †	53.4 ± 3.7 †	70.9 ± 7.0 †

All values represent average ± standard deviation

† significantly different (ANVOA, $p<0.017$)

‡ trending difference in G8-G10 comparison($P=0.033$)

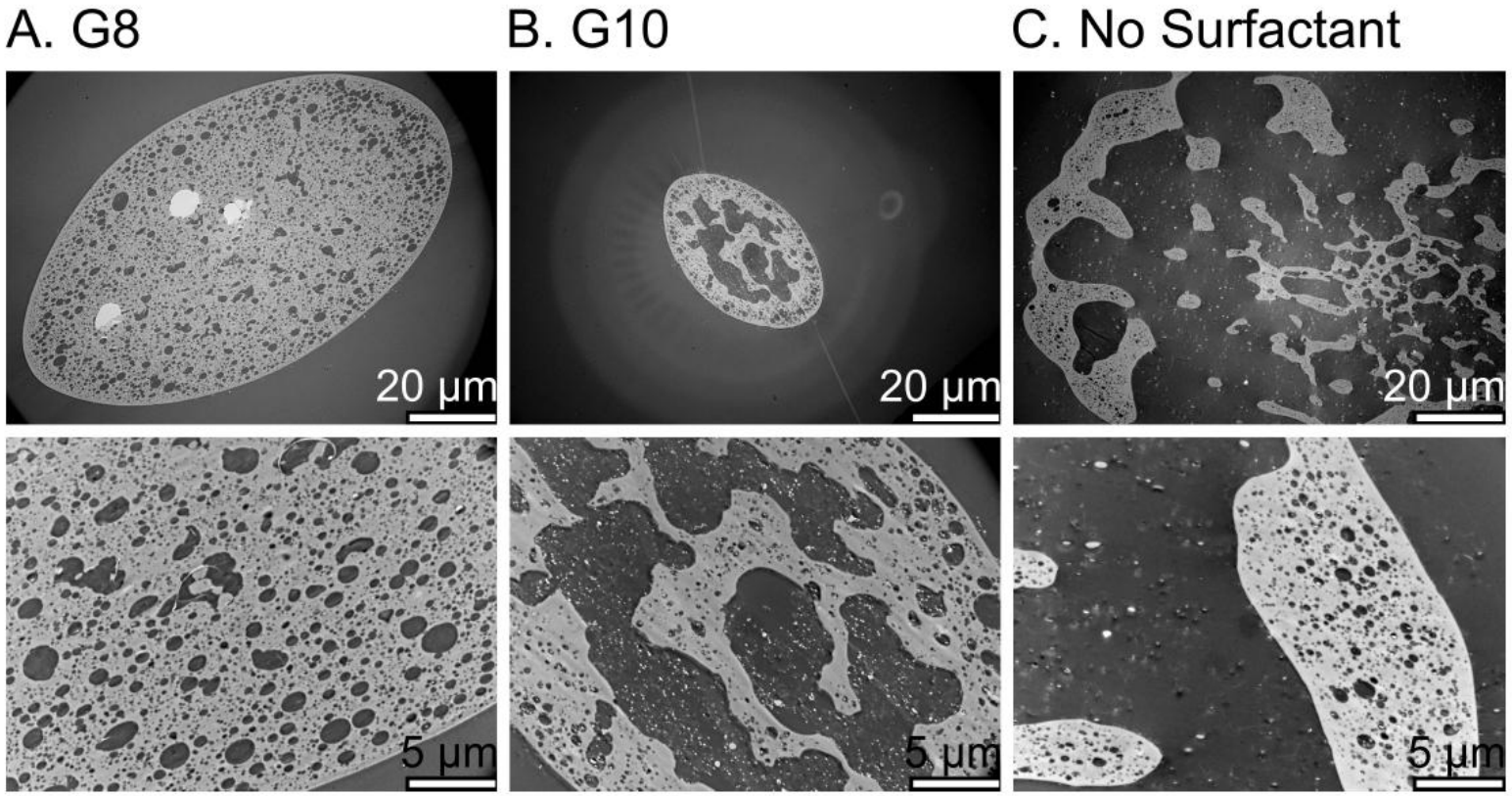

Figure 2.6 – TEM images of G8, G10, and NoSf microsphere sections demonstrating differences in internal morphology. G8 microspheres have small, discrete internal pores while G10 and NoSf microspheres have large networks of interconnected pores. Top row scale bar is 20 µm, bottom row scale bar is 5 µm.

conclude that NoSf microspheres had net water influx, because 71 % of their internal volume was unoccupied by polymer. This would also have contributed to their large size, upwards of 300 μm. G8 formulations most likely had net loss of internal aqueous phase volume, while in G10 formulations water influx was very minor, or the efflux-influx rates were near equilibrium.

Encapsulation Efficiency & Drug Release

Encapsulation efficiency was 47±6 % in G8, 69±7 % in G10, and 65±25 % in NoSf microspheres (Table 2.4). Encapsulation of BSA in G8 microspheres was the lowest and is believed to result from the net loss of the primary aqueous phase during microsphere preparation. Another potential reason could be that our method of measuring encapsulated BSA does not detect denatured and surface adsorbed protein. This effect would result in our lower measurement of BSA in G8 microspheres, because we find more BSA is adsorbed at the water-DCM interface in the presence of G8 surfactant (Figure 2.10). Furthermore, the higher reported adsorption of BSA at the water-DCM interface in and G10 microspheres was more consistent between formulations compared to the NoSf microspheres. This deviation in the group lacking surfactant is thought to be attributed to poor primary emulsion stability. The more coarse emulsion is less stable which could lead to and would lead to the large amount of aqueous phase exchange that occurred during microsphere synthesis, as seen by morphological analysis. Resulting from the high degree of variance in the NoSf group, a comparison of all groups by ANOVA did not reveal a significant difference in encapsulation efficiency. However, a t-test comparing G8 and G10 alone is significant for higher BSA encapsulation in the G10 formulation ($P=0.017$).

Drug release curves are presented in two ways. In Figure 2.7, the drug release is represented as the percent of BSA released divided by the initial weight of microspheres in the drug release media. The second set of curves depict the percent of BSA released compared to the total BSA loaded in the microsphere (Figure 2.8). The release of BSA from our formulations followed a commonly reported tri-phasic pattern beginning with an initial burst-release phase, then a lag phase, and terminating with a continued release phase.

Individual comparisons between curves in Figure 2.7 were conducted with RM-ANOVA. They demonstrated that G8 microspheres release BSA significantly slower over the 36 day period compared to NoSf and G10 microspheres ($P<0.017$). This result is consistent with the tighter control of internal morphology in the G8 microspheres. G10 is also trending toward slower release rates compared to NoSf microspheres ($P=0.043$). However, in the last two weeks of release the G10 formulation elutes a large amount of BSA that causes this formulation to "catch-up" to the NoSf formulation. The morphological assessment of G10 microspheres shows that they have larger internal porosity than G8 microspheres, but smaller pore space than NoSf microspheres. This evidence partially supports the intermediate release pattern of G10 microspheres.

When release was demonstrated as a measure of the percent of mg of BSA released per mg of total BSA loaded we find very similar patterns (Figure 2.8). G8 and G10 microspheres release their loaded BSA much slower when compared to NoSf microspheres ($P<0.017$ and $P=0.022$, respectively).

Burst-release, the rapid release of drug in the initial 24 hours of elution, was compared between formulations. High burst-release is not desirable, because it can lead to rapid loss of encapsulated drug and potentially toxic levels of drug

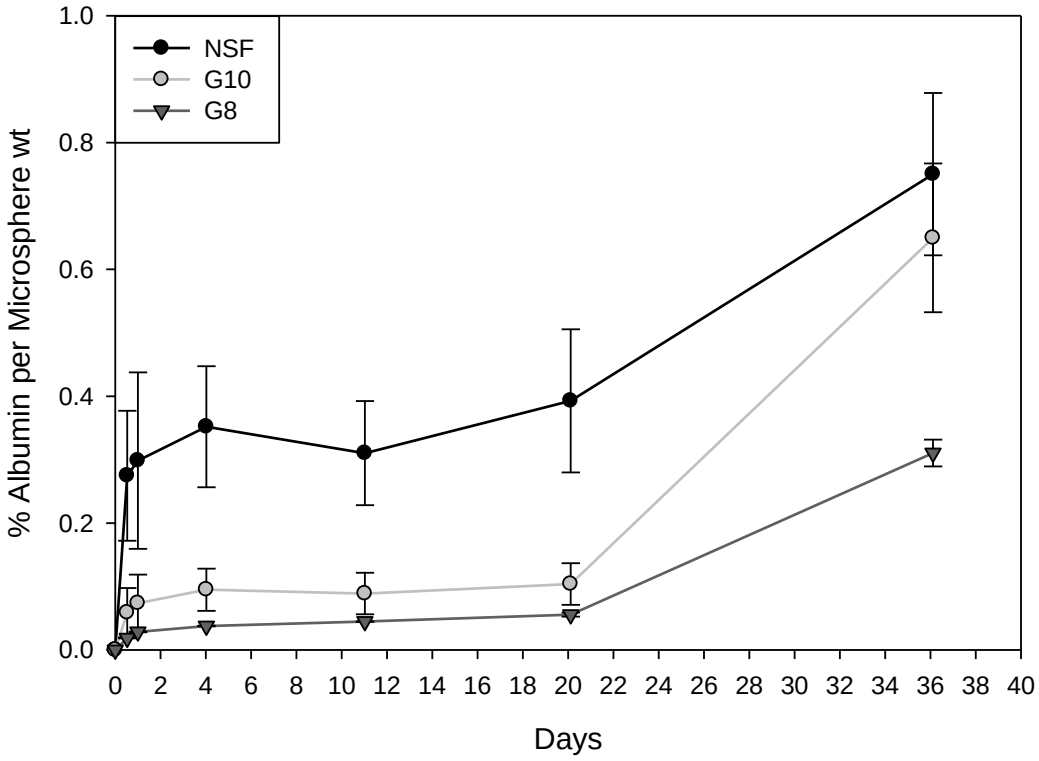

Figure 2.7 – Percent cumulative albumin release by microsphere weight calculated as: cumulative mg albumin released per total mg microspheres. RM-ANOVA for all treatment groups was significant (P=0.004). Individual comparisons between treatment groups by RM-ANOVA reveal G8 microsphere release drug significantly slower than both G10 and NoSf microspheres (P=0.013 & P=0.012). G10 microspheres trend toward slower release rates compared to the NoSf formulation (P=0.043).

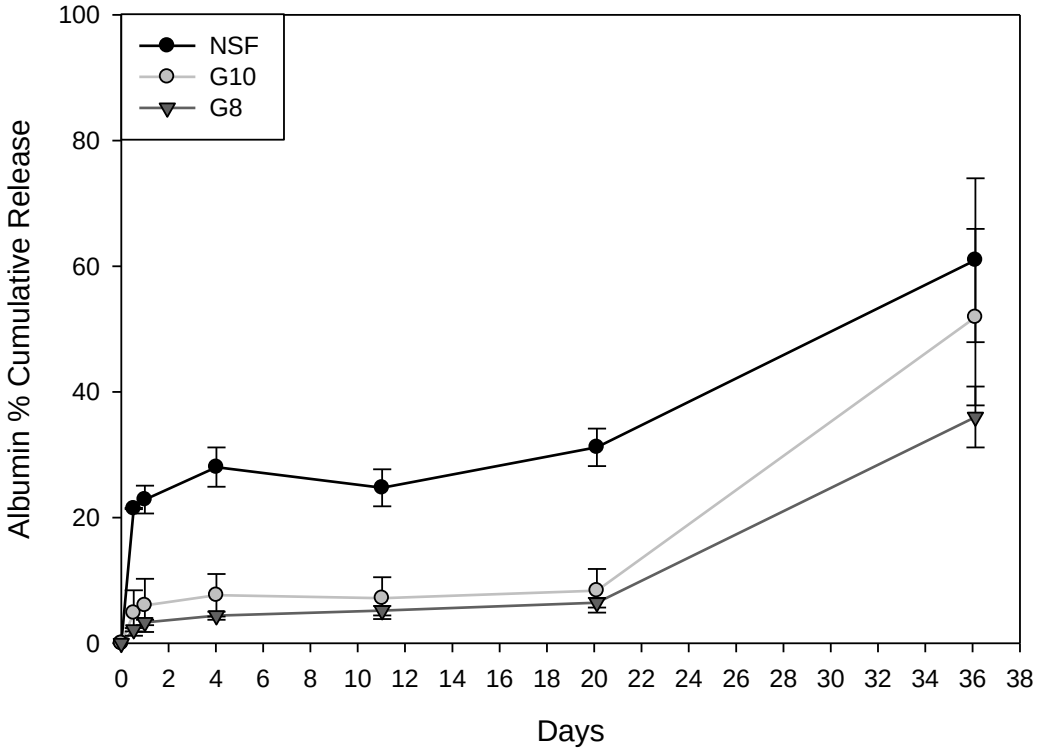

Figure 2.8 – Percent cumulative albumin release by total albumin loading calculated as: cumulative mg albumin released per total mg encapsulated albumin. RM-ANOVA for all treatment groups was significant (P=0.004). Individual comparisons between treatment groups by RM-ANOVA reveal G8 microsphere release drug significantly slower than NoSf microspheres (P=0.002) while G10 strongly trends toward slower release compared to the NSF group (P=0.022).

in the tissue. NoSf microspheres demonstrated a high burst-release where 23 % of encapsulated BSA was released in 24 hours. At 3 and 6 %, G8 and G10 emulsions had significantly less burst-release compared to NoSf formulations (P=0.002 and 0.003, respectively).

Differential Scanning Calorimetry

The glass transition temperature (T_g) was determined to assess the penetration of surfactant or BSA in the PLGA matrix (Mohamed and van der Walle, 2006). Any molecule that reduces PLGA-PLGA interactions decreases the free volume between polymer chains will increase the molecular mobility of the polymer chains. This results in a plasticizing effect, whereas molecules that promote PLGA-PLGA interaction or increase free volume will achieve the opposite and are termed ant-plasticizing agents. Both surfactants and proteins in the microsphere formulation can interact within the PLGA matrix resulting in a detectable change in T_g. DSC thermograms indicate that unmodified PLGA had a T_g onset at 50.9 °C (Figure 2.9; Table 2.6). Microspheres that contained only BSA had an anti-plasticizing effect, for example increasing PLGA Tg to 52.1 °C, which is consistent with other reports (Bouissou, et al., 2006). The surfactants, when prepared in microspheres in the absence of BSA, had opposing effects on the T_g. G10 had a plasticizing effect, suggesting the molecules of this surfactant positioned themselves within the PLGA polymer network in such a way that the PLGA had more chain mobility. In contrast, addition of G8 surfactant raised the T_g from 50.9 °C to 62.2 °C, consistent with an anti-plasticizing effect. When BSA was added to the formulation along with G8 or G10 the effect was always anti-plasticizing and both formulations had a T_g at approximately 55 °C.

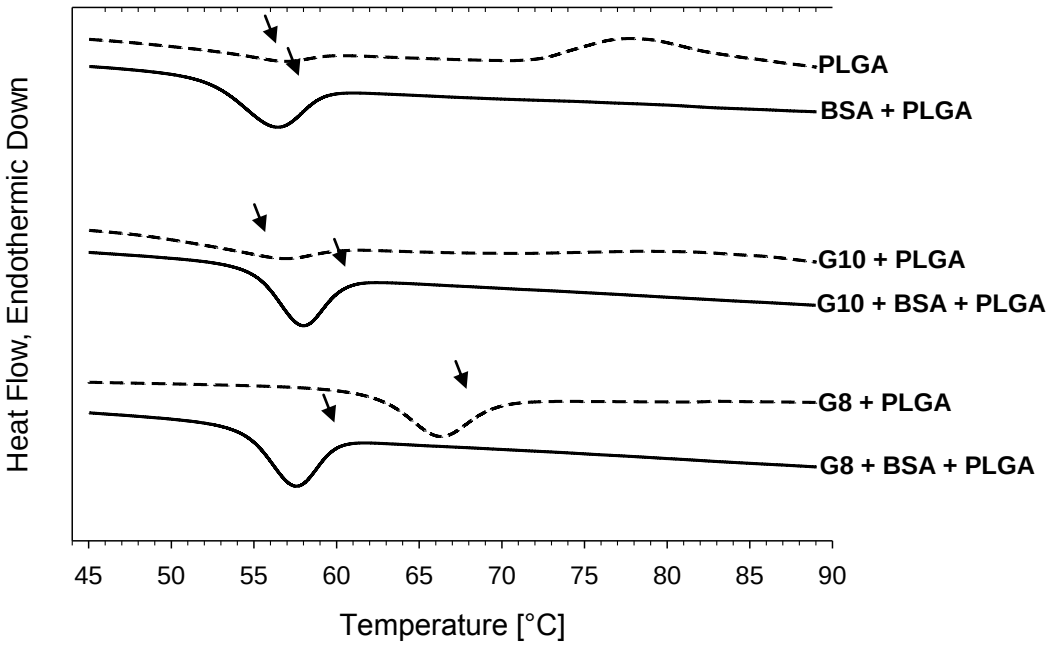

Figure 2.9 – DSC thermograms for PLGA 50:50 combined with albumin, surfactant, or both. Each treatment went through the process of microsphere synthesis by the w/o/w method followed by freeze drying prior to thermal analysis. Arrows represent an estimate of the onset T_g, while the software accentuated more precise T_g values given in table 2.6.

Table 2.6 – Onset glass transition temperature (T_g) for w/o/w microspheres prepared from the components listed below.

Microsphere Components	Onset T_g [°C]
PLGA only	50.9
PLGA + BSA	52.1
PLGA + G10	49.4
PLGA + G8	62.2
PLGA + G10 + BSA	54.9
PLGA + G8 + BSA	54.2

In situ BSA Aggregation at W/O interface

Samples from the aqueous surface layer of the two phase water-DCM solution taken after 30 min at RT revealed a decrease in concentration of diluted BSA. This was noticeable as the BSA formed a small, visible white precipitate at the surface of the W/O interface. Control samples lost only 2.7 % of the dissolved BSA from solution likely due to adsorption to the surfaces of the transfer pipette or the borosilicate test-tube. The aqueous BSA exposed to DCM containing PLGA averaged 94.0 % concentration at the end of 30 minutes which was a loss of approx 6.0 % to the DCM and glass surfaces, almost significantly different from the control treatment (Figure 2.10; $P=0.019$). When G10 was present in the organic phase a significant amount of protein, 7.3 %, was lost compared to the control group ($p<0.008$) yet this result was not different from BSA samples exposed to DCM without addition of surfactant ($P=0.150$). When G8 was present in the organic phase more BSA precipitated out of solution at about 12.0 %, a significant difference from all groups ($p<0.008$).

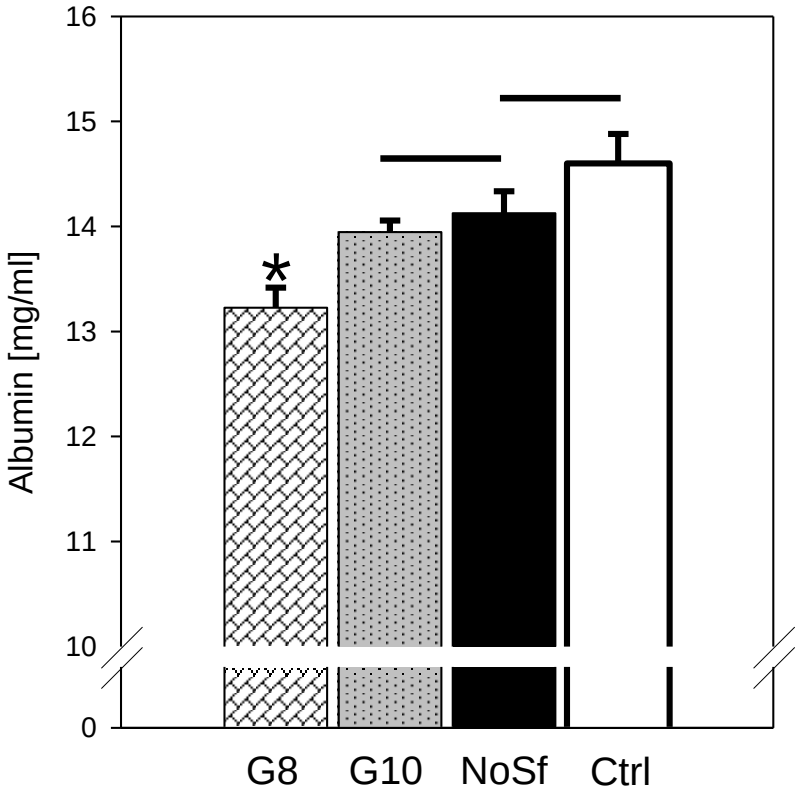

Figure 2.10 – Albumin recovered from the aqueous phase after exposure of albumin solution (15 mg/ml) to DCM as a single W/O interface.

DISCUSSION

For assessment of emulsion stability we used a creaming analysis which is a measurement of the velocity of the dispersed water phase as it rises toward the surface of the emulsion. Stokes' Law demonstrates that the velocity of a spherical particle moving through a medium is related to the square of its radius (relevant equations can be found in Hiemenez & Rajagopalan, 1997. Our emulsion analysis is a comparison of water droplet diameter with these assumptions: the dispersed phase consists of non-aggregated and spherical water droplets, diffusion is negligible, and the limitations of light scattering (e.g., multiple scattering and differential scattering by different droplet sizes) are consistent between emulsions. The rate of change in the turbidity curve generated by the emulsion analysis demonstrates for all formulations a rate of change that gradually increases and then decreased over time. This shape is consistent with a heterogeneous distribution of water droplet sizes, since water droplets in different size categories will move through the medium at different rates.

The choice of surfactants used in microsphere synthesis and their concentration were chosen based on the results from these emulsion analyses. We chose the surfactants associated with the largest difference in creaming rate (G8 and G10), because they would likely provide the most dramatic results regarding the effect of emulsifier on drug release. The concentration of surfactant in the organic phase was selected as 8.55 mM based on the information provided by emulsion analysis comparing surfactant concentration. Microspheres without surfactant were used as a reference.

Upon generating microspheres from these three formulations the G10 group had noticeably smaller microsphere diameter. Measurement performed on

SEM images demonstrated this difference. It is known that overall microsphere diameter is affected by the viscosity of the primary emulsion (Li, et al., 2008). We speculate the reduction of microsphere diameter resulted from reduced viscosity owing to the presence of G10 surfactant. However, no formal experiment was performed to test this hypothesis. It was unexpected to find that two additional hydrocarbons on the chosen surfactant could significantly influence microsphere diameter to this degree. The smaller average microsphere diameters of G10 formulations are predicted to result in more rapid BSA release (Ruan, et al., 2002). This was not evident until the final stage of BSA release starting at 20 days, where G10 microspheres released BSA more rapidly than G8 and NoSf.

Microspheres contained numerous pores on their surface. Surface porosity likely occurred where droplets of the primary emulsion were involved in nucleation with the secondary aqueous phase during microsphere preparation. At the site of nucleation PLGA was displaced, therefore leaving a void area on the microsphere surface. They may have also formed in high vacuum during gold sputtering by rupture of the microsphere surface where the surface was covered by a very thin polymer layer. These surface formations are of interest, because they have been associated with changes in drug release profile and drug encapsulation (Kang and Singh, 2001). However, in our experiment there was no significant difference in this morphological characteristic between formulations. We only distinguished a trend for increased pore area on the surface of G10 microspheres. This led us to examine the other potential contributors to the difference in drug release including internal morphology, polymer plasticity, and protein adsorption to the microsphere surface.

Internal microsphere porosity was different between formulations. This most intriguing part of these results is that there is a profound difference in internal porosity by slight changes in the added surfactant's hydrocarbon chain. This result demonstrates the effect of stabilization of the primary emulsion with surfactants. This stabilization resulted in: a) discrete internal porosity with a smaller distribution of pore sizes, and b) prevention of the seepage of water from the external aqueous phase into the interior of the microsphere. During the first two weeks of protein elution, BSA release from the microspheres was consistent with evidence from the internal morphological analysis. It is evident that smaller and more uniform internal porosity contributed to reduced BSA release for the initial 20 days of release.

The presence of additive in the PLGA matrix causes changes in the glassy state of the polymer matrix observable by changes in the glass transition temperature (T_g) (Bouissou, et al., 2006). For proteins encapsulated in PLGA microspheres, in this case BSA, it is thought that van der Waals and hydrogen bonding forces between PLGA and unfolded protein results in reduced PLGA mobility. We indicated this in our DSC results were microspheres containing BSA had slightly a higher value of T_g compared to PLGA alone. We found the addition of G8 and BSA increase microsphere T_g while G10 decreases microsphere T_g. The plasticizing effect of G10 was not found in any other additive tested. This effect leads to increase in PLGA chain mobility, the consequences of which may include more rapid drug release. However, the T_g of microspheres prepared with BSA combined with either surfactant, approx. 54 °C, were higher than microspheres prepared with BSA alone. This increase may represent the trapping of more molecules within the PLGA matrix, including encapsulated BSA. Although individual interactions cannot be fully addressed by this analysis we may describe the addition of surfactant to result in higher BSA-

PLGA association and slower release of BSA from the matrix. This PLGA associated BSA may not be freed until significant degradation of the polymer has occurred.

Lastly, the surface adsorption of BSA was studied. We found that the precipitation of BSA at the W/O interface was minimal when surfactants were not present in the organic phase. This is not surprising given the gentle mixing conditions in this experiment. These results are consistent with studies that demonstrate the sorption of BSA at a water-DCM interface is low even under more intense mixing conditions (Sah, 1999; Sah, 1999). Furthermore, addition of surfactant increased the adsorption of protein at the W/O interface. In G8 emulsions, more protein was precipitated at the interface compared to G10 and NoSf emulsions. It is unexpected that presence of surfactant would increase surface adsorption of BSA, because surfactant localization at the W/O interface is expected to prevent BSA interaction with the organic solvent. Surfactant-BSA interaction could be the cause. Albumin is known to have approx. 15 binding sites for G8 and G10, yet this binding does not cause conformational change in aqueous buffer (Wasylewski and Kozik, 1979). The surfactants appear benign to BSA conformation in aqueous buffer. However, in the presence of water-DCM interface the activity of surfactant-protein complexes is thought to be unstable and result in protein conformational change. Kwon et al. (2001) show similar results where alkyl glycoside interaction with the peptide insulin cause increased insulin precipitation in the presence of a water-DCM interface (Kwon, et al., 2001)

CONCLUSIONS

Alkyl glucosides are good candidate surfactants for use in constructing implantable PLGA devices, because of their biocompatibility and ability to modulate protein release. By analysis of primary emulsions in the double-

emulsion method we were able to select an alkyl glucoside HLB and concentration which lead to better control of internal microsphere morphology. This morphology, owing to small differences in surfactant structure, lead to a range of BSA release kinetics. Reduction in the initial burst release from microspheres was consistent with small and discrete internal microsphere porosity. This range of release kinetics is a useful tool for testing controlled release formulations where the drug dose is not known, or where rapid release is beneficial in some applications but not in others.

CHAPTER THREE
Encapsulation & Release of Thymosin B-4 from PLGA Microspheres

ABSTRACT

Thymosin β-4 (TB4) is a 43 amino acid peptide found to have regenerative properties in the ischemic myocardium. PLGA microspheres are proposed as an effective delivery method to overcome past failures in delivery of peptides to the myocardium. The purpose of this study was to encapsulate TB4 in PLGA microspheres and determine that we could show TB4 controlled release over a four week duration, consistent with the clinical timeframe of healing after an ischemic event. TB4 encapsulation was performed using the double-emulsion solvent extraction method. PLGA 50:50 with a M_w of approx. 50 kDa was used. The addition of alkyl glucoside surfactants octyl-β-D-glucopyranoside (G8) and decyl-β-D-glucopyranoside (G10) to organic phase during microsphere synthesis was performed to determine their influence on TB4 primary emulsion stability, encapsulation efficiency, and release kinetics. Microspheres prepared without surfactant were used as a reference. G8 surfactant stabilized the primary emulsion more effectively than G10 surfactant or emulsions prepared without surfactant. Encapsulation efficiency was highest in microspheres prepared with the G8 stabilized emulsions, 98.4 %. The majority of drug release occurred within the clinical timeframe of four weeks in G8 microspheres and microspheres prepared without surfactant (74 % & 73 % cumulative release, respectively). G10 microspheres released drug significantly slower after four weeks (20 % cumulative release). These results indicate the encapsulation of TB4 in PLGA microspheres using the double-emulsion method is very effective, especially in the presence of G8 surfactant. Drug release occurs within the desired clinical setting. Lastly, the release of TB4 can be reduced with the application of G10

surfactant which will be useful in future *in vitro* and *in vivo* testing, because the therapeutic dose of TB4 in humans not known.

INTRODUCTION

Irreversible damage to the heart after an ischemic events caused by coronary artery atherosclerosis, is expected to be treatable with controlled release of the therapeutic peptide TB4. TB4 is short peptide previously shown in our lab to improve heart function in a mouse model of myocardial infarction (Bock-Marquette, et al., 2004). It is also involved in progenitor cell recruitment and angiogenesis in the heart (Bock-Marquette, et al., 2009). Despite the promising effects of peptides, many have failed in humans resulting from short residence time and poor cellular uptake. To overcome this, we suggest the use of microencapsulation as a formulation for TB4. Microencapsulation can protect peptide function, improve drug half-life, and requires fewer interventions. This study describes the first controlled release PLGA microsphere formulation designed with the intention for implantation and dissemination of TB4 in the ischemic myocardium. Other applications for our TB4 microsphere formulation include accelerated wound healing, especially for diabetic ulcers, or used in combination with other drug delivery technologies.

We developed a PLGA microsphere formulation that demonstrated slow release of TB4 for four weeks *in vitro*. The double-emulsion technique was used to encapsulate TB4 within poly(lactic-co-glycolic acid) polymer microspheres. The non-ionic surfactant octyl glucopyranoside (G8) or decyl glucopyranoside (G10) were used to increase emulsion stability, which is known to affect microsphere morphology and drug release kinetics. Primary emulsions were prepared using 8.55 mM of G8, or G10 surfactant in the organic phase of the

primary emulsion. Microspheres prepared without surfactant were used as a reference. These emulsions were subjected to primary emulsion stability testing by comparison of creaming rate. We completed double-emulsion microsphere formation by adding these primary emulsions to a secondary water phase. The elution of TB4 from these three microsphere formulations was carried out for 28 days to determine the effect of the presence of surfactant and surfactant type on the peptide release pattern. By emulsion analysis, we determined that G10 significantly increased the rate of primary emulsion creaming compared to emulsions generated with G8 or no surfactant. Surprisingly, this reduction in emulsion stability resulted in microspheres with slower release rates of TB4.

MATERIALS & METHODS

Thymosin β-4 (*Homo sapiens*) (TB4) was synthesized by the Protein Chemistry Technology Core facility at UT Southwestern with the sequence:

[Ac-**S**-**D**-**K**-**P**-**D**-**M**-**A**-**E**-**I**-**E**-**K**-**F**-**D**-**K**-**S**-**K**-**L**-**K**-**K**-**T**-**E**-**T**-**Q**-**E**-**K**-**N**-**P**-**L**-**P**-**S**-**K**-**E**-**T**-**I**-**E**-**Q**-**E**-**K**-**Q**-**A**-**G**-**E**-**S**-COOH]

The Mw of TB4 is 4963.5 Da and contains an acetylated N-terminus. Dichloromethane (DCM), poly(vinyl alcohol) (PVA), phosphate buffered saline (PBS), and the bicinchoninic acid assay (BCA assay) were purchased from Sigma-Aldrich. PLGA with a 50:50 ratio of lactic acid to glycolic acid and inherent viscosity of 0.35 - 0.45 dL/g (M_w 41 – 59 kDa) was purchased from Lakeshore Biomaterials. Alkyl glucoside surfactants were purchased from Anatrace. Trifluoroacetic acid, and acetonitrile were purchased from Fisher Scientific. All other chemicals were purchased from Sigma-Aldrich.

Microsphere Synthesis

Microspheres were synthesized by the water-in-oil-in-water (w/o/w) double-emulsion method. Briefly, 250 mg PLGA 50:50 was dissolved in 5.0 ml DCM. The indicated amount of surfactant was carefully weighed and added to the DCM-PLGA mixture. To generate the primary emulsion, 200 µl of 2.5% (w:v) TB4 in water was pipetted into the DCM-PLGA-surfactant mixture. The coarse emulsion was vortexed for 10 sec followed by indirect sonication. Sonication was achieved using a cup-horn sonication probe (Soncis & Materials Inc. model CV17) with a circulating bath of water and glycol maintained at 1.1 ± 1 °C. The emulsion was sonicated in a 50 ml Erlenmeyer flask with a flat bottom to increase surface area for transmission of acoustic energy to the emulsion. To generate the second emulsion, the sonicated mixture was added dropwise to a beaker containing 20 ml of 1.0 % (w:v) PVA being stirred at 300 rpm with an overhead stirrer (Caframo model BDC 250). DCM was extracted at RT for 6.0 hrs. The resulting microspheres were washed to remove small particles and excess PVA using a 15 µm sieve (BioDesign Inc. of New York). Microspheres were frozen in liquid nitrogen and freeze dried in a small vacuum chamber with a liquid nitrogen moisture trap.

Emulsion Analysis

This analysis was performed by generating primary emulsions containing TB4 and G8, G10, or no surfactant (NoSf) in the organic phase. Primary emulsions were prepared by the method described in microsphere synthesis. Directly after sonication the primary emulsion was transferred to a 2.0 mm path-length quartz cuvette and sealed with a Teflon stopcock. Rapid creaming of the emulsion was achieved by placing the cuvettes in a bench-top centrifuge at 28 x gravity and measuring the change in turbidity at specific timepoints up to 12 minutes, temperature was maintained at 25°C.

Encapsulation Efficiency (EE)

Drug loading efficiency was calculated for TB4 by carefully weighing Approx. 15 mg microspheres into borosilicate vials. 1.0 ml of chloroform was added to the microspheres to dissolve the polymer followed by addition of 1.0 ml of PBS buffer to extract the TB4. TB4 concentration was determined by reverse phase HPLC (method described in following section). EE is calculated as the percent of TB4 recovered from the formulation divided by the amount of TB4 used to generate the formulation, 5.0 mg. Each surfactant group was analyzed in triplicate.

TB4 Release

2.0 ml phosphate buffered saline (PBS) was added to 75 mg of microspheres, the exact weight of microspheres was carefully recorded. TB4 release was carried out in borosilicate vials in an oven at 37 ± 1.0 °C rotating horizontally at approx. 10 rpm. 1.0 ml of drug release media was collected and replaced with fresh PBS at pre-determined timepoints. TB4 in the collected drug release medium was quantified by reverse phase HPLC (Dionix, UltiMate 3000) equipped with porous channel monolith type column (Proswift® RP-2H; phenyl surface chemistry; dimensions 4.6 × 50 mm). The mobile phases consisted of A: 95 % H_2O, 5.0 % acetonitrile and 0.1 % TFA and B: 95% acetonitrile, 5.0 % H_2O H and 0.1 % TFA. The mobile phase decreased from 99 % A to 15 % A in 2.75 minutes using a gradient method with flow rate of 2.5 ml/min (see Appendix part C for program information). Detection of TB4 was set at 214 nm with TB4 retention time at approx. 1.27 minutes.

RESULTS

Emulsion Analysis

Emulsion analysis demonstrated the rising of the cloudy emulsion water droplets in the dichloromethane over time. The initial turbidity of G10 emulsions was significantly lower than the G8 and NoSf emulsions ($P<0.001$). This suggests that the total distribution of water droplets in the G10 emulsion does not scatter as much light as the G8 and NoSf emulsion. Upon creaming of these three emulsions at accelerated gravity we found G10 emulsions remained less turbid than G8 or NoSf emulsions throughout the creaming analysis ($P<0.001$ and $P=0.014$, respectively; Figure 3.10).

Encapsulation Efficiency (EE)

EE was high in all formulations, but nearly 100 percent in when G8 surfactant was used in the organic phase. EE was detected in NoSf microspheres at 74.8±20.2 %, in 82.1±8.3 %, and 98.4±2.7 % in G8 (Figure 3.2). G8 encapsulation was significantly higher than the other two microsphere formulations ($P<0.01$). We were pleased to see that the small and water soluble TB4 was entrapped within microspheres with high efficiency. It appears that the G8 surfactant facilitates the retention of TB4 during the process of microsphere synthesis.

TB4 Release

Drug release from TB4 microsphere formulations were compared in two ways. The first was the cumulative percent of TB4 released calculated as the cumulative release of TB4 per mg of microspheres (Figure 3.3). The elution pattern in this analysis shows a minimal initial release for all formulations below 10 % of the total encapsulated drug that was followed by a two week lag phase where release in all formulations remained under 20 %. At 14 days, drug release

rates increased substantially in the G8 and NoSf formulations while the only slightly increased in the G10 formulation. Upon completion of the 28 day elution period, 74 % TB4 release was accounted for in the G8 formulation, 73 % in NoSf, and 20 % in G10 microspheres. G10 microspheres released significantly less TB4 over time compared to G8 and NoSf microspheres (RM ANOVA: $P<0.001$ and $P=0.005$, respectively), and there was no difference in release between G8 and NoSf microspheres. We also observed for NoSf and G8 formulations the total weight of drug released is higher in the TB4 formulations compared to the BSA formulations at 28 days (Table 3.1).

The second comparison of TB4 drug release shows the cumulate percent of TB4 release (Figure 3.4). This is calculated as the cumulative mg of TB4 released per mg of TB4 loaded in the microsphere formulation (determined by EE analysis). We find a similar tri-phasic pattern of drug release as well as the same slow elution of TB4 from G10 microspheres compared to G8 and NoSf formulations ($P<0.001$ and $P=0.014$, respectively).

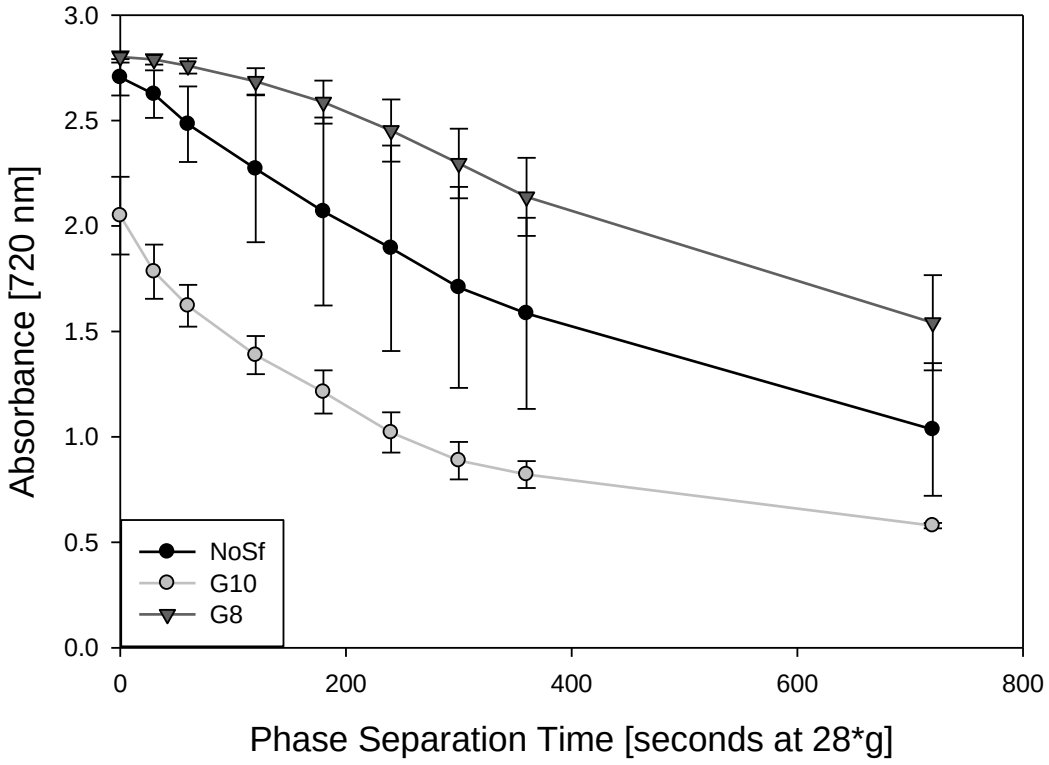

Figure 3.1 – Emulsion analysis of TB4 primary emulsions generated with alkyl glucosides G8, G10, or no surfactant. RM-ANOVA for all treatment groups was significant ($P<0.001$). Individual comparisons by RM-ANOVA demonstrate the turbidity of G10 emulsions decreases significantly faster than G10 and NoSf emulsions ($P<0.001$ & $P = 0.014$).

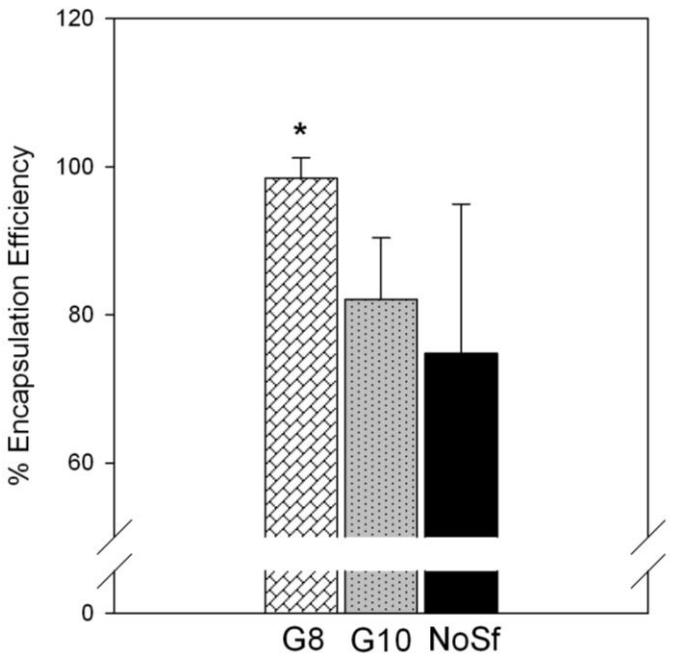

Figure 3.2 – TB4 encapsulation efficiency calculated as the percent of TB4 loaded per theoretical loading (5 mg). Encapsulation efficiency was significantly higher in G8 microspheres ($P<0.01$).

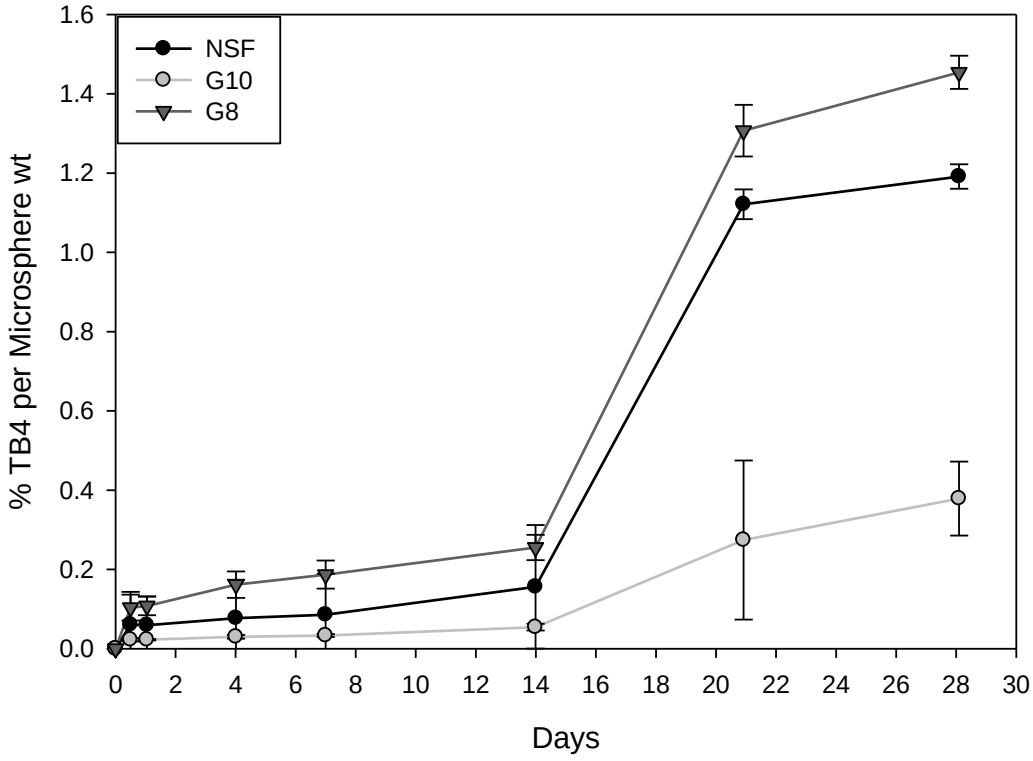

Figure 3.3 – Percent cumulative TB4 release by microsphere weight calculated as: cumulative mg TB4 released per total mg microspheres. RM-ANOVA for all treatment groups was significant ($P<0.001$). Individual comparisons between treatment groups by RM-ANOVA reveal G10 microsphere release drug significantly slower than both G8 and NoSf microspheres ($P<0.017$).

Table 3.1 – Percent cumulative mg drug release per mg microspheres at 28 days

Formulation	BSA	TB4
NoSf	0.6%	1.2%
G10	0.4%	0.4%
G8	0.2%	1.5%

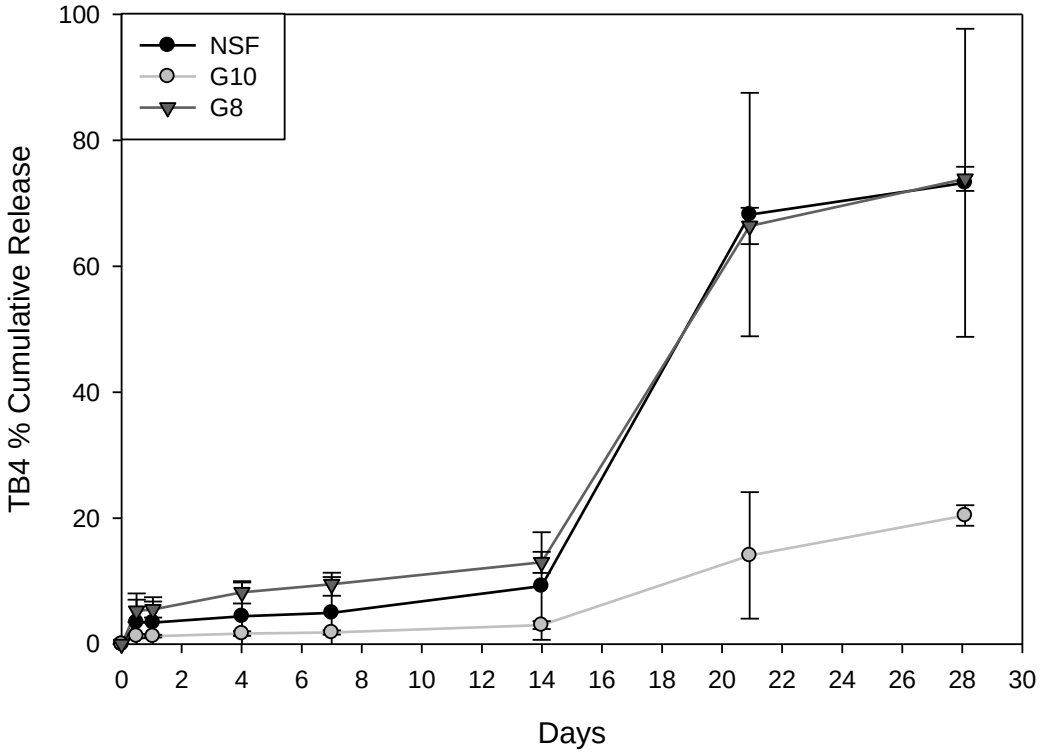

Figure 3.4 – Percent cumulative TB4 release by total TB4 loading calculated as: cumulative mg TB4 released per total mg encapsulated TB4. RM-ANOVA for all treatment groups was significant (P=0.002). Individual comparisons between treatment groups by RM-ANOVA reveal G10 microsphere release drug significantly slower than both G8 and NoSf formulations (P<0.017).

DISCUSSION

The encapsulation and release of TB4 from PLGA microsphere was successful and there are a number of beneficial outcomes from this analysis. One, we were able to retain TB4 in the microspheres during synthesis with high efficiency. This result is important because the cost of drug formulations is a significant issue when performed in large scale with synthetic peptides. Secondly, we demonstrated release of TB4 within a timeframe relevant to the healing of myocardial infarction, 28 days (Sun, et al., 2000). Lastly, we were able to modulate the release kinetics of TB4 with the addition of alkyl glucoside surfactants. G8 surfactant resulted in about three-quarters of TB4 to be released after 28 days. In G10 surfactants the release that occurred over this duration was about a third of the mass of TB4 that released from the G8 microspheres.

Difference between TB4 and BSA primary emulsions were observed. One of these differences was that G10 primary emulsions were less stable than the NoSf group in the TB4 experiment (P=0.014) whereas they are equally as stable in the BSA experiment (P=0.667). Another contrasting result was that G8 emulsions were equally as stable as NoSf in the TB4 formulations (P=0.099) whereas G8 emulsions were more stable than both NoSf and G10 in the BSA formulations (P=0.027 and P=0.003, respectively). These differences are attributed to differing interactions in the system when TB4 was substituted for BSA. TB4 is smaller (5 kDa) and very water soluble (Ch. 1, Figure 1.9, hydropathy plot calculated from TB4 primary sequence) compared to BSA which is large (66.5 kDa) and globular with many hydrophobic residues. Owing to the lack of hydrophobic residues, TB4 is also likely to be less surface active in relation to BSA. Furthermore, interaction between the added alkyl glucosides and

TB4 are different compared to interactions between alkyl glucosides and BSA. BSA is known to bind hydrocarbon chains such as those present on the hydrophobic portion of alkyl glucosides (Wasylewski and Kozik, 1979). The difference in TB4 surface activity and alkyl glucoside interactions are two potential contributors to the difference in emulsion stability and would be a focal point for further studies on these TB4 microsphere formulations.

Interpretation of the emulsion analysis results with respect to drug release revealed that reduced rates of emulsion creaming did not correlate with slower overall release of drug from the microspheres. Our previous experience in the BSA studies demonstrated that the G8 emulsion was significantly more stable than NoSf and G10 emulsions. G8 emulsions lead to more uniform and smaller internal porosity. The drug release from G8 microspheres was the slowest of all three formulations, partially owing to tighter control of the internal morphology. Therefore we could interpret greater emulsion stability as predictive of slower release rates of BSA. Concerning TB4 release, G8 and NoSf emulsions were significantly more stable than G10 emulsions. However, the release of drug from G8 and NoSf microspheres was more rapid compared to G10 microspheres in the 28 day release period. We observed a significant difference in emulsion stability does result in significant changes in drug release. However, we are unable to predict whether that change will be an increase or a decrease in release rates. This suggests a few things about our emulsion analysis: one, carrying out the analysis for a longer period of time may provide a more complete picture needed to compare TB4 emulsions, and two, the predictive ability of the emulsion analysis used to compare surfactants may be confined to each unique microsphere formulation.

A third possibility regarding the emulsion analysis involves a light scattering effect. The significantly lower initial absorbance of the G10 emulsions suggests that a significant portion of the emulsion was not scattering light with as much intensity as the G8 and NoSf treatment groups. The initial absorbance value of this emulsion was approx. 2 AU. This was the lowest of all emulsions tested, even including the albumin experiments. It may be resulting from the presence of very small water droplets in the emulsion that does not scatter light with as much intensity as larger droplets. If this is the case, it suggests that the G10 emulsion contains a significant amount of very small water droplets below 720 nm in diameter. If this is the case, G10 may be the most stable emulsion by our criteria of small water droplets. Furthermore, microspheres prepared with G10 surfactant would show the smallest internal pores. Dissection of the microsphere and viewing by TEM would provide evidence to support this hypothesis.

Overall, EE was high in when encapsulating TB4 in microspheres. Most interesting is that in TB4, the addition of G8 surfactants sustained significantly higher rates of drug loading while in BSA microspheres, addition of G8 was consistent with the lowest encapsulation rates. We hypothesize that the difference in EE between BSA and TB4 microspheres arises from the different interactions that occur at the water-DCM interface during microsphere synthesis. BSA cannot tolerate sonication of the water-in-oil primary emulsion as effectively as TB4 owing to the complex secondary structure of BSA. The result of this harsh treatment would be BSA denaturation, aggregation, and precipitation at the water-oil interface. Our method of calculating drug loading requires re-suspension of the microspheres in organic solvent followed by extraction of water-soluble molecules into an aqueous buffer solution at pH 7.4. The content of loaded protein is quantified from the aqueous buffer. If the encapsulated BSA within the microspheres was denatured and precipitated it would not partition into the

organic phase and would be undetected by HPLC. TB4, however, contains nearly all hydrophilic amino acid residues and may be more resistant to aggregation and precipitation. Therefore it would be more accessible to be quantified by our EE analysis. This hypothesis is supported by an alternative analysis of EE performed on BSA microspheres. We extracted BSA from PLGA microspheres by rapid degradation of the PLGA with in 0.1 N NaOH and 0.1 % SDS (sodium dodecyl sulfate). The detergent in this method, SDS, re-suspends precipitated BSA. Protein in the degraded microsphere solutions was quantified with a bicinchoninic acid assay (BCA). The BCA assay works in a non-specific way of detecting any molecule with an amide bond. Results from the BCA assay show BSA loading was 97±7 % for G8, 107±12 % for G10, and 85±11 % for NoSf formulations. The drawback to the BCA assay is that it has poor accuracy at low protein concentrations.

Electron microscopy showing both internal and external morphology of the TB4 formulations would provide important evidence for the effects these surfactants have on the microsphere formulation. We would be especially interested to see if the more rapid releasing G8 and NoSf formulations have larger and more interconnected internal pores.

CONCLUSIONS

Analysis of double-emulsion microspheres for the extended release of TB4 was performed. Emulsion stability results predicted a significantly different creaming rate in the G10 microspheres compared to G8 and NoSf microspheres which was consistent with a significantly different drug release pattern. The lower initial absorbance by the G10 emulsion suggests that light scattering is not similar to the G8 and NoSf emulsions. The stability of the G10 emulsion was

lower than that of G8 and NoSf emulsions leading us to believe that the emulsion would result in a more porous microsphere interior, faster rates of diffusion and finally a higher burst release of TB4. This was not the case showing that analysis of other factors affecting drug release is required to determine why G10 and G8 surfactants lead to variations in TB4 release kinetics. The TB4 formulations generated here demonstrate release kinetics that fit the important timeframe of the healing process of myocardial infarction, and the addition of alkyl glucosides resulted in a range of release kinetics that will be useful in future *in vivo* and *in vitro* experimentation.

CHAPTER FOUR
Stability of Encapsulated Proteins

ABSTRACT

The secondary structure of a protein is typically essential for its proper function. The process of microencapsulation exposes protein to organic solvents and polymer surfaces where unfolding can occur. This is exacerbated by the intensity of mixing used to generate the emulsion, primarily sonication. We hypothesized the addition of alkyl glycosides would inhibit the exposure of a model protein to the water-DCM interface and aid in maintaining the secondary structure of BSA during double-emulsion synthesis. Changes to secondary structure of proteins can be determined by FT-IR Spectroscopy. The advantage to this method is that the regions of the IR spectrum at which protein secondary structure absorb, the amide I and II regions, encompass wavenumbers where PLGA does not interfere. Therefore BSA structure can be measured without deconstructing the microsphere. The purpose of this chapter was to compare BSA secondary structure after microencapsulation with or without surfactant added to the organic phase of the primary emulsion. Our results indicate BSA maintains more native secondary by percent alpha-helical content when G8 surfactant is present. Microspheres prepared without surfactant show slightly less BSA alpha-helical structure followed by microspheres prepared with G10 surfactant. These results did not reach statistical significance. We determined that sources of variation include poor signal strength in the amide I region of the IR spectra, inadequate controls, and absorbance of water from microsphere exposure to ambient relative humidity. Solutions to these issues include encapsulating higher amounts of BSA in the microspheres, re-lyophilizing the albumin after purchasing from the vendor, and storing microspheres in a vacuum between pellet preparation and analysis.

INTRODUCTION

The stability of proteins and peptides after encapsulation and release from PLGA microspheres is important because controlled release from degradable polymers is one of the few effective delivery strategies for these molecules. Stability refers to changes to the native primary or secondary structure of these molecules. The secondary structure of proteins can be altered during the processing of microspheres, especially when they are exposed to water-organic solvent interfaces. This results in a denatured protein which typically leads to irrecoverable loss of protein function. In the case primary structure, there are two potential alterations that can cause loss of function. One being chain scission caused by the acidic environment which results in two or more fragments. In another mechanism, lactic acid and glycolic acid monomers freed from degrading PLGA have functional end-groups that can covalently attach to labile amino acid R-groups. This reaction can be detrimental to peptides where alterations to one or two amino acid R-groups can greatly alter their function such as in receptor-ligand binding.

The denaturing of proteins can occur in microspheres during processing by the energy of mixing, exposure to organic solvents, adsorption at the water-oil interface, or adsorption to PLGA surface of the microsphere (Chesko, et al., 2005; Kang, et al., 2002). The study of protein precipitation during the emulsification process has been performed. It was found that addition of PVA to the aqueous phase of a W/O emulsion reduces the amount of lysozyme precipitation at the W/O interface resulting in 31% more active lysozyme remaining in the aqueous phase (van de Weert, et al., 2000). This study also demonstrates that addition of PLGA to the organic phase reduces the stabilizing effect of surfactants. Wei et al.

(2007) analyzed destabilization of a large 191 amino acid peptide, GH, at the W/O interface with the addition of surfactants (Wei, et al., 2007). In this work, Pluronic F127 was the most successful surfactant at preventing GH aggregation at the water-DCM interface. The protective effect of Pluronic F127 was shown to be effective in a concentration dependent manner. Both PVA and Tween 20 also provided a slight protective effect.

The addition of surfactants to microsphere formulations has been used to reduce the degree of structural perturbations to encapsulated proteins. Lecithin, a biosurfactant found in the cell membrane of both plants and animals was added to the primary emulsion of double-emulsion microspheres to determine its ability to stabilize bovine carbonic anhydrase (Sandor, et al., 2002). The addition of this surfactant preserved the protein activity at nearly 100 % compared to 73 % activity in microspheres prepared without surfactant. The biological efficacy of a protein comprised of an immunoglobulin-type beta-fold domain, FIII9'-10, was incorporated in the W/O/W process with surfactant molecules to determine if improvements in stability could be achieved (Bouissou, et al., 2004). The inclusion of the surfactants Igepal CA-630 or Triton X-100 were capable of maintaining levels of FIII9'-10's effects in a cell attachment assay close to those in the control group. In the work by van de Weert and Bouissou two common surfactants were tested, Tween 20 and Tween 80. The Tween surfactants did not reduce protein aggregation. These surfactants are very common therefore it is important to note that that the hydrophilic PEG segments in Tweens tend to prefer the organic phase in this specific water-DCM emulsion system. The solubility of PEG in the organic phase reduces the surface activity of these surfactants and is proposed to be the reason for their inability to improve protein structure in double-emulsion synthesis.

Form this work we can conclude that the presence of surfactant in the primary emulsion step of double-emulsions can be effective in preserving protein function. The most effective surfactant may be specific to the encapsulated protein's structure or chemistry.

The study of protein conformational changes after microencapsulation has been accomplished using biological assays as well as direct structural analysis. Bioassays involve collecting the released peptide and applying it to an assay where biological function is measured. This can involve quantifying its catalytic properties or studding its effect on cells *in vitro* and is considered to be highly important because these tests directly measure the functionality of the released molecule. Direct measurement of protein conformation can also be assessed to determine structural alterations during processing and release from microspheres. The two most utilized methods to determine changes to protein secondary structure are Fourier transform infrared spectroscopy (FT-IR) and circular dichroism (CD).

Secondary Structure Quantification of Proteins by FT-IR Spectroscopy

FT-IR can be used to determine secondary structural elements of a protein including β-sheets, α-helices, and random coils. We are especially concerned with the content of α-helices, because they can be used to indicate preservation of a protein's native conformation after the processing steps performed in microsphere synthesis (Fu, et al., 1999). The advantage of this method is that the structure of the encapsulated protein can be assessed without extraction from the microspheres. This is possible because PLGA does not absorb in the IR regions that are used to characterize protein structure. These regions are called the amide I and amide II regions. Most analyses are performed on the amide I region,

because it is centered on the wavenumber 1652 cm^{-1}. A peak at this wavenumber corresponds with protein α-helical structures. Also in this region, β-sheets correspond to peaks at 1629, 1638, and 1977 cm^{-1}. Unordered loops and turns are accounted for at 1646, 1672, and 1686 cm^{-1}. Detailed descriptions of this method have been provided by Fu, 1999 and Yang, 1999.

The research outlined in this section aims to provide evidence that alkyl glucoside surfactants will improve the retention of protein secondary structure during encapsulation by the double-emulsion method. By occupying the water-oil interface with surfactant, the exposure of BSA to the water-oil interface is expected to be reduced. This would result in a greater concentration of albumin being encapsulated in the native conformation compared to microspheres prepared without any surfactant.

METHOD

We encapsulated BSA in microspheres containing 8.55 mM of G8, or G10 surfactant as well as microspheres that did not contain any additional surfactant. These microspheres were prepared by the method outlined in Ch. 2. To remove as much residual water as possible, microspheres were freeze-dried in a vacuum container with a liquid nitrogen vapor trap for 48 hours prior to analysis. For each treatment group, five unique IR spectra were taken from dried microspheres formed into a 1 - 2 mm potassium bromide pellet using a model Bruker Vector 22 IR Spectrophotometer with software Opus v. 6.5 (Bruker Optics). The IR band region between 1600 cm-1 and 1700 cm^{-1}, which corresponds to the amide I region, was collected. The second derivative of each unique spectrum was obtained and normalized. Gaussian curve fitting was applied to determine the area under each peak of the second derivative spectrum. The peak at

approximately 1655 cm^{-1} is known to be associated with α-helical content of proteins (Yang, et al., 1999). In order to determine the percent α-helical content for each spectrum, the area under the curve at 1655 cm^{-1} was divided by the combined area under each Gaussian curve in the amide I region. All five unique spectra from each group were averaged and compared using ANOVA.

RESULTS AND DISCUSSION

Averaged second derivative spectra reveal the peak centered around 1655 cm^{-1} corresponding to absorption of α-helical regions is the largest peak in the amide I region (Figure 4.1). Analysis of the area under this peak compared to the surrounding peaks through Gaussian curve fitting gives % α-helical content. This analysis indicates that G8 microspheres have higher α-helical content (29±10 %) compared to G10 (21±5 %) and NSF (24±7 %) microspheres (Figure 4.2). The statistical analysis shows the ANOVA model to be significant (P=0.005, power=0.858). However, all pairwise multiple comparisons are insignificant except between G8 and the lyophilized BSA. In this case we conclude that the addition of surfactant was not effective in preserving α-helical continent of encapsulated albumin.

This insignificant result in comparison of α-helical content between BSA in different states came from the high variability we confronted in performing this analysis. Sample preparation is not typically a source of variability in FT-IR; however, absorbance of the PLGA polymer in the amide one region can be a source of interference (Yang, et al., 1999). Furthermore, the signal strength of the spectra we collected was very low (testimony of Dr. Brian Edwards at UTA chemistry core facility) which could be owing to low albumin content of the samples or limitations of the instrument. A further complication of this analysis is

that the lyophilized albumin control contained an unexpectedly low percentage of α-helical content (8±1 %) which is inconsistent with findings in the literature that show α-helical content to be approx. 31 ± 1 % (Fu, et al., 1999). Re-lyophilizing the albumin from the vendor may produce a lyophilized control with the previously reported alpha-helical content. Another source of variation could be the presence of water in the sample. Despite having lyophilized microspheres prior to analysis, the analysis was very time consuming and during this time our microspheres were exposed ambient relative humidity. Humidity is known to be absorbed by microspheres during storage resulting in changes to the PLGA matrix (Bouissou, et al., 2006). Careful control of water in the sample will be necessary as this may be a source of variability. This may even include storage of samples awaiting analysis in a vacuum with desiccant between preparation and analysis of other treatment groups.

A more accurate analysis of albumin α-helical content could be established by performing this experiment in conjunction with CD in order to confirm the FT-IR results. However, the significance of surfactant stabilization of protein secondary structure after encapsulation in PLGA microspheres is best interpreted when *in vitro* functional analysis is also available for the released protein. Without this we can only speculate that an additive to the microsphere formulation is effective in preserving protein activity.

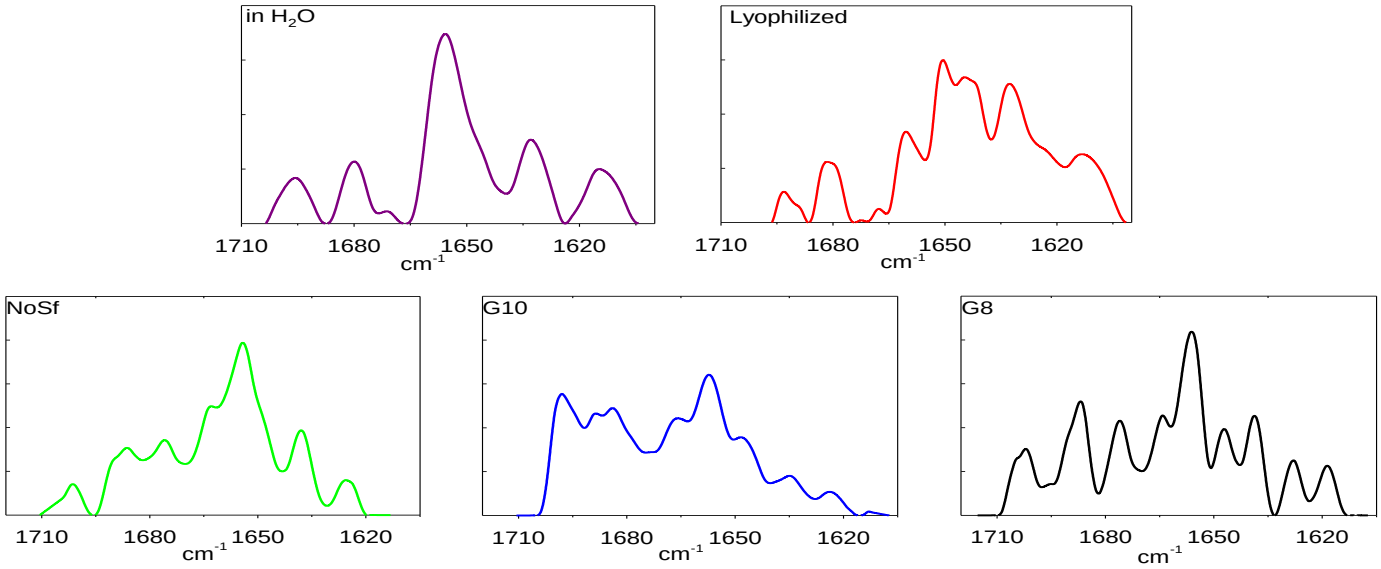

Figure 4.1 – Average second derivative IR spectra of albumin in the Amide I region. Albumin is in different states including: lyophilized crystals, dissolved in H_2O, encapsulated in G8, G10, or NoSf microsphere formulations. The tallest peaks centered around 1655 cm-1 represent α-helical secondary structure of albumin.

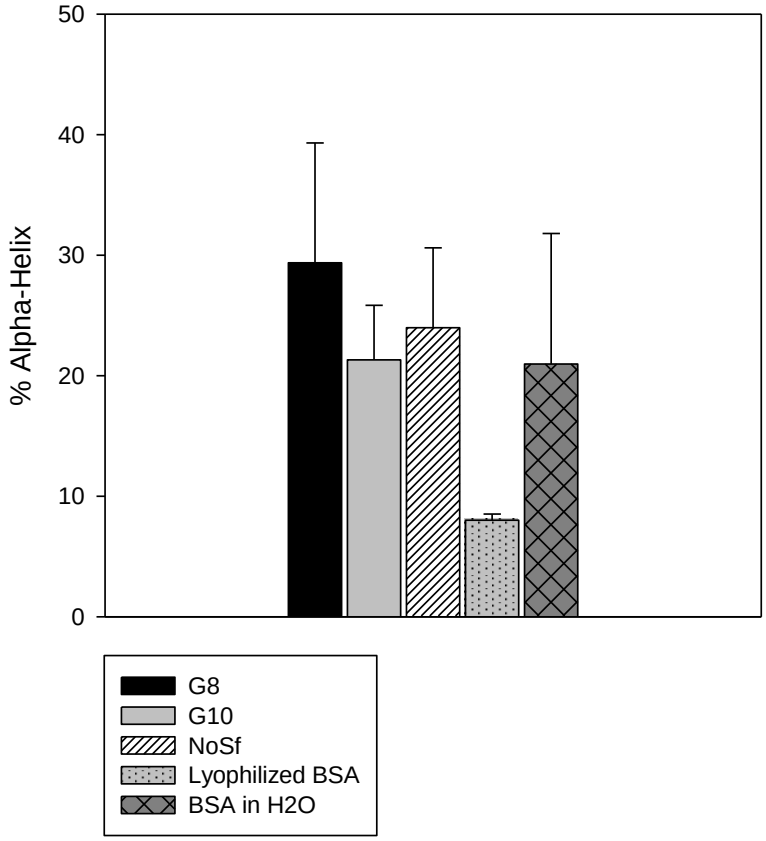

Figure 4.2 – Percent α-helical content of BSA in different states determined from amide I region in FT-IR spectra. G8, G10, and NoSf are microsphere formulations. The Full ANOVA model was significant (P=0.005). Individual comparisons between treatments show G8 has significantly more α-helical content than lyophilized albumin (P<0.005).

CHAPTER FIVE
Primary Structure Modifications of Peptides in PLGA Matrices

ABSTRACT

Covalent modification to protein and peptide amino acid R-groups can occur when exposed to the degradation products of PLGA. The rate of these chemical reactions increases in degrading PLGA microspheres resulting from low pH and the accumulation of PLGA degradation products in the microsphere interior (see Ch. 1, Degradation of PLGA & PLGA Microspheres). TB4 contains a number of labile amino acid R-groups that are known to be involved in a covalent modification called acylation. Acylation results in the addition of a lactic acid (LA) or glycolic acid (GA) monomer to the primary amine found on lysine or peptide the N-terminus. These modifications may inhibit the function of TB4 eluted from the PLGA matrix. The purpose of this chapter is to outline our development of a Liquid Chromatography-Mass Spectrometry (LC-MS) method for the quantification of acylated peptide exposed to PLGA degradation products. We incubated a model peptide, insulin, in low and high concentration LA solutions and collected aliquots at predetermined time points for LC-MS analysis. LC-MS analysis of insulin incubated in 50% LA for 21 days demonstrated the acylation reaction had occurred. Insulin molecules with masses corresponding to the covalent attachment of 1 to 4 LA monomers were present in this solution. The insulin mass spectrum also revealed numerous peaks relating to unknown chemical entities. We conclude this method of analysis will require the ability to carefully identify molecules producing the unknown peaks in the mass spectrum before it can be applicable for rapid quantification of TB4 covalent modification.

INTRODUCTION

In the last part of this thesis on surfactant stabilization of PLGA microspheres will contain a discussion on recent work in the arena of the stability of peptides and proteins. This includes difficult to detect alterations to peptide primary structure that go beyond chain scission, which is relatively straightforward to detect using SDS-PAGE. These alterations are the covalent attachment of PLGA degradation products to labile amino acids on the peptide chain.

Our interest in the generation of peptide impurities from degrading PLGA microspheres results from the potential for these reactions to inhibit the function of TB4 *in vivo*. Assessment of TB4 primary structure reveals nine lysine and four serine residues that are potential targets for covalent modification by lactic or glycolic acid monomers. We proceeded to establish a method to quantify these additions to the peptide chain using insulin as a model peptide. Our work in this area was blunted because of the time consuming process of collecting and analyzing this data. However, I have included information regarding the concepts in this field and our results in order to demonstrate the potential for its use in future experiments as well as to point out its difficulties.

As previously mentioned, the non-uniform degradation of PLGA microspheres causes a high concentration of acidic degradation products within the microsphere interior. This leads to acidic conditions with pH values around

1.5 - 4.7. The acidic microenvironment inside the microspheres can induce several chemical changes to encapsulated peptides. For instance, deamidation and covalent dimerization of insulin has been regarded as the major factor of peptide and protein instability within PLGA microspheres (Rothen-Weinhold, et al., 2000). In addition to deamidation and covalent dimerization, an acylation reaction can occur between peptides and PLGA catalyzed by an acidic environment. Lucke et al. (2002) have demonstrated that in this acylation reaction, the degradation of PLA and PLGA microspheres can result in covalent addition of LA and GA units to encapsulated peptides (Lucke, et al., 2002). Amino acids that are a target for acylation need to carry nucleophilic functional groups, such as primary amines. Similarly, the N-terminal amine group of a peptide could act as a nucleophile for the acylation reaction.

The source of the acylation reaction could be the result of many factors. The presence of LA or GA monomers in solution may be the only necessary factor in generating peptide acylation products. The pH of the reaction environment appears to play a major role in the mechanism of the acylation reaction (Lucke, et al., 2002). Also, Peptide adsorption to the hydrophobic PLGA polymer surface could be another source of acylation.

Promising solutions to reduce the acylation of labile amino acids by degrading lactic acid polymers include the following list derived from Sophocleous 2009:

- Increasing the microclimate pH from 2 to 6 (Lucke, et al., 2002; Murty, et al., 2003)
- Shielding the reactive amino group on the peptide by PEGylation (Na and DeLuca, 2005)

- Reducing polymer hydrolysis rate by encapsulating in PLGAs of high lactic:glycolic ratio (Murty, et al., 2003)
- Facilitating the release of water-soluble oligomers, for example by using PEG as a porogen (Jiang and Schwendeman, 2001)
- Prevent sorption of peptide to polymer chains with divalent cations such as CaCl2 MnCl2 (Sophocleous, et al., 2009)

The primary structure of TB4 demonstrates it has a high number of potential acylation sites. This information directed us toward establishing a method to detect covalent modification of peptides after release within degrading microspheres. The goal of this experimental pathway was to determine how much released TB4 was composed of acylation products, and whether they would have a detrimental effect on the therapeutic function of TB4. To begin, we established a method to detect acylation of the 51 amino acid insulin after incubation in lactic acid solutions.

MATERIALS & METHODS

85% Lactic acid (LA) solution (Arcos Organics) was purchased from Fisher Scientific. Lyophilized Bovine insulin (51 amino acids, Mw 5734 Da) was purchased from Sigma-Aldrich. All other chemicals for chromatography including acetonitrile and TFA were of HPLC grade and were purchased from Sigma-Aldrich. Filtered and UV treated DI water from a Barnstead filtration system was used.

Incubation of Insulin in Lactic Acid Solutions

LA solutions of 50, 20, 10, 5, and 1 % were generated by diluting LA solution in water. Insulin was added to each solution to generate corresponding

insulin concentrations of 179, 191, 196, 198, and 200 μg/ml. The solutions were incubated at 37 °C in polypropylene tubes for 28 days. 1.0 ml aliquots of the incubating solutions were drawn at 1, 8, 14, 21, and 28 days.

Liquid Chromatography-Mass Spectrometry (LC-MS)

Native insulin and insulin from lactic acid solutions were analyzed using a Shimadzu LCMS-IT-TOF (Shimadzu Scientific Instruments, Inc., Columbia, MD, USA). Insulin was separated by reverse phase chromatography using a C18 column. A gradient method was used starting with 90% A and decreasing to 10% A in 30 minutes. Mobile phase A consisted of 90 % H_2O, 10 % acetonitrile and 0.1 % TFA, and mobile phase B consisted of 90 % acetonitrile, 10 % H_2O and 0.1 % TFA. The IT-TOF was operated in the negative ionization mode with a spray voltage of −3.5 kV, and a scan range of 750–1260 m/z.

RESULTS & DISCUSSION

Results were obtained from native insulin and insulin incubated in 50 % LA solution for 21 days. Elution of native insulin from the C18 column occurred at approx. 13 min as a single peak. MS shows this peak consisted of insulin carrying four (+) charges. The mass of this peak was 5734.68 Da (Figure 5.1).

LA incubated insulin eluted from the C18 column as a bimodal peak between 12 and 15 min. MS analysis revealed this peak to contain molecules carrying 5, 6, or 7 (+) charges (Figure 5.2). The 7 H^+ region was between 800 – 850 m/z, the 6 H^+ region between 950 – 1010 m/z, and the 5 H^+ region between 1125 – 1250 m/z. Analysis of each region showed the presence of native insulin as well as insulin carrying a mass corresponding to covalent addition of 1, 2, 3 or 4 LA monomers.

The results of our LC-MS analysis demonstrates the good potential for screening of peptides released from PLGA microspheres for covalent modifications. This analysis is straight forward to interpret when the mass of the covalently added molecule is known. For example, from the m/z plots generated in this experiment we could quickly decipher the covalently modified insulin when one or more LA units were added. However, there are many other unidentified peaks in this sample. Some are likely the result of deamidation of insulin, but many peaks remain to be characterized.

We have learned that the LCMS method is simple to perform with the benefit of quickly producing information about the chemicals present in a solution containing a peptide of interest. The drawback of this method is that unknown peaks are difficult to interpret requiring more time for analysis. Despite the difficulty of peak interpretation, the 50 % LA solution sample was a good candidate for preliminary testing, because acylation reaction conditions are more favorable in a high LA concentration and high acidic environment. Nevertheless, it may be owing to this solution of high LA concentration that there were so many unidentifiable peaks on the spectrum.

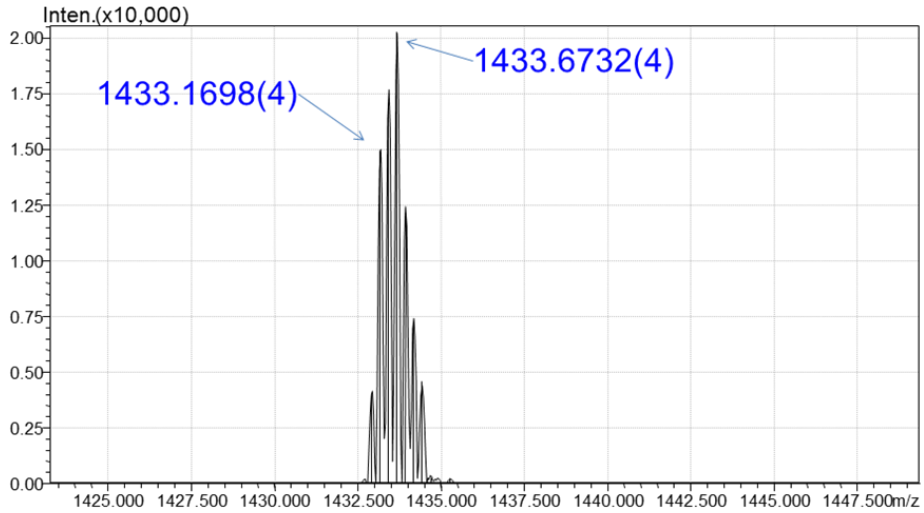

Figure 5.1 – Mass to charge ratio of native insulin with total mass of 5734.68 Da.

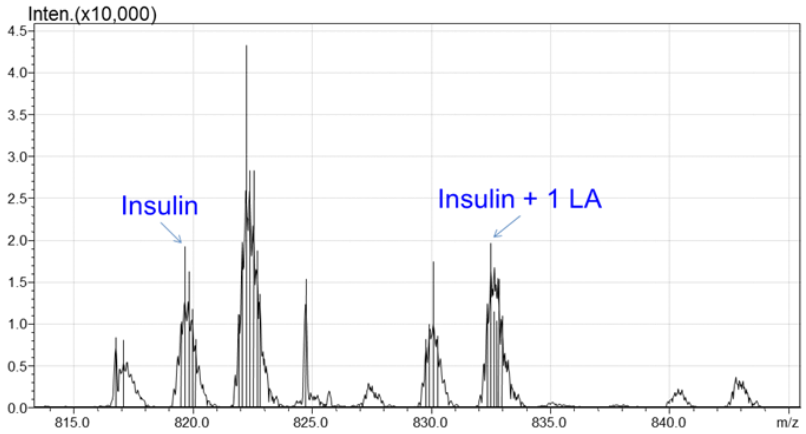

(A)

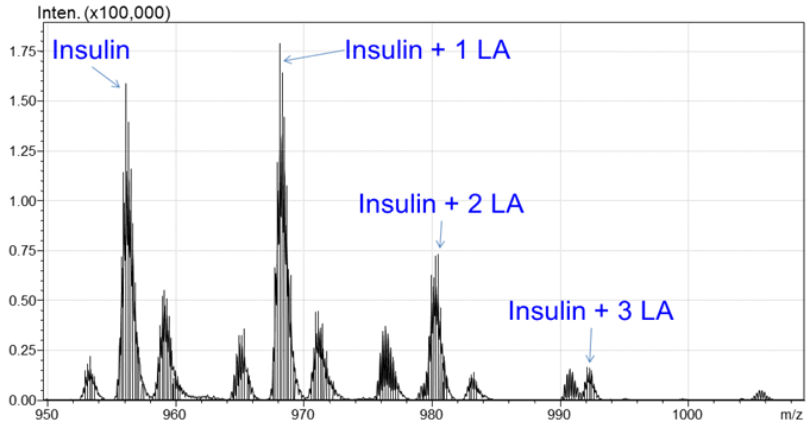

(B)

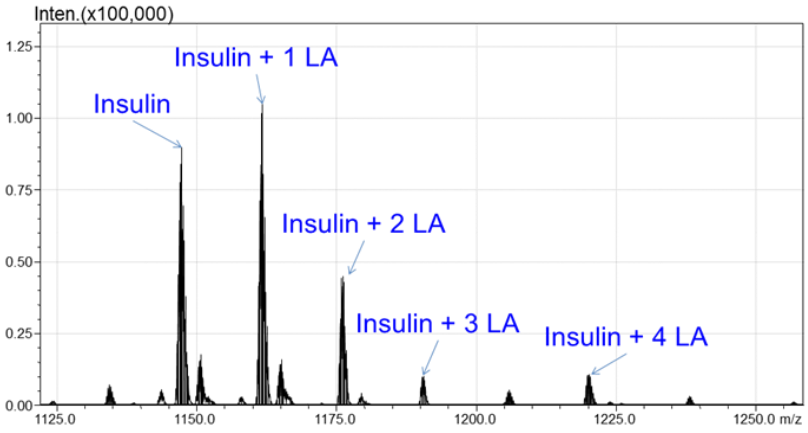

(C)

Figure 5.2 – Mass to charge ratio of insulin after incubation in 50 % LA solution for 21 days. (A) The 7 H^+ region, (B) the 6 H^+ region, and (C) the 5 H^+ region.

CHAPTER SIX
Future Directions

Surfactant Additives & PLGA Microspheres

The application of surfactants to microsphere formulations is a field that has shown solutions to some of the numerous difficulties involved in the controlled release of biological molecules from polymer matrices. Some of these include altering drug release rates, and improving the stability of encapsulated proteins and peptides. We have explored in detail the addition of a group of alkyl glucoside surfactants to PLGA microsphere formulations for the controlled release of the protein BSA and the peptide TB4. Our results demonstrate that the release kinetics of these biological molecules can be modulated by only small changes in surfactant structure. Furthermore, we have reduced the commonly reported problem of burst-release in BSA releasing microspheres by application of surfactants. Careful attention to specific attributes of these surfactants including HLB number and concentration played a critical role in our results.

The future of improving controlled release from PLGA matrices with surfactant additives remains an area that warrants extensive study. There are a number of biologically safe surfactant molecules that are commercially available that have not been explored in microsphere formulations. Furthermore, using chemical synthesis techniques, it should possible to customize surfactants to interact within the microsphere system in such a way that they establish desirable release kinetics and improve the stability of encapsulated molecules. Already, customized amphiphilic polymers designed to protect encapsulated proteins have appeared in scientific journals (Kim, et al., 2005). Surfactants that play a dual role of improving drug release as well as maintaining drug stability will be one focus for this technology in the future.

There are a number of applications of the primary W/O emulsions that will benefit from the research described here. These include drug coating of implantable devices for local controlled release. This has especially been important in development of intravascular stents. Drug releasing stents can be utilized in cardiac applications to release drugs that prevent re-occlusion of the vessels after implantation, or to aid in maintaining or improving a patient's heart function. Similar devices can be used to locally deliver chemotherapy to tumor vasculature. The W/O emulsion can also be precipitated into other configurations that are useful for mucosal, ocular, or dermal delivery of drugs. Regardless of the final geometry of the polymer device, the primary emulsion imparts important characteristics to the stability, encapsulation, and release of drug from the matrix.

TB4 Controlled Release in vitro and in vivo

The research presented in this dissertation leads to two future directions of experimentation regarding the controlled release of TB4. One direction is to understanding of the effects our surfactants play in TB4 elution from microspheres. The experiments presented in Ch. 2 and 3 demonstrate G8 reduces the release of BSA yet has little effect on the release of TB4, while G10 reduces release rates in both formulations but has low lower emulsion stability in TB4 compared to BSA. Initially it would be important to perform morphological analysis with SEM and TEM to determine how the surfactants impact microsphere morphology in the TB4 formulation. Microsphere morphology plays a key role in drug release kinetics as we have already explored with BSA release in Ch 2. We may find that tighter control of internal microsphere porosity does not relate to emulsion stability in the TB4 formulation as it did in the BSA work. Surface adsorption studies at the W/O interface would be another component of

further research on TB4 formulations. The surface adsorption of the encapsulated drug may play a role equally as important as internal microsphere morphology. In general, TB4 has higher EE and greater drug release overall. This may actually be the result of fewer drug molecules being adsorbed to PLGA in the TB4 formulation. Lastly, pursuing mass spectrometry to analyze covalent modifications to peptide primary structure would be of interest to quantify the amount of peptide impurities being released from the microspheres.

The second direction that would be of great benefit to pursue is the analysis of cellular response to released peptide over the four week duration of TB4 elution. These experiments include routine toxicity testing *in vitro*, such as an MTT assay. We are also interested in the response of endothelial cells to the controlled release of TB4 *in vitro*. Previously we were able to show that TB4 increases the development of capillary-like tube formation in human coronary endothelial cells (Bock-Marquette, et al., 2009). By employing an endothelial cell 'sprouting' assay, such as the one designed by Davis, 2008, we can quantify the induction of capillary-like tubes in coronary endothelial cells with controlled release of TB4 from microspheres. Other endpoints of this experiment include cell sprouting, cell survival, attachment, and analysis of gene expression in angiongeic pathways. A similar result in endothelial cell activation from externally administered TB4 and microsphere eluted TB4 would demonstrate the advantage to the single dose controlled release formulation. This information would establish strong evidence for *in vivo* testing with small animal models of MI.

APPENDIX A
Volume & Mole Fraction of Microsphere Formulation

For reference to our formulation I have provided the necessary information to perform calculation of the volume fraction and mole fraction of the microsphere formulation used where G8 is the surfactant at 8.55 mM. The pie graphs that follow represent each chemical's portion of the final microsphere formulation (figure A.1 & A.2).

Table A.1 – Physical properties of materials used in microsphere synthesis

Reagent	Density [g/cm3]*	Weight [mg]	Volume [ml]	Mw [g/mol]	Moles (ni)
Dichloromethane	1.33	6650	5.00	119.4	5.6E-02
Water	0.932	186.4	0.20	18	1.0E-02
PLGA 50:50	1.25	250	0.20	50000	5.0E-06
Surfactant (G8)	0.9	12.5	0.01	734.1	1.7E-05
Drug*	1	5	0.01	4963.5	8.7E-07

*Thymosin β-4 was the drug used in this calculation with the density estimated

*Absolute density of PLGA is approximately 1.34 g/cm^3. Particles formulated from this material are expected to be less dense and we used an estimate in the range of 1.21 to 1.29 g/cm^3 (Arnold, et al., 2007).

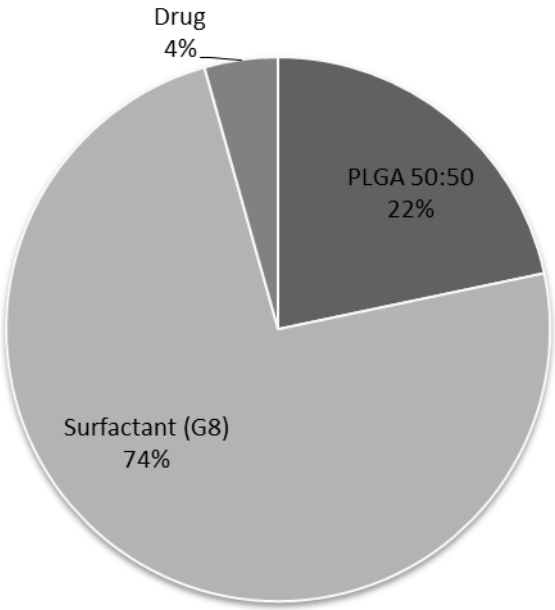

Figure A.1 – Mole fraction of lyophilized microspheres.

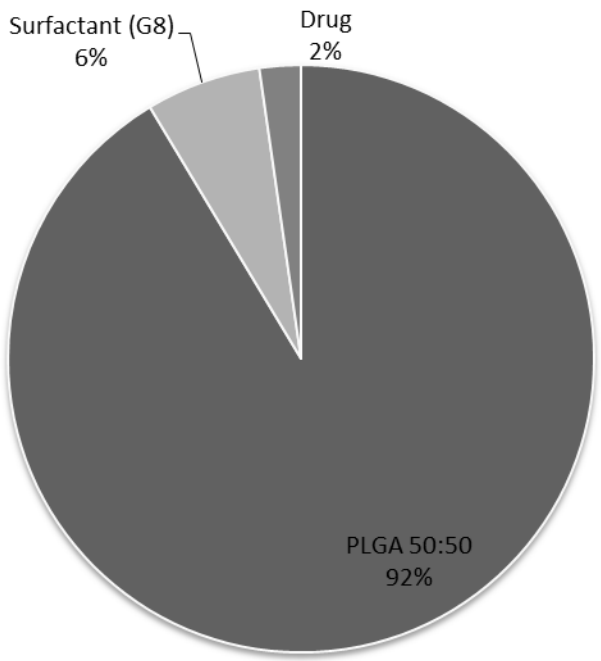

Figure A.2 – Volume fraction of lyophilized microspheres.

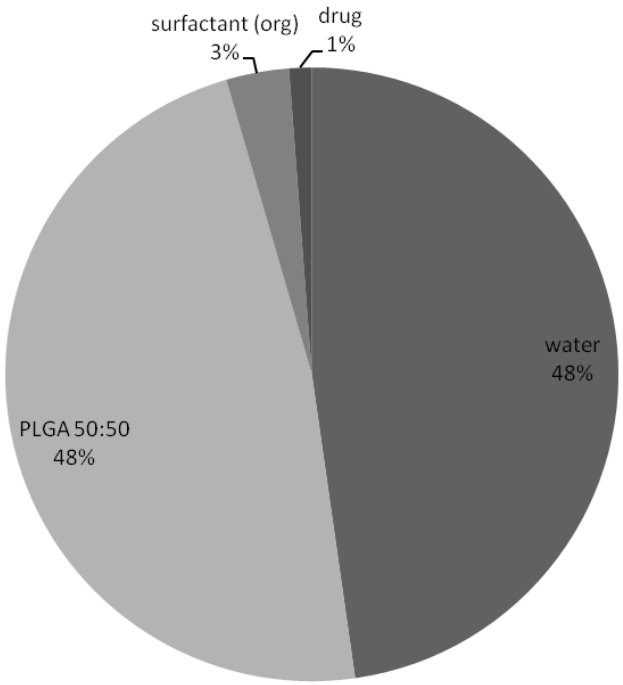

Figure A.3 – Volume fraction of microsphere formulation after extraction of organic solvent but prior to removal of internal aqueous phase water.

APPENDIX B
Estimation of Droplet Radius in Emulsion Analysis

$$R_s = \left(\frac{9\eta v}{2(\rho_2 - \rho_1)g}\right)^{1/2} \quad \textbf{(Eq. 4)}$$

Parameters

Viscosity (η) [P*s]	4.40E-03
Velocity (v) [cm/second] (1.5 cm/ 720 s)	2.08E-03
Density of Water (ρ_2) [g/cm^3]	0.932
Density of DCM (ρ_1) [g/cm^3]	1.33
28*gravity (g) [cm/s^2]	27440

Assumptions

- Water droplets are spherical
- Diffusion is negligible
- Water droplets do not coagulate or combine and act as independent units
- Viscosity of phases are not affected by dissolved molecules
- Velocity of water droplets are not affected by surface adsorbed molecules
- Gravity remained constant and acceleration/deceleration of the centrifuge is not taken into account

Solution

Time (s)	Cutoff Droplet Diameter (μm)
30	6.0
60	4.3
120	3.0
180	2.5
240	2.1
300	1.9
360	1.7
720	1.2

APPENDIX C
Program Files for Albumin & Thymosin B-4 Reverse Phase Chromatography

Dionix® Albumin Program

TempCtrl = On
Temperature.Nominal = 30.0 [°C]
Temperature.LowerLimit = 28.0 [°C]
Temperature.UpperLimit = 32.0 [°C]
EquilibrationTime = 0.5 [min]
ReadyTempDelta = 1.0 [°C]
Pressure.LowerLimit = 73 [psi]
Pressure.UpperLimit = 2799 [psi]
MaximumFlowRampDown = Infinite
MaximumFlowRampUp = Infinite
%A.Equate = "Empty"
%B.Equate = "0.1% TFA 5%ACN 95%H20" (Solution A was placed on the 'B' pump line)
%C.Equate = "0.1% TFA 95%ACN 5%H2O" (Solution B was placed on the 'C' pump line)
%D.Equate = "Empty"
DrawSpeed = 5.000 [µl/s]
DrawDelay = 3000 [ms]
DispSpeed = 20.000 [µl/s]
DispenseDelay = 0 [ms]
WasteSpeed = 32.000 [µl/s]
SampleHeight = 2.000 [mm]
InjectWash = NoWash
LoopWashFactor = 2.000
PunctureOffset = 0.0 [mm]
PumpDevice = "Pump"
InjectMode = Normal
SyncWithPump = On
Data_Collection_Rate = 5.0 [Hz]
ResponseTime = 2.000 [s]
UV_VIS_1.Wavelength = 214.0 [nm]
UV_VIS_1.Bandwidth = 2 [nm]
UV_VIS_1.RefWavelength = 600.0 [nm]
UV_VIS_1.RefBandwidth = 1 [nm]
UV_VIS_2.Wavelength = 280.0 [nm]
UV_VIS_2.Bandwidth = 2 [nm]
UV_VIS_2.RefWavelength = 600.0 [nm]
UV_VIS_2.RefBandwidth = 1 [nm]
UV_VIS_3.Wavelength = 220.0 [nm]
UV_VIS_3.Bandwidth = 2 [nm]
UV_VIS_3.RefWavelength = 600.0 [nm]
UV_VIS_3.RefBandwidth = 1 [nm]
AutoTrayShakeTimes = 1

-4.000 Flow = 2.500 [ml/min]
%B = 99.0 [%] (Solution A was placed on the 'B' pump line)
%C = 1.0 [%] (Solution B was placed on the 'C' pump line)
%D = 0.0 [%]

0.000 Autozero
Flow = 2.500 [ml/min]

%B = 99.0 [%]
%C = 1.0 [%]
%D = 0.0 [%]
Wait UV.Ready and Pump.Ready and ColumnOven.Ready and Sampler.Ready and PumpModule.Ready
Inject
UV_VIS_1.AcqOn
UV_VIS_2.AcqOn
UV_VIS_3.AcqOn
Flow = 2.500 [ml/min]
%B = 99.0 [%]
%C = 1.0 [%]
%D = 0.0 [%]

4.000 Flow = 2.500 [ml/min]
%B = 20.0 [%]
%C = 80.0 [%]
%D = 0.0 [%]

5.000 Flow = 2.500 [ml/min]
%B = 20.0 [%]
%C = 80.0 [%]
%D = 0.0 [%]

6.000 Flow = 2.500 [ml/min]
%B = 15.0 [%]
%C = 85.0 [%]
%D = 0.0 [%]

8.000 Flow = 2.500 [ml/min]
%B = 15.0 [%]
%C = 85.0 [%]
%D = 0.0 [%]

8.100 Flow = 2.500 [ml/min]
%B = 99.0 [%]
%C = 1.0 [%]
%D = 0.0 [%]

UV_VIS_1.AcqOff
UV_VIS_2.AcqOff
UV_VIS_3.AcqOff
End

Dionix® Thymosin Beta-4 Program

TempCtrl = On
Temperature.Nominal = 30.0 [°C]
Temperature.LowerLimit = 25.0 [°C]
Temperature.UpperLimit = 35.0 [°C]
EquilibrationTime = 0.5 [min]
ReadyTempDelta = 1.0 [°C]
Pressure.LowerLimit = 73 [psi]
Pressure.UpperLimit = 2799 [psi]

MaximumFlowRampDown = Infinite
MaximumFlowRampUp = Infinite
%A.Equate = "Empty"
%B.Equate = "0.1% TFA 5%ACN 95%H20" (Solution A was placed on the ‘B’ pump line)
%C.Equate = "0.1% TFA 95%ACN 5%H2O" (Solution B was placed on the ‘C’ pump line)
%D.Equate = "Empty"
DrawSpeed = 5.000 [µl/s]
DrawDelay = 3000 [ms]
DispSpeed = 20.000 [µl/s]
DispenseDelay = 0 [ms]
WasteSpeed = 32.000 [µl/s]
SampleHeight = 2.000 [mm]
InjectWash = NoWash
LoopWashFactor = 2.000
PunctureOffset = 0.0 [mm]
PumpDevice = "Pump"
InjectMode = Normal
SyncWithPump = On
Data_Collection_Rate = 5.0 [Hz]
ResponseTime = 2.000 [s]
UV_VIS_1.Wavelength = 214.0 [nm]
UV_VIS_1.Bandwidth = 2 [nm]
UV_VIS_1.RefWavelength = 600.0 [nm]
UV_VIS_1.RefBandwidth = 1 [nm]
UV_VIS_2.Wavelength = 220.0 [nm]
UV_VIS_2.Bandwidth = 2 [nm]
UV_VIS_2.RefWavelength = 600.0 [nm]
UV_VIS_2.RefBandwidth = 1 [nm]
UV_VIS_3.Wavelength = 280.0 [nm]
UV_VIS_3.Bandwidth = 2 [nm]
UV_VIS_3.RefWavelength = 600.0 [nm]
UV_VIS_3.RefBandwidth = 1 [nm]
AutoTrayShakeTimes = 1

-3.000 Flow = 2.500 [ml/min]
%B = 99.0 [%] (Solution A was placed on the ‘B’ pump line)
%C = 1.0 [%] (Solution B was placed on the ‘C’ pump line)
%D = 0.0 [%]

0.000 Autozero
Flow = 2.500 [ml/min]
%B = 99.0 [%]
%C = 1.0 [%]
%D = 0.0 [%]
Wait UV.Ready and Pump.Ready and ColumnOven.Ready and Sampler.Ready and PumpModule.Ready
Inject
UV_VIS_1.AcqOn
UV_VIS_2.AcqOn
UV_VIS_3.AcqOn
Flow = 2.500 [ml/min]
%B = 99.0 [%]
%C = 1.0 [%]
%D = 0.0 [%]

2.500 Flow = 2.500 [ml/min]
%B = 50.0 [%]
%C = 50.0 [%]
%D = 0.0 [%]

2.750 Flow = 2.500 [ml/min]
%B = 15.0 [%]
%C = 85.0 [%]
%D = 0.0 [%]

4.750 Flow = 2.500 [ml/min]
%B = 15.0 [%]
%C = 85.0 [%]

4.850 Flow = 2.500 [ml/min]
%B = 99.0 [%]
%C = 1.0 [%]
%D = 0.0 [%]

UV_VIS_1.AcqOff
UV_VIS_2.AcqOff
UV_VIS_3.AcqOff

BIBLIOGRAPHY

References

Aiello, L.P., *et al.* (1994) Vascular endothelial growth factor in ocular fluid of patients with diabetic retinopathy and other retinal disorders, *N Engl J Med*, **331**, 1480-1487.

Alonso, M.J., *et al.* (1993) Determinants of release rate of tetanus vaccine from polyester microspheres, *Pharm Res*, **10**, 945-953.

Arnold, M.M., *et al.* (2007) NanoCipro encapsulation in monodisperse large porous PLGA microparticles, *J Control Release*, **121**, 100-109.

Athanasiou, K.A., Niederauer, G.G. and Agrawal, C.M. (1996) Sterilization, toxicity, biocompatibility and clinical applications of polylactic acid/polyglycolic acid copolymers, *Biomaterials*, **17**, 93-102.

Bertram, J.P., *et al.* (2010) Using polymer chemistry to modulate the delivery of neurotrophic factors from degradable microspheres: delivery of BDNF, *Pharm Res*, **27**, 82-91.

Blanco, D. and Alonso, M.J. (1998) Protein encapsulation and release from poly(lactide-co-glycolide) microspheres: effect of the protein and polymer properties and of the co-encapsulation of surfactants. In, *Eur J Pharm Biopharm*. Netherlands, pp. 285-294.

BlancoPrieto, M.J., *et al.* (1996) Study of the influence of several stabilizing agents on the entrapment and in vitro release of pBC 264 from poly(lactide-co-glycolide) microspheres prepared by a W/O/W solvent evaporation method, *Pharmaceut Res*, **13**, 1127-1129.

Bock-Marquette, I., *et al.* (2004) Thymosin beta4 activates integrin-linked kinase and promotes cardiac cell migration, survival and cardiac repair, *Nature*, **432**, 466-472.

Bock-Marquette, I., *et al.* (2009) Thymosin beta4 mediated PKC activation is essential to initiate the embryonic coronary developmental program and epicardial progenitor cell activation in adult mice in vivo, *J Mol Cell Cardiol*, **46**, 728-738.

Bouissou, C., *et al.* (2004) Controlled release of the fibronectin central cell binding domain from polymeric microspheres. In, *J Control Release*. Netherlands, pp. 557-566.

Bouissou, C., *et al.* (2006) The influence of surfactant on PLGA microsphere glass transition and water sorption: remodeling the surface morphology to attenuate the burst release, *Pharm Res*, **23**, 1295-1305.

Camarata, P.J., *et al.* (1992) Sustained release of nerve growth factor from biodegradable polymer microspheres, *Neurosurgery*, **30**, 313-319.

Carrascosa, C., *et al.* (2004) Microspheres containing insulin-like growth factor I for treatment of chronic neurodegeneration, *Biomaterials*, **25**, 707-714.
Cassimeris, L., *et al.* (1992) Thymosin beta 4 sequesters the majority of G-actin in resting human polymorphonuclear leukocytes, *J Cell Biol*, **119**, 1261-1270.
Cha, H.J., Jeong, M.J. and Kleinman, H.K. (2003) Role of thymosin beta4 in tumor metastasis and angiogenesis, *J Natl Cancer Inst*, **95**, 1674-1680.
Chesko, J., *et al.* (2005) An investigation of the factors controlling the adsorption of protein antigens to anionic PLG microparticles, *J Pharm Sci*, **94**, 2510-2519.
Cho, K.Y., *et al.* (2001) Protein release microparticles based on the blend of poly(D,L-lactic-co-glycolic acid) and oligo-ethylene glycol grafted poly(L-lactide), *J Control Release*, **76**, 275-284.
Christian, T.F., Schwartz, R.S. and Gibbons, R.J. (1992) Determinants of infarct size in reperfusion therapy for acute myocardial infarction, *Circulation*, **86**, 81-90.
Cleek, R., *et al.* (1997) Microparticles of poly(dl-lactic-co-glycolic acid)/poly(ethylene glycol) blends for controlled drug delivery, *Journal of Controlled Release*, **48**, 259-268.
Cleland, J., *et al.* (1997) Local controlled delivery of vascular endothelial growth factor provides neovascularization, *Proc Int Symp Control Del Bioact Mater* **24**.
Cleland, J.L., *et al.* (2001) Development of poly-(D,L-lactide--coglycolide) microsphere formulations containing recombinant human vascular endothelial growth factor to promote local angiogenesis, *J Control Release*, **72**, 13-24.
Cooper, L.T., Jr., *et al.* (2001) Proteinuria in a placebo-controlled study of basic fibroblast growth factor for intermittent claudication, *Vasc Med*, **6**, 235-239.
Cui, F., *et al.* (2005) Preparation and characterization of melittin-loaded poly (DL-lactic acid) or poly (DL-lactic-co-glycolic acid) microspheres made by the double emulsion method, *J Control Release*, **107**, 310-319.
Davies, J. (1957) A quantitative kinetic theory of emulsion type, I. Physical chemistry of the emulsifying agent, *Proceedings of the International Congress of Surface Activity*, 426-438.
Diaz, R.V., Llabres, M. and Evora, C. (1999) One-month sustained release microspheres of 125I-bovine calcitonin. In vitro-in vivo studies, *J Control Release*, **59**, 55-62.
Ehtezazi, T., Washington, C. and Melia, C.D. (1999) Determination of the internal morphology of poly (D,L-lactide) microspheres using stereological methods, *J Control Release*, **57**, 301-314.
Flint, E.B. and Suslick, K.S. (1991) The temperature of cavitation, *Science*, **253**, 1397-1399.

Fournier, E., *et al.* (2003) Biocompatibility of implantable synthetic polymeric drug carriers: focus on brain biocompatibility, *Biomaterials*, **24**, 3311-3331.
Freedman, S.B. and Isner, J.M. (2001) Therapeutic angiogenesis for ischemic cardiovascular disease, *J Mol Cell Cardiol*, **33**, 379-393.
Freeman, K.W., Bowman, B.R. and Zetter, B.R. (2011) Regenerative protein thymosin beta-4 is a novel regulator of purinergic signaling, *FASEB J*, **25**, 907-915.
Fu, K., *et al.* (1999) FTIR characterization of the secondary structure of proteins encapsulated within PLGA microspheres, *J Control Release*, **58**, 357-366.
Fuchs, S., *et al.* (2003) Catheter-based autologous bone marrow myocardial injection in no-option patients with advanced coronary artery disease: a feasibility study, *J Am Coll Cardiol*, **41**, 1721-1724.
Gleason, J.D., *et al.* (2002) Myocardial drug distribution pattern following intrapericardial delivery: an MRI analysis, *J Cardiovasc Magn Reson*, **4**, 311-316.
Grant, D.S., *et al.* (1995) Matrigel induces thymosin beta 4 gene in differentiating endothelial cells, *J Cell Sci*, **108 (Pt 12)**, 3685-3694.
Griffin, W. (1954) Calculation of HLB Values of Non-Ionic Surfactants, *Journal of the Society of Cosmetic Chemists* **5**, 259.
Grizzi, I., *et al.* (1995) Hydrolytic degradation of devices based on poly(DL-lactic acid) size-dependence, *Biomaterials*, **16**, 305-311.
Grossman, P.M., *et al.* (2002) Incomplete retention after direct myocardial injection, *Catheter Cardiovasc Interv*, **55**, 392-397.
Hamano, K., *et al.* (2001) Local implantation of autologous bone marrow cells for therapeutic angiogenesis in patients with ischemic heart disease: clinical trial and preliminary results, *Jpn Circ J*, **65**, 845-847.
Hao, X., *et al.* (2007) Angiogenic effects of sequential release of VEGF-A165 and PDGF-BB with alginate hydrogels after myocardial infarction, *Cardiovasc Res*, **75**, 178-185.
Hiemenez, P. and Rajagopalan, R. (1997) *Principles of Colloid and Surface Chemistry: Third Edition.* CRC Press, Boca Raton, Florida.
Hinds, K.D., *et al.* (2005) PEGylated insulin in PLGA microparticles. In vivo and in vitro analysis, *J Control Release*, **104**, 447-460.
Hof, R.P., *et al.* (1981) Trapping and intramyocardial distribution of microspheres with different diameters in cat and rabbit hearts in vitro, *Basic Res Cardiol*, **76**, 630-638.
Hofmann, M., *et al.* (2005) Monitoring of bone marrow cell homing into the infarcted human myocardium, *Circulation*, **111**, 2198-2202.
Hsieh, P.C., *et al.* (2006) Controlled delivery of PDGF-BB for myocardial protection using injectable self-assembling peptide nanofibers, *J Clin Invest*, **116**, 237-248.

Huff, T., *et al.* (2001) beta-Thymosins, small acidic peptides with multiple functions, *Int J Biochem Cell Biol*, **33**, 205-220.
Huh, K., Cho, Y. and Park, K. (2003) PLGA-PEG Block Copolymers for Drug Formulations, *Drug Development & Delivery*, **3**.
Iwakura, A., *et al.* (2003) Intramyocardial sustained delivery of basic fibroblast growth factor improves angiogenesis and ventricular function in a rat infarct model, *Heart Vessels*, **18**, 93-99.
Jain, R.A. (2000) The manufacturing techniques of various drug loaded biodegradable poly(lactide-co-glycolide) (PLGA) devices., *Biomaterials*, **21**, 2475-2490.
Jain, R.K., *et al.* (2007) Antiangiogenic therapy for normalization of atherosclerotic plaque vasculature: a potential strategy for plaque stabilization, *Nat Clin Pract Cardiovasc Med*, **4**, 491-502.
Jiang, W. and Schwendeman, S.P. (2001) Stabilization and controlled release of bovine serum albumin encapsulated in poly(D, L-lactide) and poly(ethylene glycol) microsphere blends, *Pharm Res*, **18**, 878-885.
Kang, F., *et al.* (2002) Lysozyme stability in primary emulsion for PLGA microsphere preparation: effect of recovery methods and stabilizing excipients, *Pharm Res*, **19**, 629-633.
Kang, F. and Singh, J. (2001) Effect of additives on the release of a model protein from PLGA microspheres, *AAPS PharmSciTech*, **2**, 30.
Kang, F. and Singh, J. (2003) Conformational stability of a model protein (bovine serum albumin) during primary emulsification process of PLGA microspheres synthesis, *Int J Pharm*, **260**, 149-156.
Kim, H.K. and Park, T.G. (2004) Comparative study on sustained release of human growth hormone from semi-crystalline poly(L-lactic acid) and amorphous poly(D,L-lactic-co-glycolic acid) microspheres: morphological effect on protein release, *J Control Release*, **98**, 115-125.
Kim, J.H., *et al.* (2005) Stability of bovine serum albumin complexed with PEG-poly(L-histidine) diblock copolymer in PLGA microspheres, *J Control Release*, **109**, 86-100.
Kobayashi, T., *et al.* (2002) Thymosin-beta4 regulates motility and metastasis of malignant mouse fibrosarcoma cells, *Am J Pathol*, **160**, 869-882.
Kostanski, J.W., *et al.* (2000) Effect of the concurrent LHRH antagonist administration with a LHRH superagonist in rats, *Pharm Res*, **17**, 445-450.
Kowalski, A., Duda, A. and Penczek, S. (2000) Kinetics and Mechanism of Cyclic Esters Polymerization Initiated with Tin(II) Octoate. 3. Polymerization of l,l-Dilactide, *Macromolecules*, **33**, 7359–7370.
Kwon, Y.M., *et al.* (2001) In situ study of insulin aggregation induced by water-organic solvent interface, *Pharm Res*, **18**, 1754-1759.

Kyte, J. and Doolittle, R.F. (1982) A simple method for displaying the hydropathic character of a protein, *J Mol Biol*, **157**, 105-132.

Laham, R.J., *et al.* (2005) Transendocardial and transepicardial intramyocardial fibroblast growth factor-2 administration: myocardial and tissue distribution, *Drug Metab Dispos*, **33**, 1101-1107.

Laham, R.J., *et al.* (2003) Intrapericardial administration of basic fibroblast growth factor: myocardial and tissue distribution and comparison with intracoronary and intravenous administration, *Catheter Cardiovasc Interv*, **58**, 375-381.

Laham, R.J., *et al.* (1999) Local perivascular delivery of basic fibroblast growth factor in patients undergoing coronary bypass surgery: results of a phase I randomized, double-blind, placebo-controlled trial, *Circulation*, **100**, 1865-1871.

Lam, X.M., Duenas, E.T. and Cleland, J.L. (2001) Encapsulation and stabilization of nerve growth factor into poly(lactic-co-glycolic) acid microspheres. In, *J Pharm Sci*. 2001 Wiley-Liss, Inc. and the American Pharmaceutical Association, United States, pp. 1356-1365.

Lam, X.M., *et al.* (2000) Sustained release of recombinant human insulin-like growth factor-I for treatment of diabetes, *J Control Release*, **67**, 281-292.

Langmuir, I. (1917) The Constitution and Fundamental Properties of Solids and Liquids. II, *Journal of the American Chemical Society*, **39**, 1848-1906.

Lazarous, D.F., *et al.* (1997) Pharmacodynamics of basic fibroblast growth factor: route of administration determines myocardial and systemic distribution, *Cardiovasc Res*, **36**, 78-85.

le Maire, M., Champeil, P. and Moller, J.V. (2000) Interaction of membrane proteins and lipids with solubilizing detergents, *Biochim Biophys Acta*, **1508**, 86-111.

Leighton, T. (1994) *The Acoustic Bubble*. Academic Press, Inc., San Diego, California.

Li, M., Rouaud, O. and Poncelet, D. (2008) Microencapsulation by solvent evaporation: state of the art for process engineering approaches, *Int J Pharm*, **363**, 26-39.

Liu, Y., *et al.* (2006) Effects of basic fibroblast growth factor microspheres on angiogenesis in ischemic myocardium and cardiac function: analysis with dobutamine cardiovascular magnetic resonance tagging, *Eur J Cardiothorac Surg*, **30**, 103-107.

Low, T.L. and Goldstein, A.L. (1982) Chemical characterization of thymosin beta 4, *J Biol Chem*, **257**, 1000-1006.

Low, T.L., Hu, S.K. and Goldstein, A.L. (1981) Complete amino acid sequence of bovine thymosin beta 4: a thymic hormone that induces terminal

deoxynucleotidyl transferase activity in thymocyte populations, *Proc Natl Acad Sci U S A*, **78**, 1162-1166.

Luan, X. and Bodmeier, R. (2006) Influence of the poly(lactide-co-glycolide) type on the leuprolide release from in situ forming microparticle systems, *J Control Release*, **110**, 266-272.

Lucerna, M., *et al.* (2007) Vascular endothelial growth factor-A induces plaque expansion in ApoE knock-out mice by promoting de novo leukocyte recruitment, *Blood*, **109**, 122-129.

Lucke, A., *et al.* (2002) The effect of poly(ethylene glycol)-poly(D,L-lactic acid) diblock copolymers on peptide acylation, *J Control Release*, **80**, 157-168.

Lucke, A., Kiermaier, J. and Gopferich, A. (2002) Peptide acylation by poly(alpha-hydroxy esters), *Pharm Res*, **19**, 175-181.

Malinda, K.M., *et al.* (1999) Thymosin beta4 accelerates wound healing, *J Invest Dermatol*, **113**, 364-368.

Mani, K. and Kitsis, R.N. (2003) Myocyte apoptosis: programming ventricular remodeling, *J Am Coll Cardiol*, **41**, 761-764.

Meinel, L., *et al.* (2001) Stabilizing insulin-like growth factor-I in poly(D,L-lactide-co-glycolide) microspheres, *J Control Release*, **70**, 193-202.

Mohamed, F. and van der Walle, C.F. (2006) PLGA microcapsules with novel dimpled surfaces for pulmonary delivery of DNA. In, *Int J Pharm*. Netherlands, pp. 97-107.

Murty, S.B., *et al.* (2003) Identification of chemically modified peptide from poly(D,L-lactide-co-glycolide) microspheres under in vitro release conditions, *AAPS PharmSciTech*, **4**, E50.

Na, D.H. and DeLuca, P.P. (2005) PEGylation of octreotide: I. Separation of positional isomers and stability against acylation by poly(D,L-lactide-co-glycolide), *Pharm Res*, **22**, 736-742.

Nihant, N., *et al.* (1995) Polylactide Microparticles Prepared by Double Emulsion-Evaporation: II. Effect of the Poly(Lactide-co-Glycolide) Composition on the Stability of the Primary and Secondary Emulsions *Journal of Colloid and Interface Science*, **173**, 55-65.

Nihant, N., *et al.* (1994) Polylactide microparticles prepared by double emulsion/evaporation technique. I. Effect of primary emulsion stability., *Pharm Res*, **11**, 1479 - 1484.

Okada, H., *et al.* (1994) Preparation of three-month depot injectable microspheres of leuprorelin acetate using biodegradable polymers, *Pharm Res*, **11**, 1143-1147.

Ostgren, C.J., *et al.* (2000) Associations between smoking and beta-cell function in a non-hypertensive and non-diabetic population. Skaraborg Hypertension and Diabetes Project, *Diabet Med*, **17**, 445-450.

Paillard-Giteau, A., *et al.* (2010) Effect of various additives and polymers on lysozyme release from PLGA microspheres prepared by an s/o/w emulsion technique. In, *Eur J Pharm Biopharm*. 2010 Elsevier B.V, Netherlands, pp. 128-136.

Pean, J.M., *et al.* (1998) NGF release from poly(D,L-lactide-co-glycolide) microspheres. Effect of some formulation parameters on encapsulated NGF stability, *J Control Release*, **56**, 175-187.

Penicka, M., *et al.* (2005) Images in cardiovascular medicine. Early tissue distribution of bone marrow mononuclear cells after transcoronary transplantation in a patient with acute myocardial infarction, *Circulation*, **112**, e63-65.

Perin, E.C., *et al.* (2003) Transendocardial, autologous bone marrow cell transplantation for severe, chronic ischemic heart failure, *Circulation*, **107**, 2294-2302.

Philp, D., *et al.* (2003) Thymosin beta 4 and a synthetic peptide containing its actin-binding domain promote dermal wound repair in db/db diabetic mice and in aged mice, *Wound Repair Regen*, **11**, 19-24.

Platel, R., Hodgson, L. and Williams, C. (2008) Biocompatible Initiators for Lactide Polymerization, *Poly. Rev.*, **48**, 11-63.

Ratner, B. and Hoffman, A. (2004) *Biomaterials Science, Second Edition: An Introduction to Materials in Medicine*. Elsevier Inc., San Diego, California.

Reimer, K.A. and Jennings, R.B. (1979) The "wavefront phenomenon" of myocardial ischemic cell death. II. Transmural progression of necrosis within the framework of ischemic bed size (myocardium at risk) and collateral flow, *Lab Invest*, **40**, 633-644.

Reimer, K.A., *et al.* (1977) The wavefront phenomenon of ischemic cell death. 1. Myocardial infarct size vs duration of coronary occlusion in dogs, *Circulation*, **56**, 786-794.

Roger, V.L., *et al.* (2011) Heart disease and stroke statistics--2011 update: a report from the American Heart Association, *Circulation*, **123**, e18-e209.

Rosa, G.D., *et al.* (2000) Influence of the co-encapsulation of different non-ionic surfactants on the properties of PLGA insulin-loaded microspheres, *J Control Release*, **69**, 283-295.

Rothen-Weinhold, A., *et al.* (2000) Formation of peptide impurities in polyester matrices during implant manufacturing, *Eur J Pharm Biopharm*, **49**, 253-257.

Rothstein, S.N., Federspiel, W.J. and Little, S.R. (2009) A unified mathematical model for the prediction of controlled release from surface and bulk eroding polymer matrices, *Biomaterials*, **30**, 1657-1664.

Ruan, G., Feng, S.S. and Li, Q.T. (2002) Effects of material hydrophobicity on physical properties of polymeric microspheres formed by double emulsion process, *J Control Release*, **84**, 151-160.

Sah, H. (1999) Protein behavior at the water/methylene chloride interface, *Journal of Pharmaceutical Sciences*, **88**, 1320-1325.
Sah, H. (1999) Protein instability toward organic solvent/water emulsification: implications for protein microencapsulation into microspheres, *PDA J Pharm Sci Technol*, **53**, 3-10.
Saltzman, W.M. (2001) *Drug Delivery: Engineering Principles for Drug Therapy*. Oxford University Press, Inc., New York, New York.
Sanders, M.C., Goldstein, A.L. and Wang, Y.L. (1992) Thymosin beta 4 (Fx peptide) is a potent regulator of actin polymerization in living cells, *Proc Natl Acad Sci U S A*, **89**, 4678-4682.
Sandor, M., *et al.* (2002) Effect of lecithin and MgCO3 as additives on the enzymatic activity of carbonic anhydrase encapsulated in poly(lactide-co-glycolide) (PLGA) microspheres. In, *Biochim Biophys Acta*. Netherlands, pp. 63-74.
Schwendeman, S.P., *et al.* (1996) Strategies for stabilising tetanus toxoid towards the development of a single-dose tetanus vaccine, *Dev Biol Stand*, **87**, 293-306.
Shelke, N.B., Rokhade, A.P., Aminabhavi, T.M. (2010) Preparation and Evaluation of Novel Blend Microspheres of Poly(lactic-co-glycolic)acid and Pluronic F68/127 for Controlled Release of Repaglinide, *Journal of Applied Polymer Science*, **116**, 366–372.
Shenderova, A., Ding, A. and Schwendeman, S. (2004) Potentiometric Method for Determination of Microclimate pH in Poly(lactic-co-glycolic acid) Films, *Macromolecules*, **37**, 10052–10058.
Sinha, V.R. and Trehan, A. (2003) Biodegradable microspheres for protein delivery, *J Control Release*, **90**, 261-280.
Sophocleous, A.M., Zhang, Y. and Schwendeman, S.P. (2009) A new class of inhibitors of peptide sorption and acylation in PLGA, *J Control Release*, **137**, 179-184.
Sosne, G., *et al.* (2001) Thymosin beta 4 promotes corneal wound healing and modulates inflammatory mediators in vivo, *Exp Eye Res*, **72**, 605-608.
Srivastava, D., *et al.* (2007) Thymosin beta4 is cardioprotective after myocardial infarction, *Ann N Y Acad Sci*, **1112**, 161-170.
Stamm, C., *et al.* (2003) Autologous bone-marrow stem-cell transplantation for myocardial regeneration, *Lancet*, **361**, 45-46.
Sun, Y., *et al.* (2000) Cardiac remodeling by fibrous tissue after infarction in rats, *J Lab Clin Med*, **135**, 316-323.
Suslick, K., Hammerton, D. and Cline, R. (1986) Sonochemical hot spot, *J. Am. Chem. Soc.*, **108**, 5641–5642.

Takada, S., *et al.* (1995) Application of a spray drying technique in the production of TRH-containing injectable sustained-release microparticles of biodegradable polymers, *J Pharm Sci Technol*, **49**, 180-184.
Tobio, M., *et al.* (1999) A novel system based on a poloxamer/PLGA blend as a tetanus toxoid delivery vehicle, *Pharm Res*, **16**, 682-688.
Tracy, M.A., *et al.* (1999) Factors affecting the degradation rate of poly(lactide-co-glycolide) microspheres in vivo and in vitro, *Biomaterials*, **20**, 1057-1062.
Tse, H.F., *et al.* (2003) Angiogenesis in ischaemic myocardium by intramyocardial autologous bone marrow mononuclear cell implantation, *Lancet*, **361**, 47-49.
Ungaro, F., *et al.* (2006) Microsphere-integrated collagen scaffolds for tissue engineering: effect of microsphere formulation and scaffold properties on protein release kinetics, *J Control Release*, **113**, 128-136.
van de Weert, M., *et al.* (2000) The effect of a water/organic solvent interface on the structural stability of lysozyme. In, *J Control Release*. Netherlands, pp. 351-359.
van Ruissen, F., *et al.* (1998) Differential effects of detergents on keratinocyte gene expression, *J Invest Dermatol*, **110**, 358-363.
Vert, M., Mauduit, J. and Li, S. (1994) Biodegradation of PLA/GA polymers: increasing complexity, *Biomaterials*, **15**, 1209-1213.
Virmani, R., *et al.* (2005) Atherosclerotic plaque progression and vulnerability to rupture: angiogenesis as a source of intraplaque hemorrhage, *Arterioscler Thromb Vasc Biol*, **25**, 2054-2061.
Wang, W.S., *et al.* (2004) Overexpression of the thymosin beta-4 gene is associated with increased invasion of SW480 colon carcinoma cells and the distant metastasis of human colorectal carcinoma, *Oncogene*, **23**, 6666-6671.
Wasylewski, Z. and Kozik, A. (1979) Protein--non-ionic detergent interaction. Interaction of bovine serum albumin with alkyl glucosides studied by equilibrium dialysis and infrared spectroscopy, *Eur J Biochem*, **95**, 121-126.
Wei, G., Lu, L.F. and Lu, W.Y. (2007) Stabilization of recombinant human growth hormone against emulsification-induced aggregation by Pluronic surfactants during microencapsulation, *Int J Pharm*, **338**, 125-132.
Wei, G., *et al.* (2004) The release profiles and bioactivity of parathyroid hormone from poly(lactic-co-glycolic acid) microspheres, *Biomaterials*, **25**, 345-352.
Wei, H.J., *et al.* (2007) Gelatin microspheres encapsulated with a nonpeptide angiogenic agent, ginsenoside Rg1, for intramyocardial injection in a rat model with infarcted myocardium, *J Control Release*, **120**, 27-34.
Yamamoto, T., *et al.* (1993) Thymosin beta-4 expression is correlated with metastatic capacity of colorectal carcinomas, *Biochem Biophys Res Commun*, **193**, 706-710.

Yamamoto, T., *et al.* (2001) Intramyocardial delivery of basic fibroblast growth factor-impregnated gelatin hydrogel microspheres enhances collateral circulation to infarcted canine myocardium, *Jpn Circ J*, **65**, 439-444.

Yang, T.H., *et al.* (1999) Use of infrared spectroscopy to assess secondary structure of human growth hormone within biodegradable microspheres, *J Pharm Sci*, **88**, 161-165.

Yang, Y.Y., Chung, T.S. and Ng, N.P. (2001) Morphology, drug distribution, and in vitro release profiles of biodegradable polymeric microspheres containing protein fabricated by double-emulsion solvent extraction/evaporation method, *Biomaterials*, **22**, 231-241.

Yeh, M.K., Davis, S.S. and Coombes, A.G. (1996) Improving protein delivery from microparticles using blends of poly(DL lactide co-glycolide) and poly(ethylene oxide)-poly(propylene oxide) copolymers, *Pharm Res*, **13**, 1693-1698.

ACKNOWLEDGEMENTS

I would especially like to thank my mentor J. Michael DiMaio for his guidance, support and patience over the course of my studies. The people in Dr. DiMaio's lab including Ildoko Bock-Marquette for her instruction in molecular biology and basic laboratory training, Santwana Shrivastava, and Leah Gaither. I would like to thank Robert Eberhart for his engineering advice, project guidance, and serving as my committee chair, Zoltan Schelly for allowing me to use his laboratory space at UT Arlington and for serving on my committee, and the rest of my committee members: Kevin Nelson, Noelle Williams, and Jinming Gao for their effort and advice. I would like to acknowledge Kytai Nguyen for instruction in polymer drug formulations for controlled release. I would like to thank Tré Welch for his friendship and providing access to the Surgery Research Laboratory at UT Southwestern. I would like to acknowledge Kevin Schug and Hien Nguyen for assistance with mass spectrometry equipment and data analysis. I would like to thank Brian Edwards with the UT Arlington Chemistry Core facility and Laurie Meuler with the UT Southwestern Electron Microscopy Core facility for their vital assistance with instrumentation.

This project was supported by funding from the Laurence and Susan Hirsch/Centex Distinguished Chair in Heart Disease